CHAPTER SEVEN

ANALYSIS OF RIGID RAFTS SUPPORTED BY GRANULAR PILES

7.1 INTRODUCTION

In the previous two chapters solutions have been presented for the magnitude and rate of settlement of flexible foundations supported by clay reinforced by large numbers of granular piles. In this chapter the settlement of widespread rigid foundations constructed on soil stabilised by stone columns is considered.

The concept used in Chapter 5, that except near the edges of the loaded area the behaviour of all pile-soil units is the same and thus only one pile-soil unit need be analysed, is again utilised. Analytic expressions from elasticity are derived for the stresses and displacements within a pile-soil unit resting on a rigid base which undergoes equal surface displacement.

The vertical stresses in the pile and soil computed from the elastic analysis are then used to compute moment distributions in the raft when subjected to a uniform applied pressure. Solutions are presented which show the effect of pile spacing and the material properties of the pile and soil on the settlement of the foundation and the distribution of moments across the foundation. Finally, finite element solutions to Biot's equations of consolidation are presented for the rate of settlement of the rigid raft.

7.2 ANALYSIS OF SETTLEMENT

7.2.1 Description of Problem

Fig. 7.1 shows schematically, a smooth rigid raft overlaying

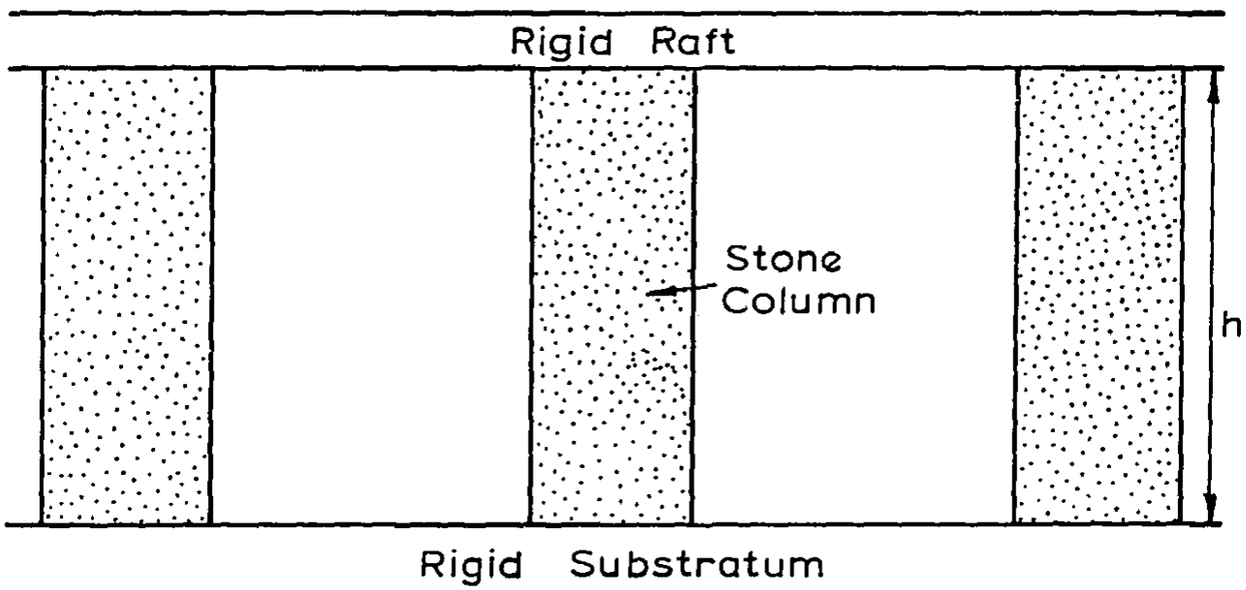

FIG. 7·1 PROBLEM DEFINITION

a layer of clay stabilised by the introduction of a large number of fully penetrating stone columns.

In general the stone columns will have been placed on a regular grid. There are three possible regular arrangements; the columns may lie on the vertices of an equilateral triangle, a square or a regular hexagon. These arrangements are illustrated in Fig. 7.2. The last case is of limited practical importance and will not be considered in detail.

Chapter 5 introduced the concept that, because of the assumption of a large number of columns, each column and the area surrounding it will respond in virtually the same fashion as those adjacent; this concept is utilised again. It follows from considerations of symmetry that the area surrounding a column (or the domain of influence) corresponding to a spacing on the vertices of equilateral triangles is a regular hexagon of side $s/\sqrt{3}$; that based on a square, is itself a square of side s; that based on the regular hexagon is an equilateral triangle of side $\sqrt{3}$ s.

It also follows from symmetry that the sides of the domains of influence are shear free and undergo no normal displacement. In order to reduce the complexity of analysis each domain is approximated by a circle of effective diameter d_e, the perimeter of which is shear free and undergoes no radial movement and which has the same area as the actual domain. This assumption leads to a considerable simplification of the geometry of the problem, as shown in Fig. 7.3. The behaviour of the stone column and the clay is approximated by assigning to them elastic Young's moduli E_1, E_2 and Poisson's ratios ν_1, ν_2 res-

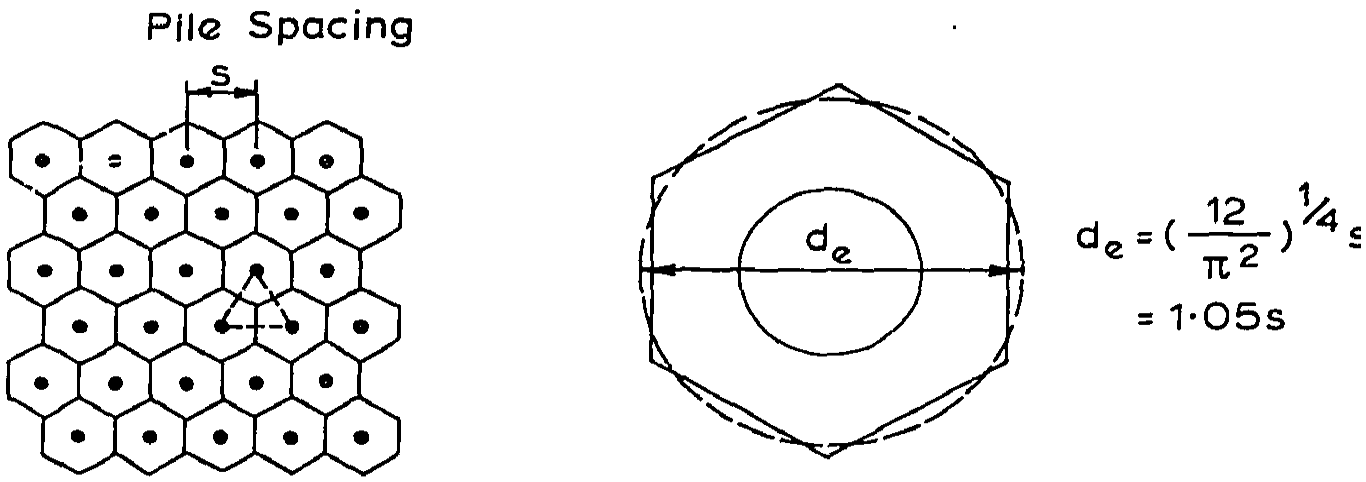

(a) Triangular Arrangement of Stone Columns

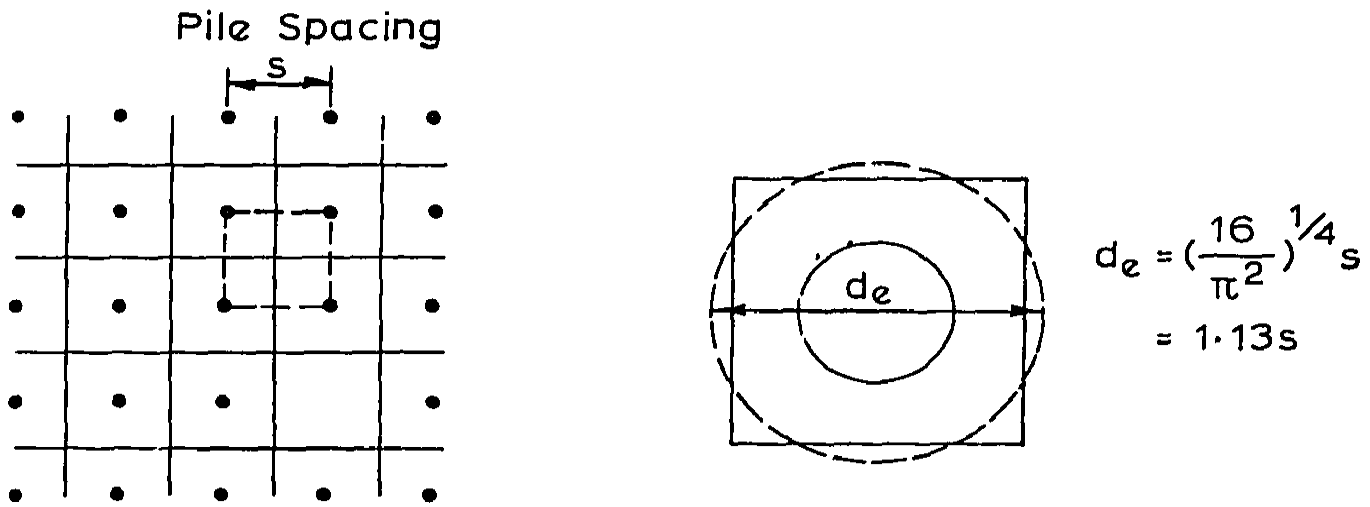

(b) Square Arrangement of Stone Columns

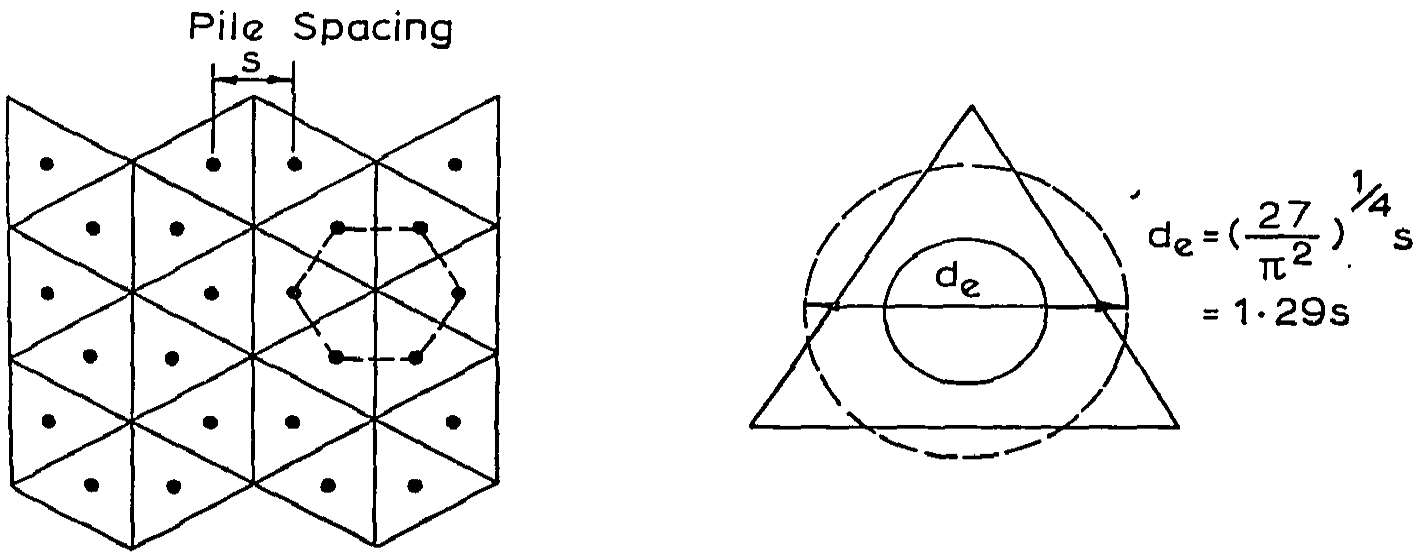

(c) Hexagonal Arrangement of Stone Columns

FIG. 7·2 VARIOUS PILE ARRANGEMENTS SHOWING THE DOMAIN OF INFLUENCE OF EACH COLUMN

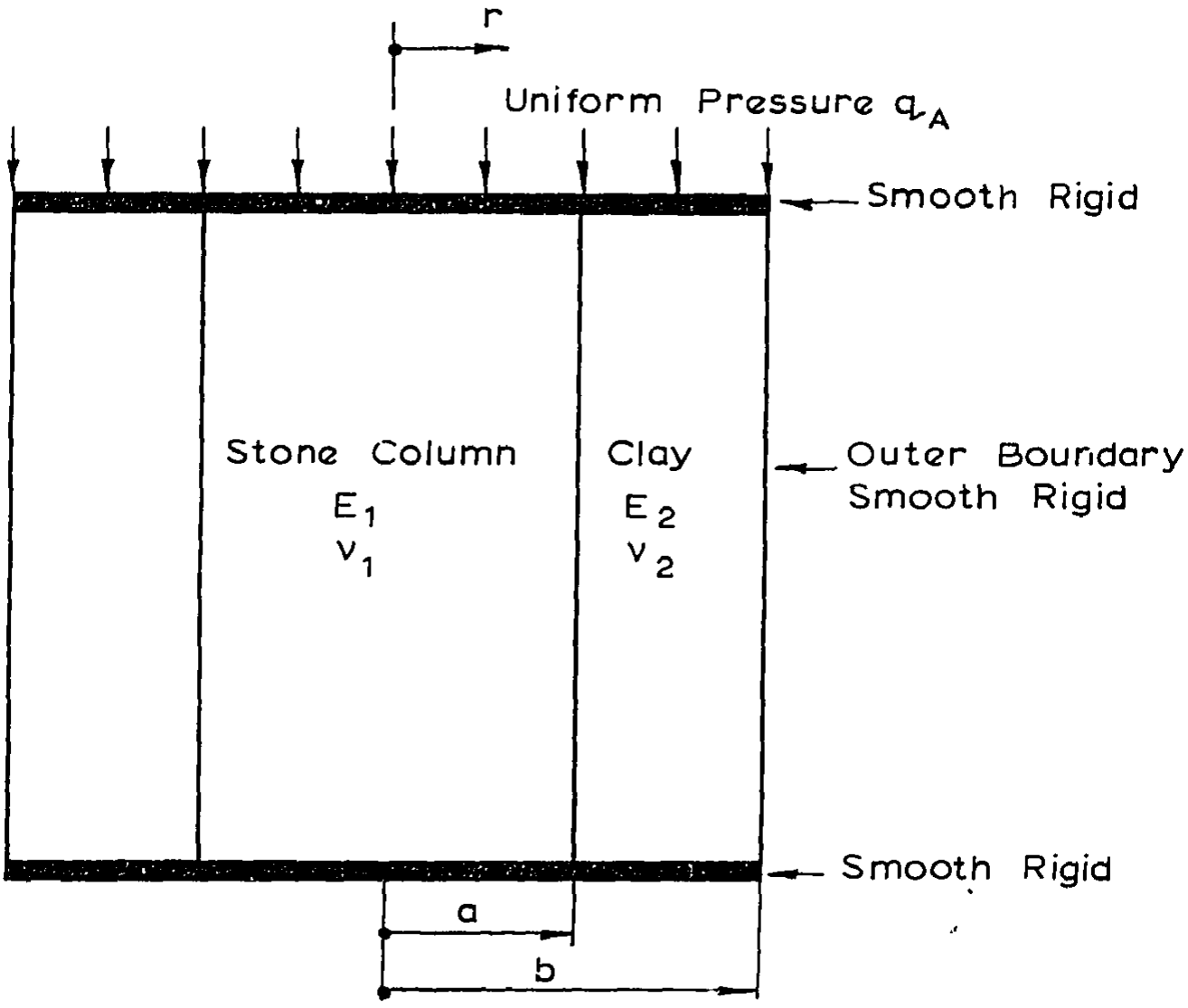

FIG. 7-3 DEFINITION OF TERMS FOR ANALYSIS OF EQUIVALENT CYLINDRICAL UNIT

pectively, where the elastic moduli are chosen to be representative of the particular stress range under consideration (Davis and Poulos, 1963; Lambe, 1964). The analysis of settlement then reduces to the analysis of the compression, of the cylindrical body shown in Fig. 7.3, between smooth (the raft) and rough (the substratum) plates, while laterally restrained by a smooth rigid wall.

Although the approximation of the actual domain by an equivalent circular domain has considerably simplified the analysis, an examination of the problem shows that a complete solution depends upon the five dimensionless parameters a/b, h/b, E_1/E_2, ν_1, ν_2.

Initially a finite element analysis was performed for representative values of these parameters. An examination of these results revealed that

(i) the vertical displacement was almost uniform on any horizontal plane and varied almost linearly from zero at the base to a maximum value at the surface

(ii) the shear stresses developed along the substratum were in general small

(iii) values of field quantities remote from the substratum were insensitive to wheter it was assumed to be perfectly rough or perfectly smooth.

These observations suggested that it might be possible to find an approximate solution to this problem, analytically.

7.2.2 Analytic Solution

As a first approximation it seems natural that the elastic body suffers no lateral strain; this will be called Solution A, and the stresses and displacements in regions 1, 2 are given below;

TABLE 7.1

SOLUTION A

A	Region 1	Region 2
ϵ_z	ϵ	ϵ
u_r	0	0
σ_r	$\lambda_1\epsilon$	$\lambda_2\epsilon$
σ_θ	$\lambda_1\epsilon$	$\lambda_2\epsilon$
σ_z	$(\lambda_1 + 2G_1)\epsilon$	$(\lambda_2 + 2G_2)\epsilon$

where it has been convenient to introduce Lame's parameters λ, G defined as

$$\lambda = \frac{E\nu}{(1+\nu)(1-2\nu)} \tag{7.1a}$$

$$G = \frac{E}{2(1+\nu)} = \text{Shear Modulus} \tag{7.1b}$$

and where

$$(\lambda + 2G) = \frac{1}{m_v} = \frac{1}{\text{Coefficient of Volume decrease}} \tag{7.1c}$$

$$\frac{\lambda}{\lambda+2G} = \frac{\nu}{1-2\nu} \tag{7.1d}$$

A comparison of solution A with numerical solutions revealed quite reasonable agreement, e.g. for a typical case where h/d = 10, b/a = 2 and E_1/E_2 = 20 (where d is the diameter of the columns = 2a), the error is 20%. The discrepancy is due to solution A not being exact since it implies a discontinuity of radial stress $\Delta\sigma_r = (\lambda_2 - \lambda_1)\varepsilon$ at the pile-soil interface.

In order to obtain an exact solution it is necessary to add to solution A, a second solution B, which corresponds to zero movement of the raft and the application of a radial traction equal and opposite to $\Delta\sigma_r$ at the pile-soil interface. This problem can be solved exactly if it is assumed that the substratum is perfectly smooth; for in this case the elastic cylinder is in a state of plane strain. Solution B is given in Table 7.2.

TABLE 7.2

SOLUTION B

B	Region 1	Region 2
ε_z	0	0
u_r	$+\delta\frac{r}{a}$	$\frac{a\delta}{r}\frac{(b^2 - r^2)}{b^2 - a^2}$
σ_r	$-2(\lambda_1 + G_1)\ \delta/a$	$\frac{2\delta a}{b^2-a^2}\ (\lambda_2 + G_2 + G_2\ \frac{b^2}{r^2})$
σ_θ	$-2(\lambda_1 + G_1)\ \delta/a$	$\frac{2\delta a}{b^2-a^2}\ (\lambda_2 + G_2 - G_2\ \frac{b^2}{r^2})$
σ_z	$-2\lambda_1\ \delta/a$	$2\lambda_2\ \frac{\delta a}{b^2-a^2}$

The value of δ (the radial displacement at the interface) is chosen so that when the two solutions are added the radial stress is

continuous across the pile-soil interface so that

$$\delta/a = F_1 \epsilon \tag{7.2a}$$

where

$$F_1 = \frac{(\lambda_1-\lambda_2)(b^2-a^2)}{2[a^2(\lambda_2+G_2-\lambda_1-G_1) + b^2(\lambda_1+G_1+G_2)]} \tag{7.2b}$$

The complete solution for a smooth substratum is obtained by addition of solutions A and B and is given below.

TABLE 7.3

SOLUTION FOR SMOOTH SUBSTRATUM - (C)

C	Region 1	Region 2
ϵ_z	ϵ	ϵ
u_r	$F_1 r\epsilon$	$[F_1 \frac{a^2}{r} \frac{(b^2-r^2)}{b^2-a^2}]\epsilon$
σ_r	$[\lambda_1 - 2(\lambda_1 + G_1)F_1]\epsilon$	$[\lambda_2 + \frac{2a^2F_1}{b^2-a^2} (\lambda_2 + G_2 + G_2 \frac{b^2}{r^2})]\epsilon$
σ_θ	$[\lambda_1 - 2(\lambda_1 + G_1)F_1]\epsilon$	$[\lambda_2 + \frac{2a^2F_1}{b^2-a^2} (\lambda_2 + G_2 - G_2 \frac{b^2}{r^2})]\epsilon$
σ_z	$[\lambda_1 + 2G_1 - 2\lambda_1 F_1]\epsilon$	$[\lambda_2 + 2G_2 + 2\lambda_2 \frac{F_1 a^2}{b^2-a^2}]\epsilon$

The relation between the strain ϵ and the average applied stress q_A can now be obtained by integrating the vertical stress across the soil surface and it is found that

$$q_A b^2 = [(\lambda_1 + 2G_1)a^2 + (\lambda_2 + 2G_2)(b^2 - a^2) - 2a^2(\lambda_1 - \lambda_2)F_1]\epsilon \tag{7.3a}$$

This may be alternatively written in the form

$$\varepsilon = F_2 \, \bar{m}_v \, q_A \tag{7.3b}$$

where $\bar{m}_v$ is the volume average of the compressibility defined by the relation

$$\frac{b^2}{\bar{m}_v} = \frac{a^2}{m_{v1}} + \frac{b^2-a^2}{m_{v2}} \tag{7.3c}$$

and where F_2 is a dimensionless factor

$$F_2 = \frac{1}{1 - \frac{2a^2}{b^2} (\lambda_1-\lambda_2) \, \bar{m}_v \, F_1} \tag{7.3d}$$

Solution C is of course not an exact solution for the situation where there is a perfectly rough base. However, as mentioned previously, numerical studies indicate that the surface vertical displacement, horizontal displacement and contact stresses are insensitive to the base condition. For example, when h/d = 5, where d is the diameter of the stone columns, and $d_e/d = 5$, which corresponds to a very shallow layer ($h/d_e = 1$), the discrepancy in surface vertical displacement and contact stresses between a finite element solution and the analytic solution is less than .5%. The discrepancy in surface horizontal displacement at the column-clay interface is 1.6%. Solution C can therefore be used with confidence to calculate these quantities.

This analytic approach has several advantages over a purely numerical approach. Firstly, the analytic solution is relatively simple

and can be calculated swiftly, in contrast a purely numerical approach would involve either, access to and the time consuming preparation of data for a finite element program; or the availability of a parametric study in the five dimensionless parameters a/b, h/b, E_1/E_2, ν_1, ν_2. Secondly, the inspection of the analytic solution reveals several important and interesting aspects of the problem, viz:

(i) The contact stress between the rigid raft and the soil is uniform over the pile and uniform over the soil:

$$\sigma_z = q_1 = [(\lambda_1+2G_1) - 2\lambda_1 F_1] F_2 \bar{m}_v q_A \qquad (7.4a)$$

for the pile

$$\sigma_z = q_2 = [(\lambda_2+2G_2) + 2\lambda_2 \frac{F_1 a^2}{b^2-a^2}] F_2 \bar{m}_v q_A \qquad (7.4b)$$

for the soil

This observation leads to a relatively simple computation of bending moments and shear forces in the raft. It is worth noting that Tanimoto (1973) adopted uniform contact stress distributions for bearing capacity and settlement computations for structures founded on clay stabilised by granular piles.

(ii) The stress state in the pile is triaxial:

$$\sigma_z = q_1 \qquad (7.4c)$$

$$\sigma_r = \sigma_\theta = \frac{\lambda_1 - 2(\lambda_1 + G_1)F_1}{\lambda_1 + 2G_1 - 2\lambda_1 F_1} q_1 \qquad (7.4d)$$

Solution C can also be used with a little modification to obtain solutions when the clay is undrained but the stone columns drained by adopting a value of $E_2 = E_{u2}$ (the undrained modulus) and allowing $\nu_2 \to \nu_u = \frac{1}{2}$. It is then found that solution C takes the form D which is given in Table 7.4.

TABLE 7.4

SOLUTION D - (CLAY UNDRAINED)

D	Region 1	Region 2
ε_z	ε	ε
u_r	$-r \frac{(b^2-a^2)}{2a^2} \varepsilon$	$\frac{r^2-b^2}{2r} \varepsilon$
σ_r	$[-G_1 + (\lambda_1 + G_1) \frac{b^2}{a^2}] \varepsilon$	$[F_3 - G_2 (1 + \frac{b^2}{r^2})] \varepsilon$
σ_θ	$[-G_1 + (\lambda_1 + G_1) \frac{b^2}{a^2}] \varepsilon$	$[F_3 - G_2 (1 - \frac{b^2}{r^2})] \varepsilon$
σ_z	$[2G_1 + \lambda_1 \frac{b^2}{a^2}] \varepsilon$	$[F_3 + 2G_2] \varepsilon$

where $F_3 = G_2 - G_1 + (\lambda_1 + G_1 + G_2) \frac{b^2}{a^2}$ (7.5a)

and $q_A = [3 (G_1 - G_2) \frac{a^2}{b^2} + (\lambda_1 + G_1 + G_2) \frac{b^2}{a^2} - 2(G_1 - G_2)] \varepsilon$ (7.5b)

A parametric study has been performed using solutions C and D to investigate the effect of the dimensionless parameters a/b, h/b, E_1/E_2, ν_1 and ν_2 on the stresses and displacements within the cylindri-

cal unit. The solutions are not affected by the dimensionless parameter h/b, due to the smooth base; furthermore, this parameter is relatively unimportant for the rough base. The stone column material deforms under drained conditions; a representative value of $\nu_1 = 0.3$ has been adopted for these analyses.

In Fig. 7.4 the vertical strain is plotted against a/b for E_1/E_2 equal to 10, 20, 30 and 40 and $\nu_1 = \nu_2 = 0.3$. The quantity $\varepsilon_z/q_A m_{v2}$ is the reduction in settlement of the clay due to the presence of the stone columns. Thus, when a/b is zero (no stone columns) there is no reduction in settlement whereas if a/b is one the clay is completely replaced by stone columns and the reduction in settlement is the ratio of the compressibilities of the stone column material and the clay.

Under undrained conditions the Poisson's ratio of the clay ν_2 is ½ whereas under drained conditions ν_2 would normally lie between .25 - .45. In Fig. 7.5 the ratio of the vertical strain of the reinforced clay to the vertical strain when $\nu_2 = .3$ (Fig. 7.4), is plotted against the complete range of Poisson's ratios ν_2. Therefore, for a particular Poisson's ratio ν_2; interpolation of Fig. 7.5 gives a correction factor to be applied to the strain obtained from Fig. 7.4. Thus, the undrained and total final settlements can be calculated. The results also illustrate the relative importance of the consolidation settlement compared with the initial undrained settlement. The consolidation settlement is reduced by decreasing the spacings of the piles.

The effect of the ratio of stiffnesses E_1/E_2 on the vertical stress in the stone column is shown in Fig. 7.6 when $\nu_1 = \nu_2 = 0.3$.

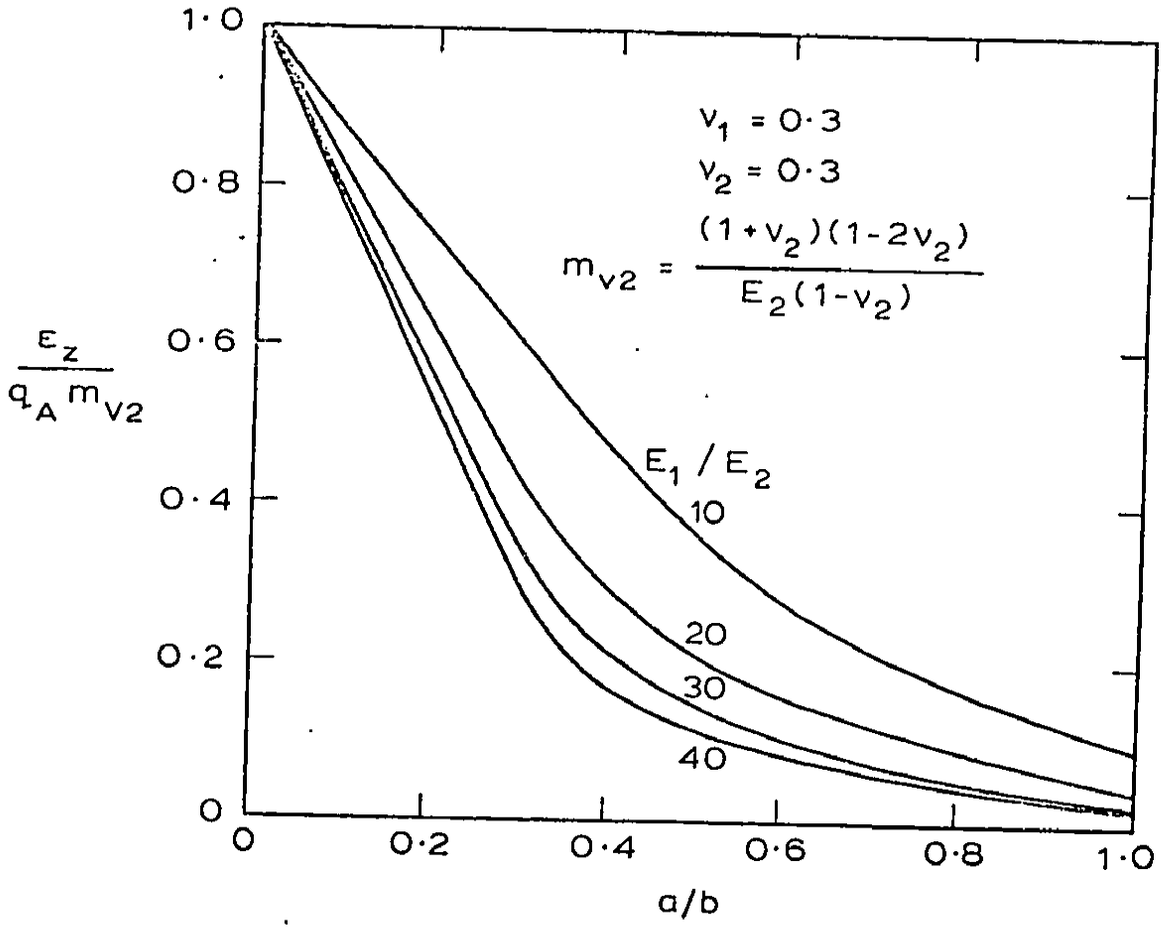

FIG. 7·4 VERTICAL STRAIN OF PILE – SOIL UNIT WITH VARYING SPACING

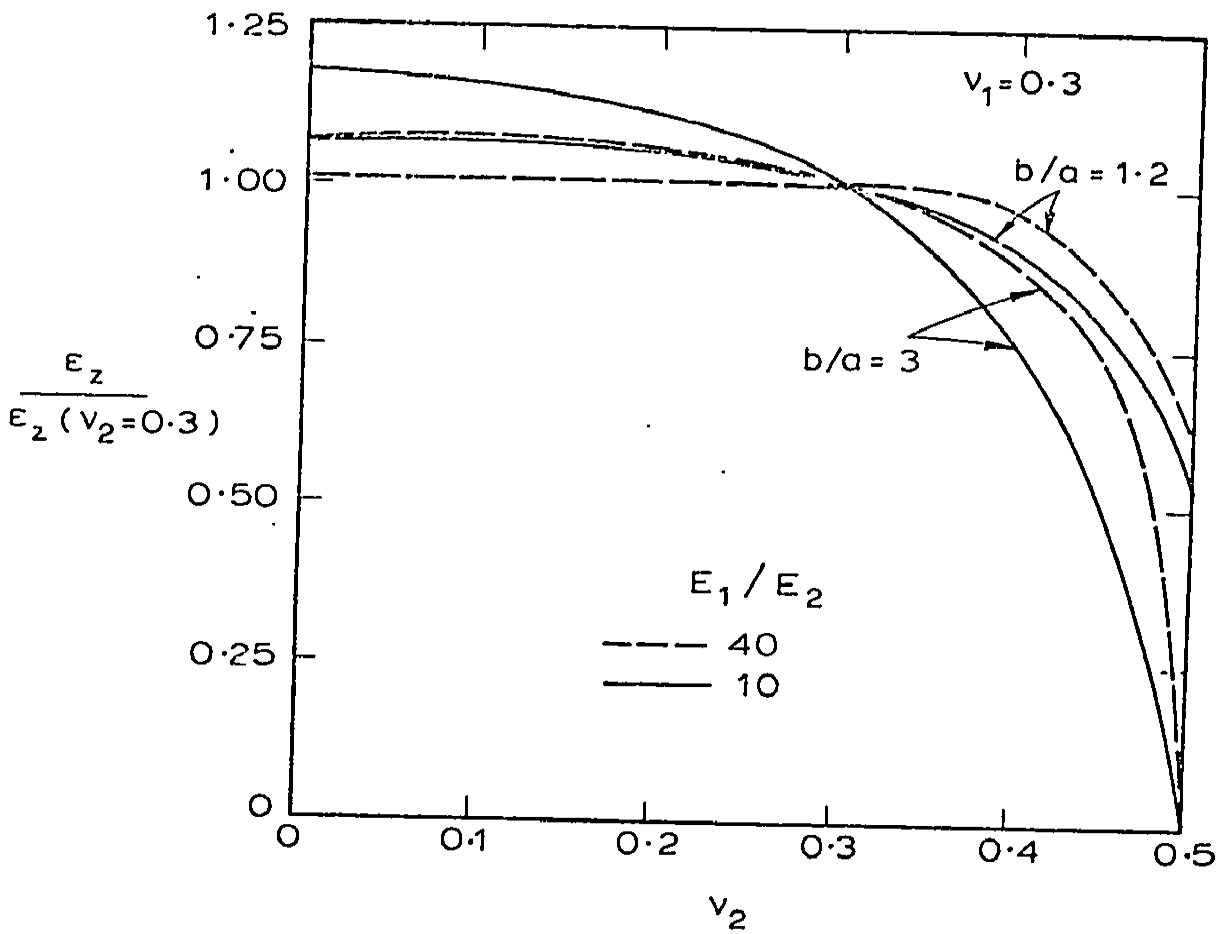

FIG. 7·5 RATIO OF STRAINS FOR CALCULATING SETTLEMENTS FOR THE COMPLETE RANGE OF POISSON'S RATIOS ν_2

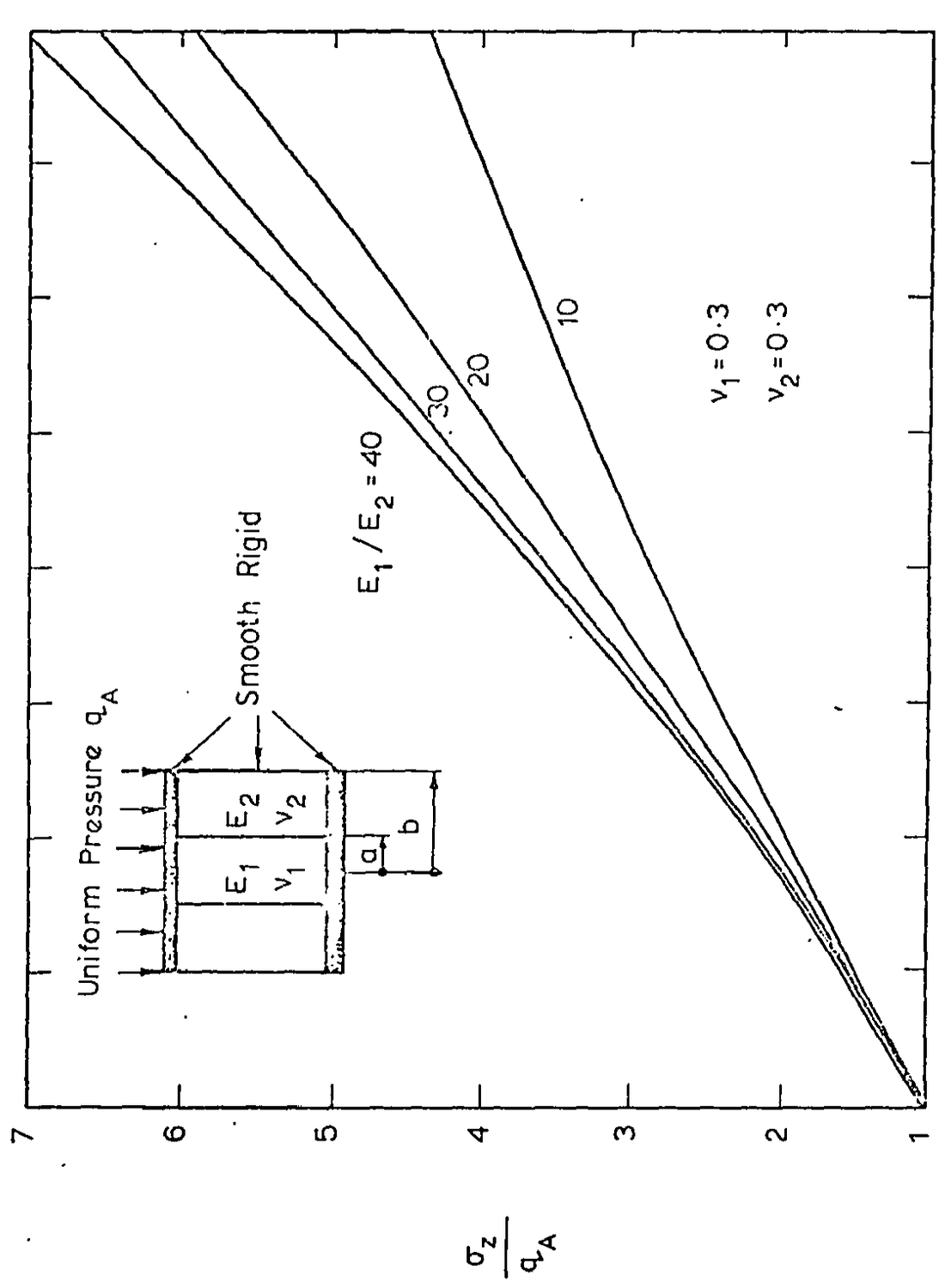

FIG. 7·6 VARIATION OF VERTICAL STRESS IN STONE COLUMN WITH b/a

The stress concentration on the column initially increases rapidly with E_1/E_2. These results suggest that the columns are used most efficiently when the raft is rigid. For a flexible raft the load is shared in the ratio of the areas of the stone columns and natural clay. As the flexibility of the raft reduces the stress in the stone column increases which results in more load being carried by the stiffer material. The ratio of the vertical to horizontal stresses in the stone column are shown in Fig. 7.7. These ratios in stress will cause confined yielding within the pile in which there is a triaxial stress state. Therefore, this confirms the approach suggested by Greenwood (1970) for estimating the ultimate load of a single column which was discussed in Chapter 2. In Chapter 5 it has been shown that although confined yielding occurs within the pile and the surrounding clay, the increase in settlement due to yielding is not significant. Thus, the results from the elastic theory are still applicable when an appropriate stiffness ratio E_1/E_2 is assigned to a given stress range. The possibility of passive failure of the clay can be estimated from the radial displacement at the column-clay interface (Fig. 7.8).

When the load is initially applied to the reinforced clay the contact stress on the clay may be greater than on the stone column. This occurs because the clay is undrained and thus behaves as an incompressible material. As the excess pore pressures are dissipated by radial flow to the stone columns, the relative stiffness of the stone columns and clay changes; under drained conditions the soil skeleton of the clay is less stiff than the granular material of the stone columns. The contact stress on the stone columns is now greater than on the clay. This 'swap-over' in the magnitude of contact stresses

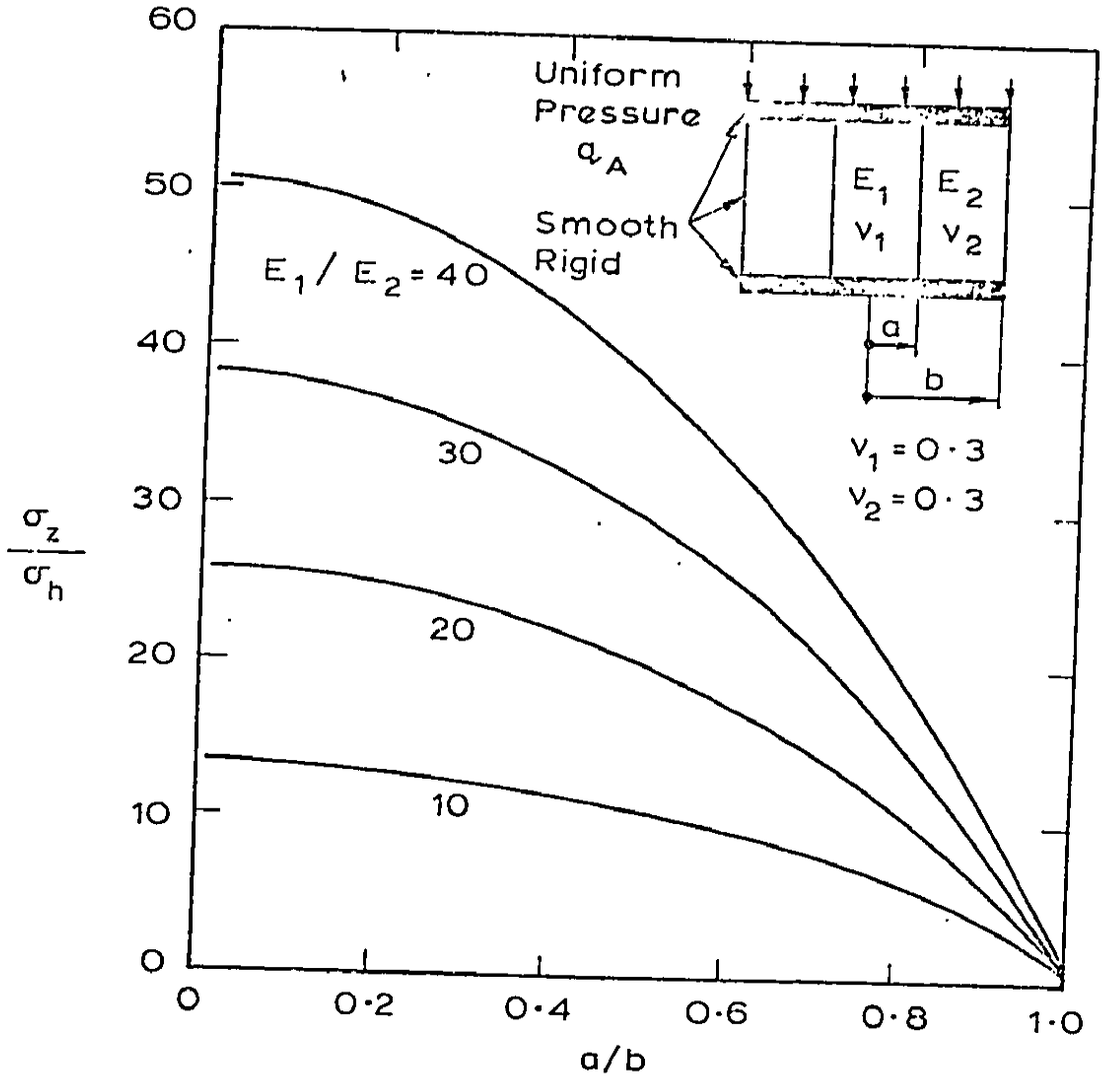

FIG. 7·7 RATIO OF VERTICAL TO HORIZONTAL STRESSES IN THE STONE COLUMN

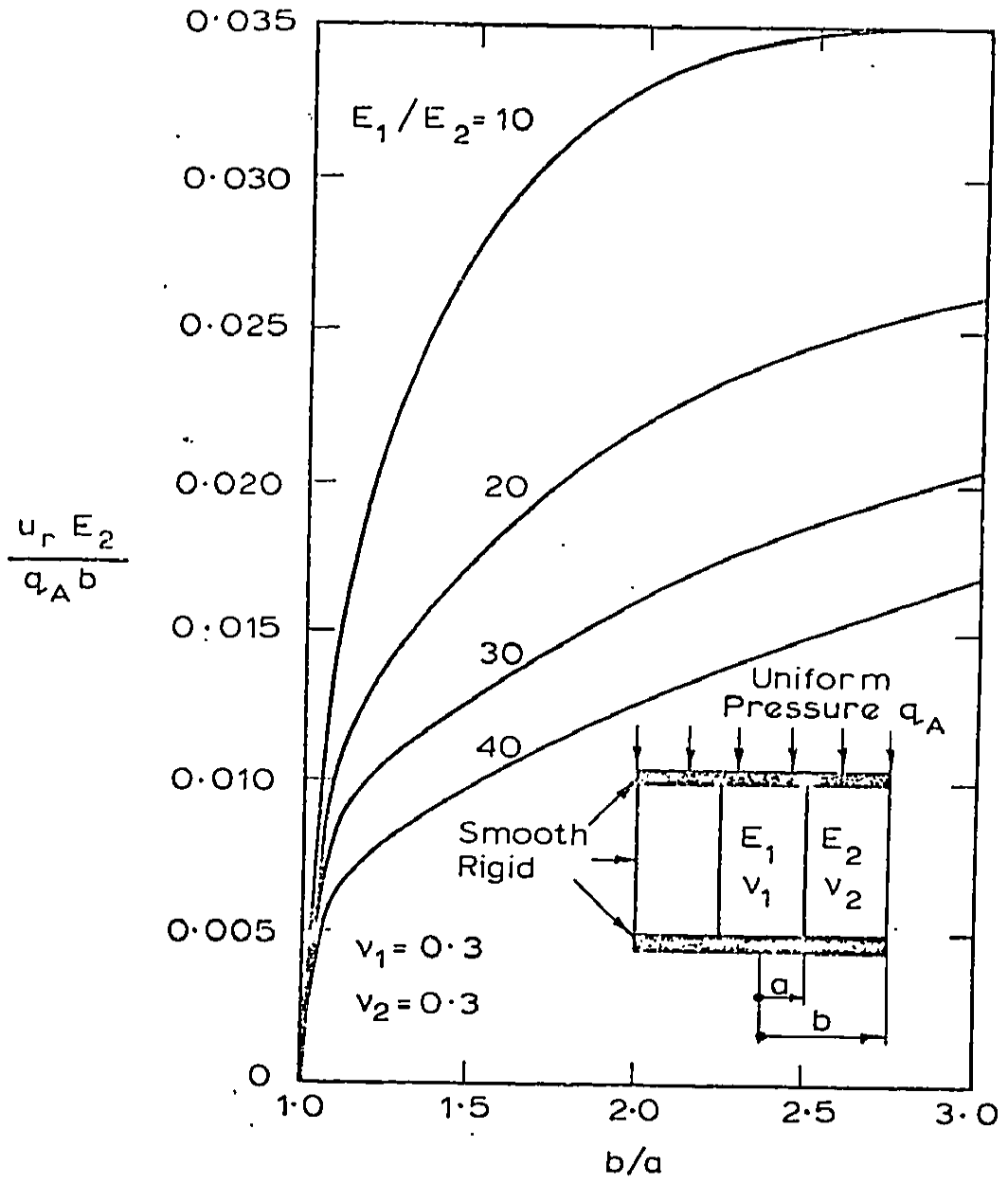

FIG. 7·8 THE RADIAL DISPLACEMENT AT THE PILE-SOIL INTERFACE

from the undrained to drained conditions is illustrated in Fig. 7.9 for b/a = 2. Therefore, as consolidation occurs the moment and shear distributions in the raft foundation alter. However, when the clay is deformed under undrained conditions, the contact stress is nearly uniform and thus the moments and shears are small when compared to those for drained conditions.

7.2.3 Effect of Domain of Influence on Solutions

The concept of equivalent diameter is widely used in Geomechanics and has led to a considerable simplification of the analysis of settlement for rigid rafts and flexible foundations (Chapter 5). It is interesting to test its validity in this context. To do this, consider the situation shown in Fig. 7.10 of a smooth base and the piles having a square domain of influence. The solution can again be obtained by superimposing two solutions; the first corresponds to uniform vertical strain and no horizontal movement, ie. solution A, and involves a discontinuity of radial stress at the pile-soil interface. The second is the plane strain solution of the body shown in Fig. 7.11 which is subjected to a radial traction equal in magnitude but opposite in sign to that induced by the first solution. It is not possible to find an analytic solution to this second problem for a non-circular domain of influence; it is however possible to find a numerical solution using a standard two dimensional finite element analysis. Once this analysis has been performed, the complete solution is given in Table 7.5.

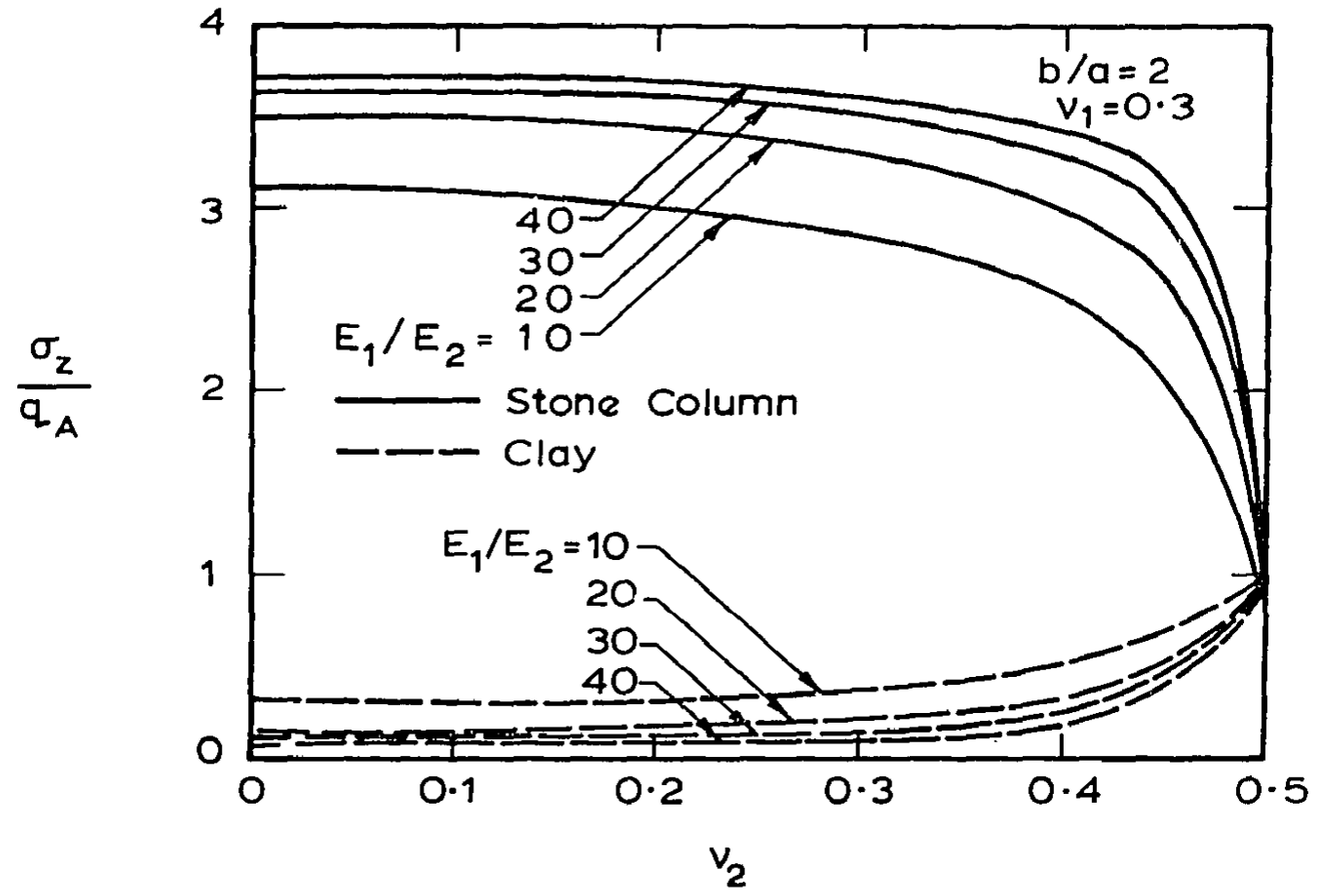

FIG. 7·9 VARIATION OF VERTICAL STRESSES WITH POISSON'S RATIO OF CLAY

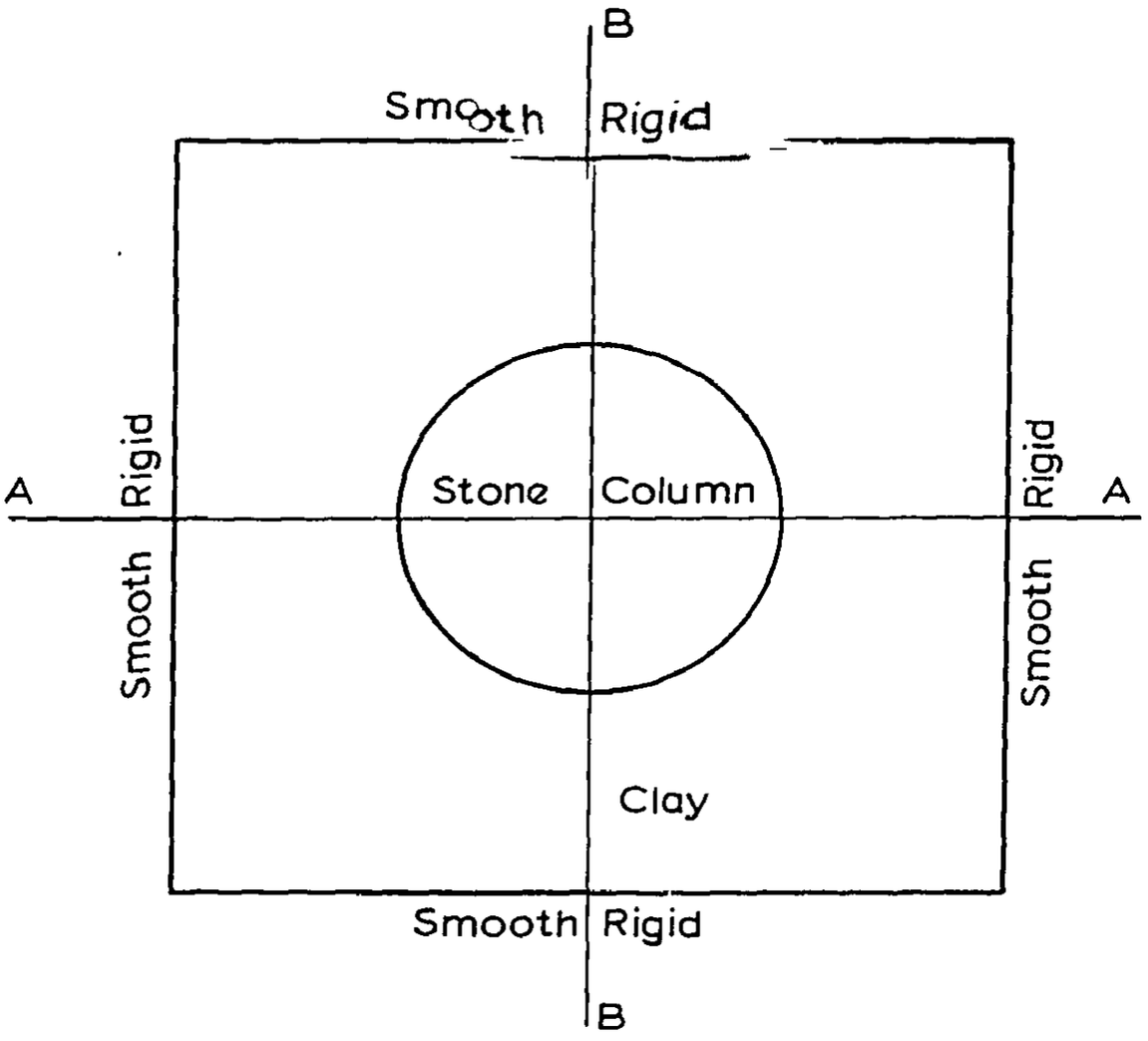

(a) Domain of Influence of Stone Column

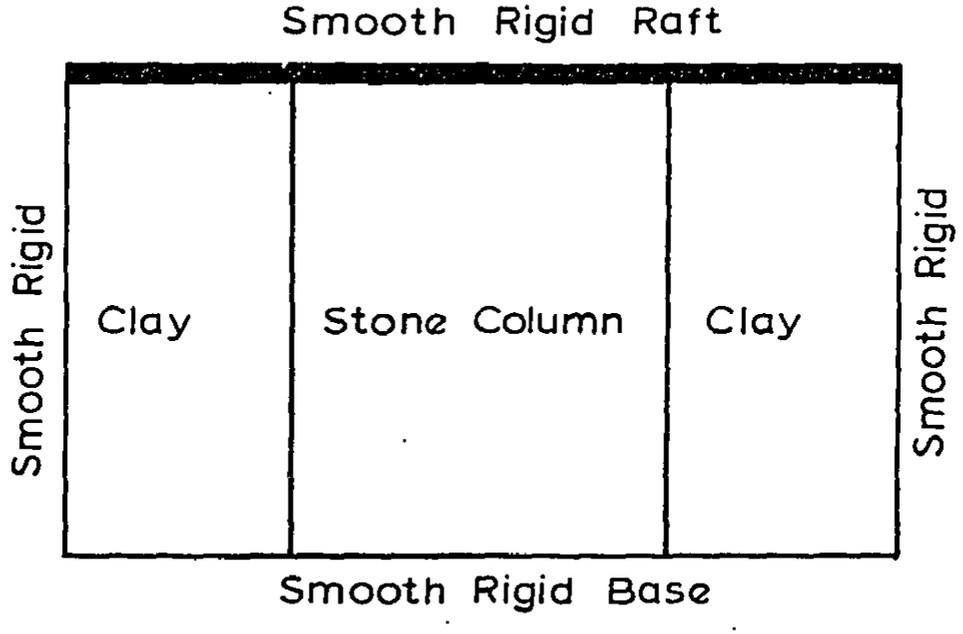

(b) Section AA: Compression of Stone Column by a Smooth Rigid Raft

FIG. 7·10 PROBLEM DEFINITION

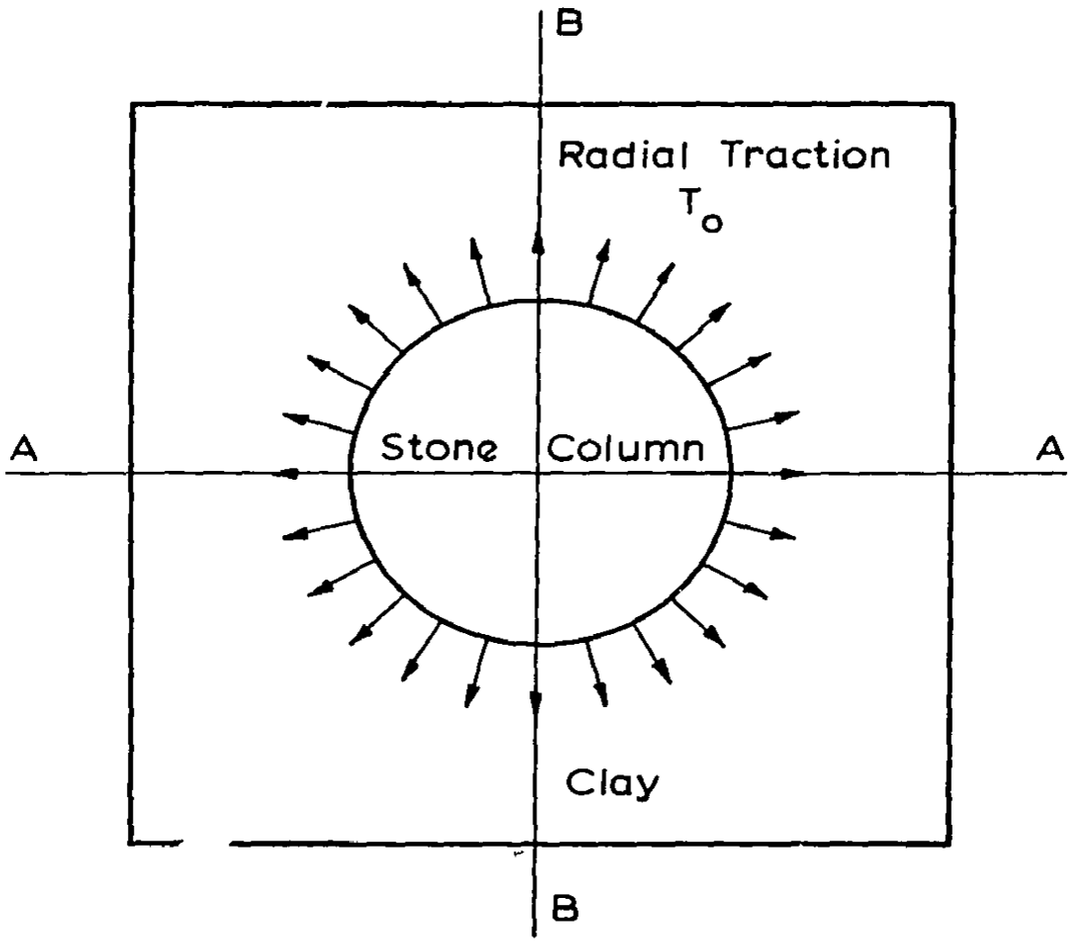

FIG. 7·11 TYPICAL SECTION FOR SOLUTION OF THE PLANE STRAIN PROBLEM

TABLE 7.5

SOLUTION FOR NON-CIRCULAR DOMAIN OF INFLUENCE

	Region 1	Region 2
ε_z	ε	ε
u_x	$f\, u_{x1}^*$	$f\, u_{x2}^*$
u_y	$f\, u_{y1}^*$	$f\, u_{y2}^*$
σ_x	$\lambda_1\varepsilon + f\, \sigma_{x1}^*$	$\lambda_2\varepsilon + f\, \sigma_{x2}^*$
σ_y	$\lambda_1\varepsilon + f\, \sigma_{y1}^*$	$\lambda_2\varepsilon + f\, \sigma_{y2}^*$
σ_z	$(\lambda_1 + 2G_1)\varepsilon + f\, \sigma_{z1}^*$	$(\lambda_2 + 2G_2)\varepsilon + f\, \sigma_{z2}^*$
σ_{xy}	$f\, \sigma_{xy_1}^*$	$f\, \sigma_{xy_2}^*$

$$f = \frac{(\lambda_1 - \lambda_2)\varepsilon}{T_o}$$

where u_{x1}^*, u_{y1}^*, σ_{x1}^* ..... denote values of displacements and stresses obtained by the finite element analysis of problem 2 with an outward radial traction T_o applied at the pile soil interface.

Once a numerical solution to problem 2 has been found, the average load acting over the raft can be calculated by integrating the vertical stress whereupon remembering that $\sigma_{z1}^* = \nu_1(\sigma_{x1}^* + \sigma_{y1}^*)$ and $\sigma_{z2}^* = \nu_2(\sigma_{x2}^* + \sigma_{y2}^*)$ under conditions of plane strain it is found that

$$\begin{aligned} q_A \times \text{Area of Domain} = {} & (\lambda_1+2G_1)\varepsilon \times \text{Area of Region 1} \\ & + (\lambda_2+2G_2)\varepsilon \times \text{Area of Region 2} \\ & + f\left[\iint_{\text{Region 1}} \sigma_{z1}^*\, dA + \iint_{\text{Region 2}} \sigma_{z2}^*\, dA\right] \end{aligned} \qquad (7.6)$$

The results for the particular situation in which $E_1/E_2 = 10$, $\nu_1 = \nu_2 = 0.3$ and $d_e/d = 2$ have been obtained. The finite element mesh used for the plane strain analysis in which a radial traction is applied to the column is shown in Fig. 7.12. Only a quarter of the square need be considered. The solution assuming this square has an equivalent circular domain of influence (solution C) has been compared with the solution obtained from the procedure outlined above for a non-circular domain of influence. Contours of percentage difference between the two solutions, for the contact stresses have been plotted in Fig. 7.13. The maximum discrepancy occurs at the interface of the column and clay diagonally opposite the corner. The agreement between the two solutions is therefore very good which indicates that solution C can be used for non-circular domains of influence using the equivalent diameter (Fig. 7.2).

7.3 ANALYSIS OF THE RAFT

In this section the reaction distributions derived in the previous section will be used to calculate the bending moments and shear forces within the raft.

7.3.1 Method of Analysis

If the vertical deflection of the raft is w then from Timoshenko and Woinowsky-Krieger (1959),

$$\nabla^4 w = p/D \qquad (7.7)$$

where $p = q_A - q_R$ is the net load distribution acting on the raft

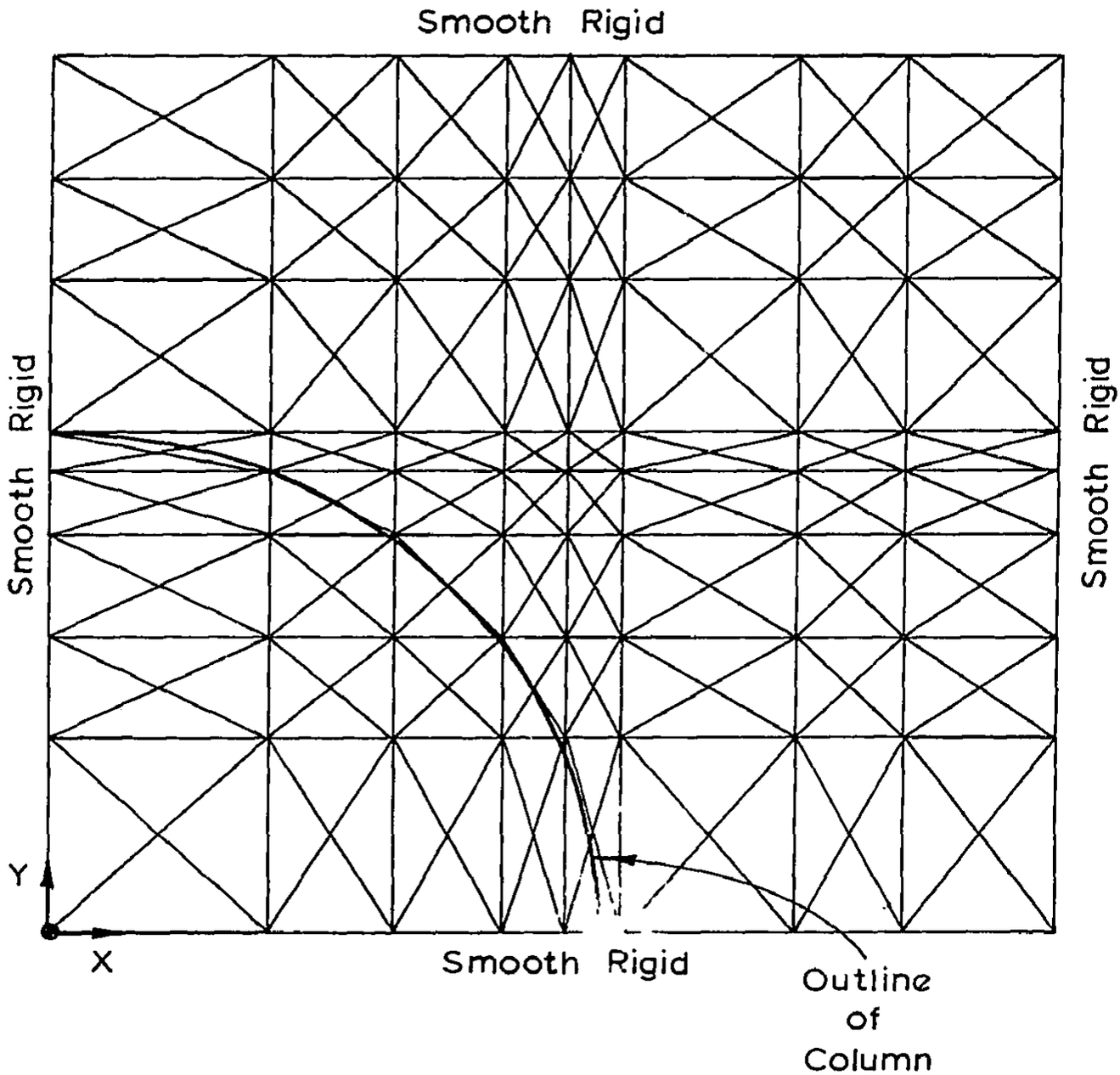

FIG. 7·12 FINITE ELEMENT MESH USED IN CHECK OF STRESSES FROM CYLINDER THEORY

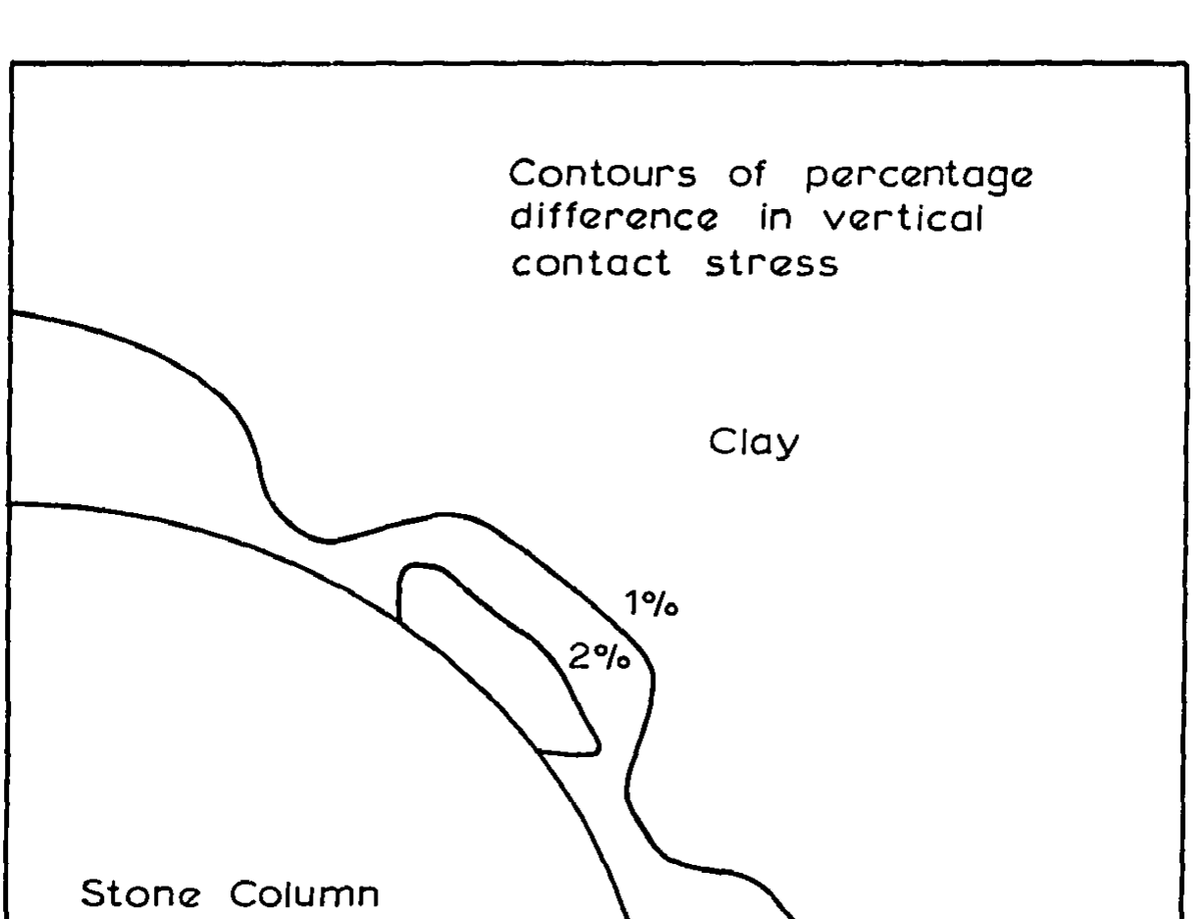

FIG. 7.6 SCHEMATIC DIAGRAM OF THE CONTOURS OF ERROR IN THE VERTICAL STRESSES

q_A = the pressure exerted by applied loads

q_R = the reaction pressure exerted by the underlying columns and soil

D = flexural rigidity of the raft.

The bending moments M_x, M_y and M_{xy} and the shear forces Q_x, Q_y are then given by

$$M_x = -D\left(\frac{\partial^2 w}{\partial x^2} + \nu \frac{\partial^2 w}{\partial y^2}\right) \qquad (7.8a)$$

$$M_y = -D\left(\frac{\partial^2 w}{\partial y^2} + \nu \frac{\partial^2 w}{\partial x^2}\right) \qquad (7.8b)$$

$$M_{xy} = D(1-\nu) \frac{\partial^2 w}{\partial x \partial y} \qquad (7.8c)$$

$$Q_x = -\frac{\partial}{\partial x} (\nabla^2 w) \qquad (7.8d)$$

$$Q_y = -\frac{\partial}{\partial y} (\nabla^2 w) \qquad (7.8e)$$

where ν is the Poisson's ratio of the raft.

There is some difficulty in applying these formulae to the case of a rigid raft ($D \to \infty$). This may be overcome by observing that for a specified net pressure $p = q_A - q_R$ the bending moments and shear forces are independent of D and thus that these values apply when $D \to \infty$, provided of course that the correct net load p, viz. that corresponding to rigid movement of the raft and soil, is used.

The concept of a domain of influence applies equally well to the raft as to the soil. As before, the domain of influence may be an equalateral triangle, a square or a regular hexagon. The boundaries

of the domain of influence will experience no shear and will have zero slope in a direction normal to the boundary.

It was shown in the previous section that the contact stress between the pile and raft and the contact stress between the soil and raft is very nearly constant. In many practical situations the applied load will be uniformly distributed over the raft and attention will be restricted to this case. Thus, if p_1 is the net pressure acting on the raft immediately above the pile and p_2 is the net pressure acting on the raft immediately above the surrounding soil, it follows from equilibrium that:

$$p_2 = \frac{p_1}{(A_p/A_D - 1)} \tag{7.9}$$

where A_p is the area of the pile

and A_D is the area of the domain of influence.

The domain of influence is approximated by a circle as was the case for the analysis of settlement. This assumption simplifies the problem considerably and it is possible, because of the circular symmetry, to obtain a simple analytic solution.

For circular symmetric deflections equation 7.7 becomes

$$\frac{1}{r}\frac{d}{dr}\, r\{\frac{d}{dr}\,[\frac{1}{r}\frac{d}{dr}\,(r\frac{dw}{dr})]\} = \frac{p_1}{D} \qquad 0 \leq r \leq a \tag{7.10a}$$

$$= \frac{p_1 a^2}{D(b^2-a^2)} \qquad a \leq r \leq b \tag{7.10b}$$

It may be shown that the solution of this equation which satisfies the

condition of zero normal slope $\partial w/\partial r$ at the outer boundary and which satisfies the continuity requirement that w and its first three derivatives must be continuous across r = a, leads to the expressions for moments and shear given in Table 7.6.

The expressions given in Table 7.6 provide a convenient method for evaluating the bending moments and shear force in the raft. However, before these may be used with any confidence it is necessary to check that the approximation of the actual domain of influence by an equivalent circle has not induced any significant error.

In order to do this consider the rectangular domain of influence, $|x| \leq A$; $|y| \leq B$ shown in Fig. 7.14. Since the net loading function p is periodic with periods π/A in the x direction and period π/B in the y direction the net load distribution can be expressed as a double Fourier series having the form:

$$p = \sum_{n=0}^{\infty} \sum_{m=0}^{\infty} \varepsilon_{mn} P_{mn}(A,B) \; A. \; B. \cos \alpha_m x \cos \beta_n y \qquad (7.11)$$

where $\varepsilon_{00} = \frac{1}{4}$

$\varepsilon_{m0} = \frac{1}{2}$ $\quad m \neq 0$

$\varepsilon_{on} = \frac{1}{2}$ $\quad n \neq 0$

$\varepsilon_{mn} = 1$ $\quad m \neq 0, \; n \neq 0$

and $\alpha_m = m \pi/A$

$\beta_n = n \pi/B$

Expressions for the coefficients $P_{mn}(A,B)$, when the net pressure has a constant value p_1 above the piles and the constant value p_2 =

TABLE 7.6

MOMENTS AND SHEARS FOR CIRCULAR DOMAIN OF INFLUENCE

	Region 1 $0 \leq r \leq a$	Region 2 $a \leq r \leq b$
$\frac{-16\ M_r}{p_1\ a^2}$	$(3+\nu)\ \frac{r^2}{a^2} + (1+\nu)\left(1 - \frac{4b^2}{b^2-a^2}\ \ell n\ \frac{b}{a}\right)$	$-\left[(3+\nu)\ \frac{r^2-2b^2}{b^2-a^2} + \frac{a^2b^2(1-\nu)}{r^2(b^2-a^2)} + \frac{(1+\nu)}{b^2-a^2}\ (a^2+b^2-4b^2\ell n\ \frac{r}{b})\right]$
$\frac{-16\ M_t}{p_1\ a^2}$	$(3\nu+1)\ \frac{r^2}{a^2} + (1+\nu)\left(1 - \frac{4b^2}{b^2-a^2}\ \ell n\ \frac{b}{a}\right)$	$-\left[(3\nu+1)\frac{(r^2-2b^2)}{(b^2-a^2)} - \frac{a^2b^2(1-\nu)}{r^2(b^2-a^2)} + \frac{(1+\nu)}{(b^2-a^2)}\ (a^2+b^2-4b^2\ell n\ \frac{r}{b})\right]$
$\frac{Q_r}{p_1\ a}$	$\frac{r}{2a}$	$\frac{1}{2}\ \frac{a}{r}\ \left[1 - \frac{r^2-a^2}{b^2-a^2}\right]$

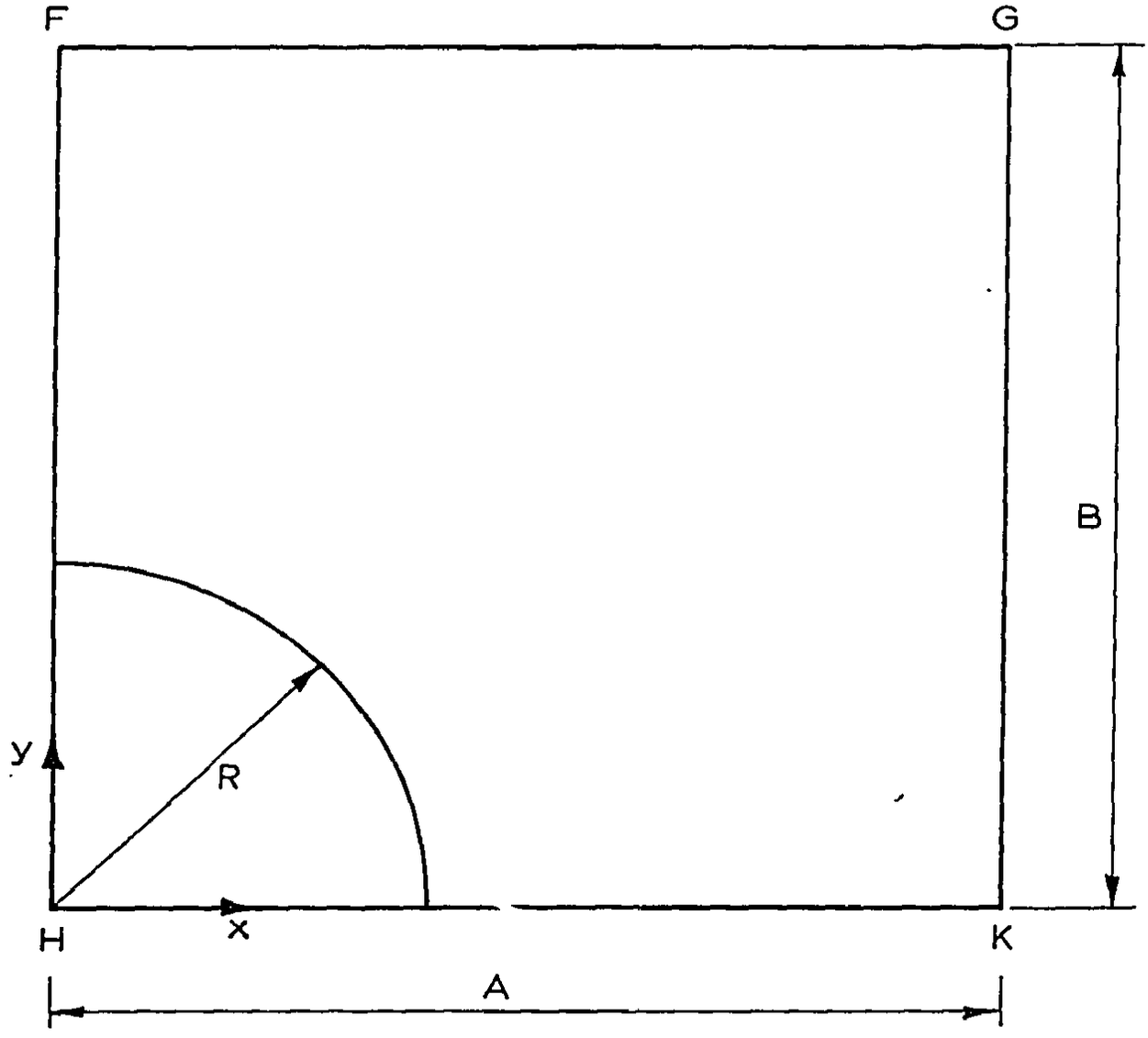

FIG. 7·14 DEFINITION OF TERMS FOR ANALYSIS OF MOMENTS IN A SQUARE DOMAIN OF INFLUENCE

$p_1 A_p/(A_D - A_p)$ above the soil, are given below for the case of a rectangular pile $|x| \leq c$, $|y| \leq d$ and a circular pile $r \leq R$:

$$P_{00} = 0 \text{ (since the net-pressure must be self equilibrating)} \quad (7.12a)$$

$$P_{mn} = (p_1 - p_2) Q_{mn} \quad (7.12b)$$

TABLE 7.7

Case	Q_{mn} $(m,n) \neq 0,0$
Rectangular Pile $\|x\| \leq c$, $\|y\| \leq d$	$\frac{4cd}{AB} \frac{\sin \alpha_m c}{\alpha_m c} \cdot \frac{\sin \beta_n d}{\beta_n d}$
Circular Pile $r \leq R$	$\frac{\pi R^2}{AB} \cdot 2 \frac{J_1(\gamma_{mn} R)}{(\gamma_{mn} R)}$

where $\gamma_{mn} = \sqrt{\alpha_m^2 + \beta_n^2}$ (7.12c)

and J_1 is the Bessel function of the first order.

The deflection of the plate can now be written in the form

$$w = w_o + \frac{p_1 - p_2}{D} \sum_{m=0}^{\infty} \sum_{n=0}^{\infty} \frac{\varepsilon_{mn} Q_{mn}}{\gamma_{mn}^4} (\cos \alpha_m x \cos \beta_n y - 1) \quad (7.13)$$

where w_o is the deflection at the origin, which can be determined from the deflection of the underlying soil. Substitution of equation 7.13 into equation 7.7 leads to the expressions for moments and shears given in Table 7.8. These expressions can be used to calculate moments and shears for a square domain of influence by taking A = B = s. They may also be used to calculate these quantities for a hexagonal domain of influence, as follows. Referring to Fig. 7.2(c) it can be seen that the

TABLE 7.8

$N_x = \frac{M_x}{p_1-p_2}$	$\sum_{m=0}^{\infty}\sum_{n=0}^{\infty} \varepsilon_{mn} Q_{mn} \frac{(\alpha_m^2+\nu\beta_n^2)}{\gamma_{mn}^4} \cos \alpha_m x \cos \beta_n y$
$N_y = \frac{M_y}{p_1-p_2}$	$\sum_{m=0}^{\infty}\sum_{n=0}^{\infty} \varepsilon_{mn} Q_{mn} \frac{(\nu\alpha_m^2+\beta_n^2)}{\gamma_{mn}^4} \cos \alpha_m x \cos \beta_n y$
$N_{xy} = \frac{M_{xy}}{p_1-p_2}$	$\sum_{m=0}^{\infty}\sum_{n=0}^{\infty} \varepsilon_{mn} Q_{mn} \frac{\alpha_m \beta_n (1-\nu)}{\gamma_{mn}^4} \sin \alpha_m x \sin \beta_n y$
$Q_x = \frac{R_x}{p_1-p_2}$	$-\sum_{m=0}^{\infty}\sum_{n=0}^{\infty} \varepsilon_{mn} Q_{mn} \frac{\alpha_m}{\gamma_{mn}^4} \sin \alpha_m x \cos \beta_n y$
$Q_y = \frac{R_y}{p_1-p_2}$	$-\sum_{m=0}^{\infty}\sum_{n=0}^{\infty} \varepsilon_{mn} Q_{mn} \frac{\beta_m}{\gamma_{mn}^2} \cos \alpha_m x \sin \beta_n y$

net load exerted on the raft can be considered to be composed of a uniform pressure (p_1-p_2) over the piles with centres $(\pm ns, \pm m\sqrt{3}\,s)$ and a uniform pressure (p_1-p_2) over piles with centres $(\frac{s}{2} \pm n\,s, \frac{\sqrt{3}\,s}{2} \pm ms)$ together with a uniform pressure p_2 over the entire raft. This leads to the following expressions for moments and shears

$$M_x = (p_1-p_2)\,[N_x' + N_x''] \qquad (7.14a)$$

$$M_y = (p_1-p_2)\,[N_y' + N_y''] \qquad (7.14b)$$

$$M_{xy} = (p_1-p_2)\,[N_{xy}' + N_{xy}''] \qquad (7.14c)$$

$$Q_x = (p_1-p_2)\,[R_x' + R_x''] \qquad (7.14d)$$

$$Q_y = (p_1-p_2)\,[R_y' + R_y''] \qquad (7.14e)$$

where $N_x' = N_x(x, y, s/2, \frac{\sqrt{3}}{2} s)$ (7.14f)

$N_x'' = N_x(x + \frac{s}{2}, y + \frac{\sqrt{3}}{2} s, s/2, \frac{\sqrt{3}}{2} s)$ etc. (7.14g)

and $p_2 = - p_1 A_p/(A_D - A_p)$ (7.14h)

$= - p_1 A_p/(\frac{\sqrt{3} s^2}{16} - A_p)$

Similar expressions involving the superposition of four terms can be found for the triangular domain of influence.

7.3.2 Effect of the Domain of Influence on the Moment and Shear Distributions Across the Raft

An investigation of the effects of the domain of influence on the moment and shear force distributions was made using the solutions presented in the previous section. Initially a comparison was made between the distribution of moments obtained using the solution for a circular domain of influence when $d_e/d = 1.5$ and those obtained from an analysis of the equivalent square domain of influence for the edge HK (Fig. 7.14).

Firstly, the pile was assumed to be rectangular as these solutions are more easily obtainable than those for a circular pile. Along the edge HK the moment M_{xy} is zero and thus M_x and M_y are principal moments. The comparison showed that the distribution of moments M_r and M_x are approximately the same. However, the distributions of M_t and M_y are considerably different with the sign of the moment having opposite signs at the shear-free edge. In order to determine whether this discrepancy is due to the assumption of a rectangular pile, the solutions

for a circular pile were obtained. The results of these comparisons are shown in Fig. 7.15. For completeness, the distribution in principal moments M_1, M_2 were obtained for the equivalent arrangement of piles (ie. a hexagonal zone of influence). The distributions of the maximum and minimum principal moments are plotted in Figs. 7.16 and 7.17 for the square and triangular arrangements along with the equivalent circular zone of influence.

Thus, if the design of the raft is one in which the profile of principal moments is to be employed (Wood, 1968) then the analytic solutions presented in the previous section can be used to determine the profiles for the given spacing of piles. If however, the design is merely based on the maximum and minimum moments, then the solutions for a circular domain of influence can be used to determine these with sufficient accuracy. Also, inspection of the results presented in Figs. 7.16 and 7.17 shows that, in practice, the magnitude of the maximum negative moment could be taken equal to the maximum positive moment which occurs at points above the centres of the piles.

The distributions of radial moment M_r and tangential moment M_t obtained from the solution for a circular domain of influence are shown in Figs. 7.18 and 7.19 for representative values of b/a. These results show that increasing the spacing of the piles causes a significant increase in the maximum positive bending moment whereas the maximum negative moment is constant. In Figs. 7.20 and 7.21 the effect of the stiffness ratio E_1/E_2 on the distribution of moments is shown when $b/a = 2$ and $\nu_1 = \nu_2 = 0.3$. Thus, the advantage of increasing the stiffness ratio E_1/E_2 when considering the settlement of the raft is partially offset by the increase in maximum bending moment.

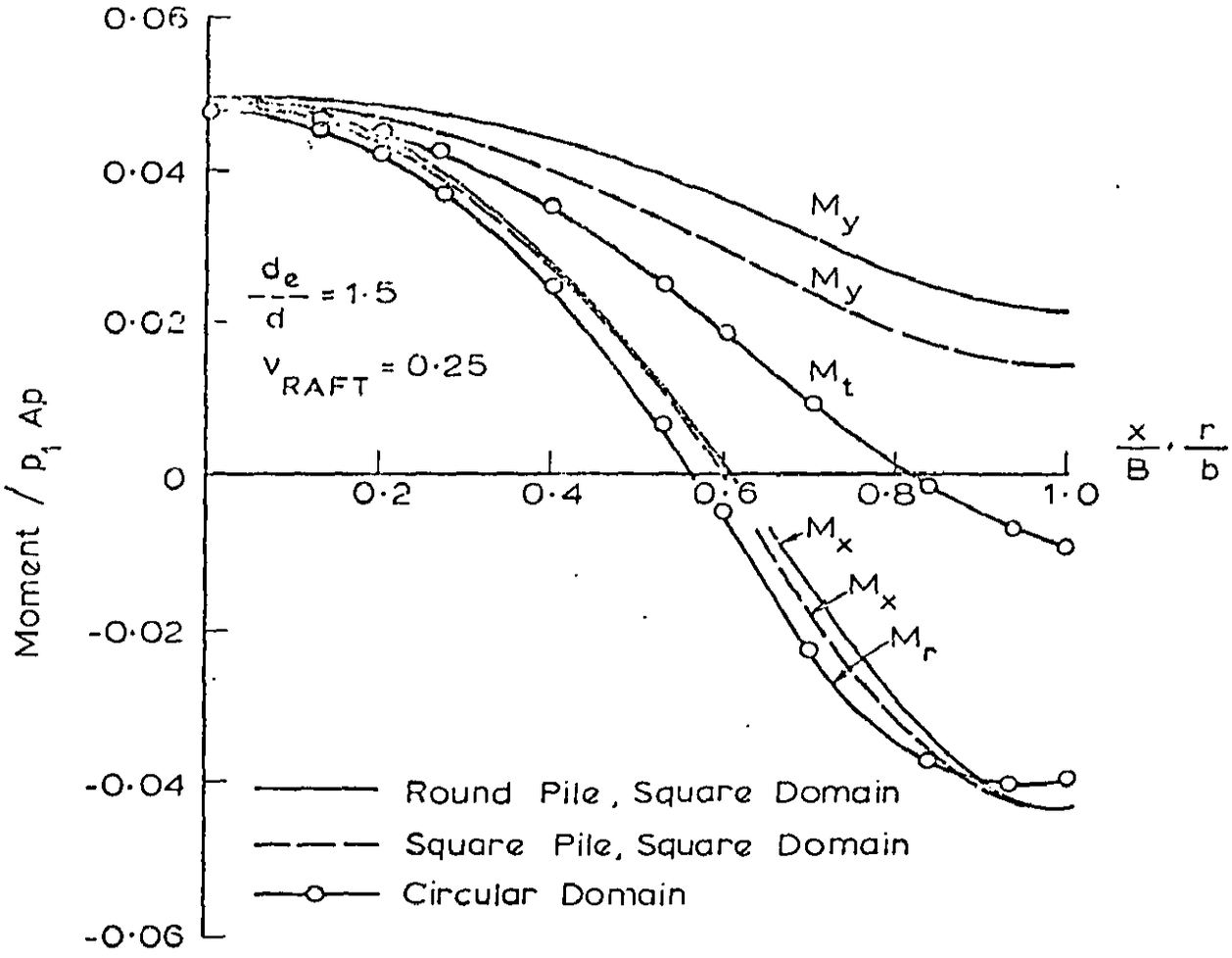

FIG. 7·15 COMPARISON BETWEEN SOLUTIONS FOR A CIRCULAR AND SQUARE DOMAIN OF INFLUENCE

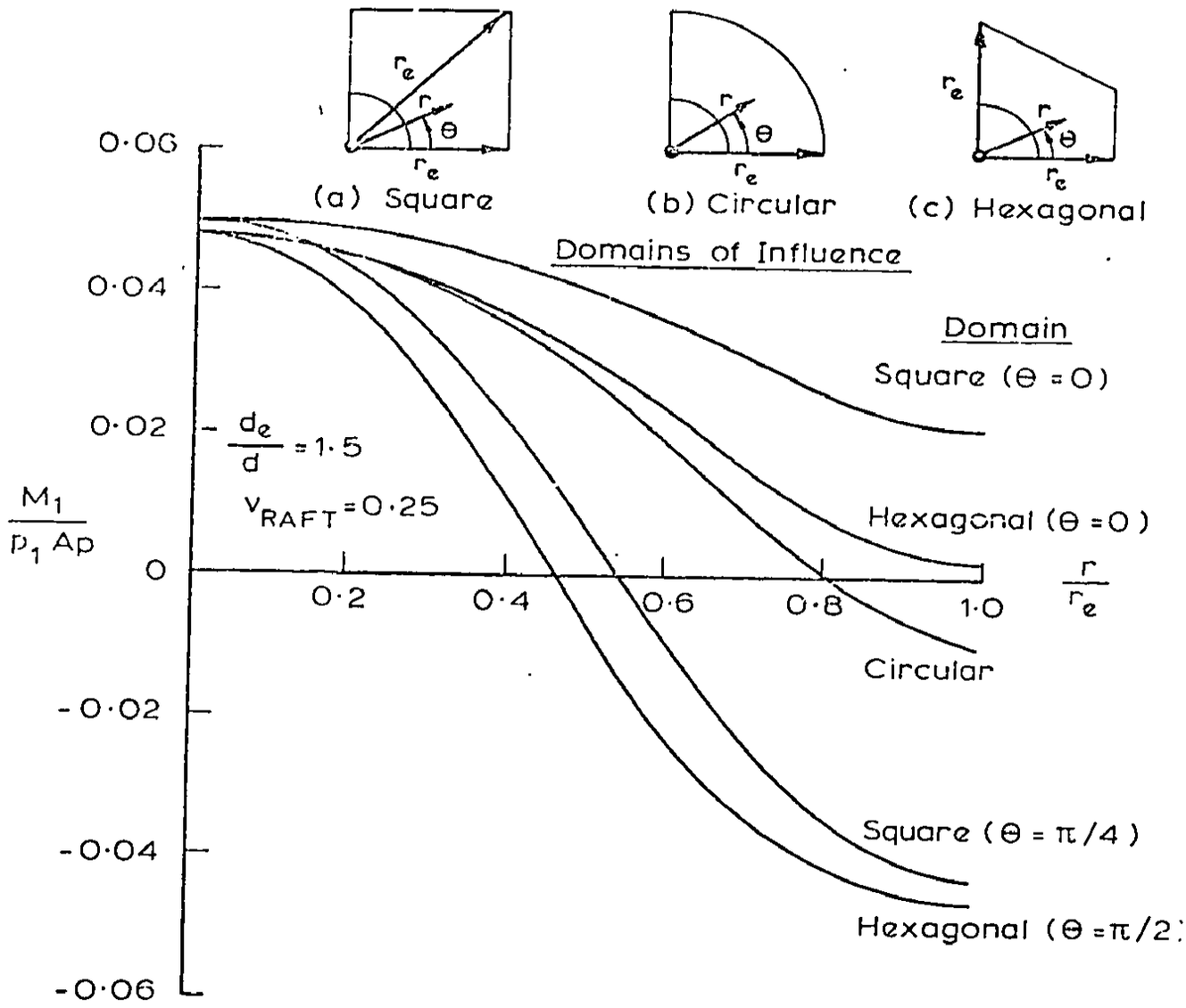

FIG. 7·16 VARIATION IN PROFILE OF M1 WITH ARRANGEMENT OF PILES

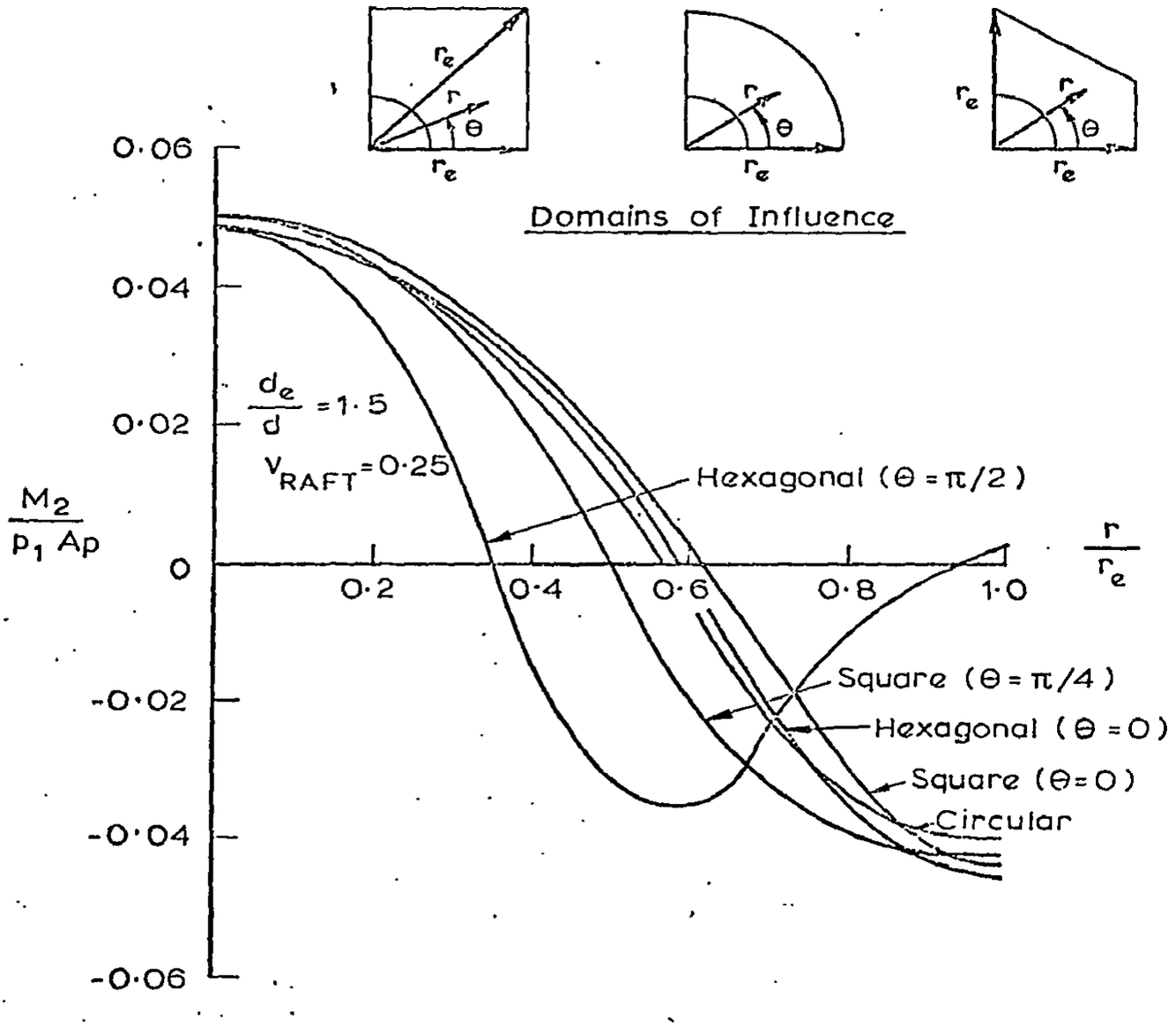

FIG. 7·17 VARIATION IN PROFILE OF M2 WITH ARRANGEMENT OF PILES

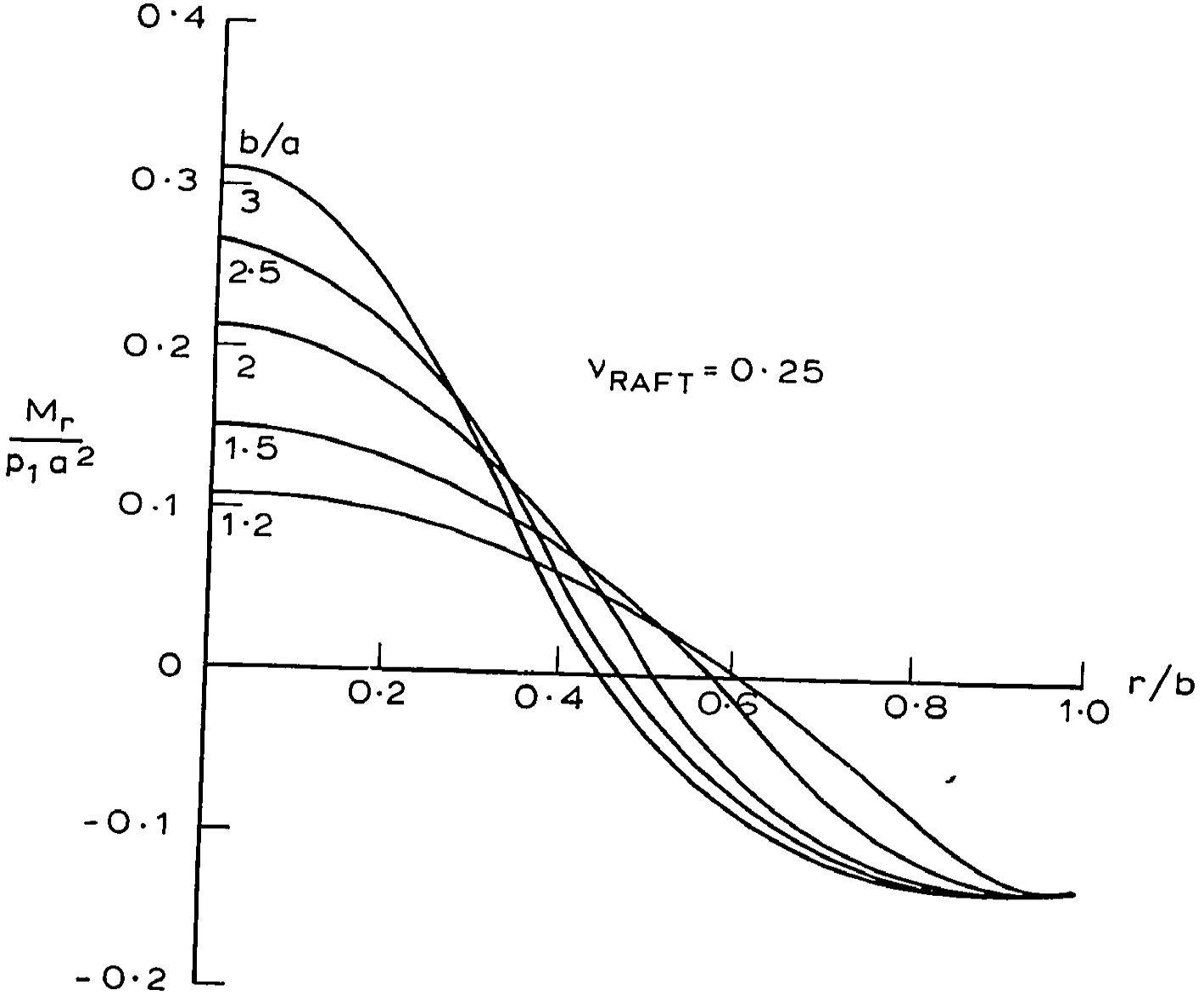

FIG. 7·18 RADIAL BENDING MOMENT DIAGRAMS

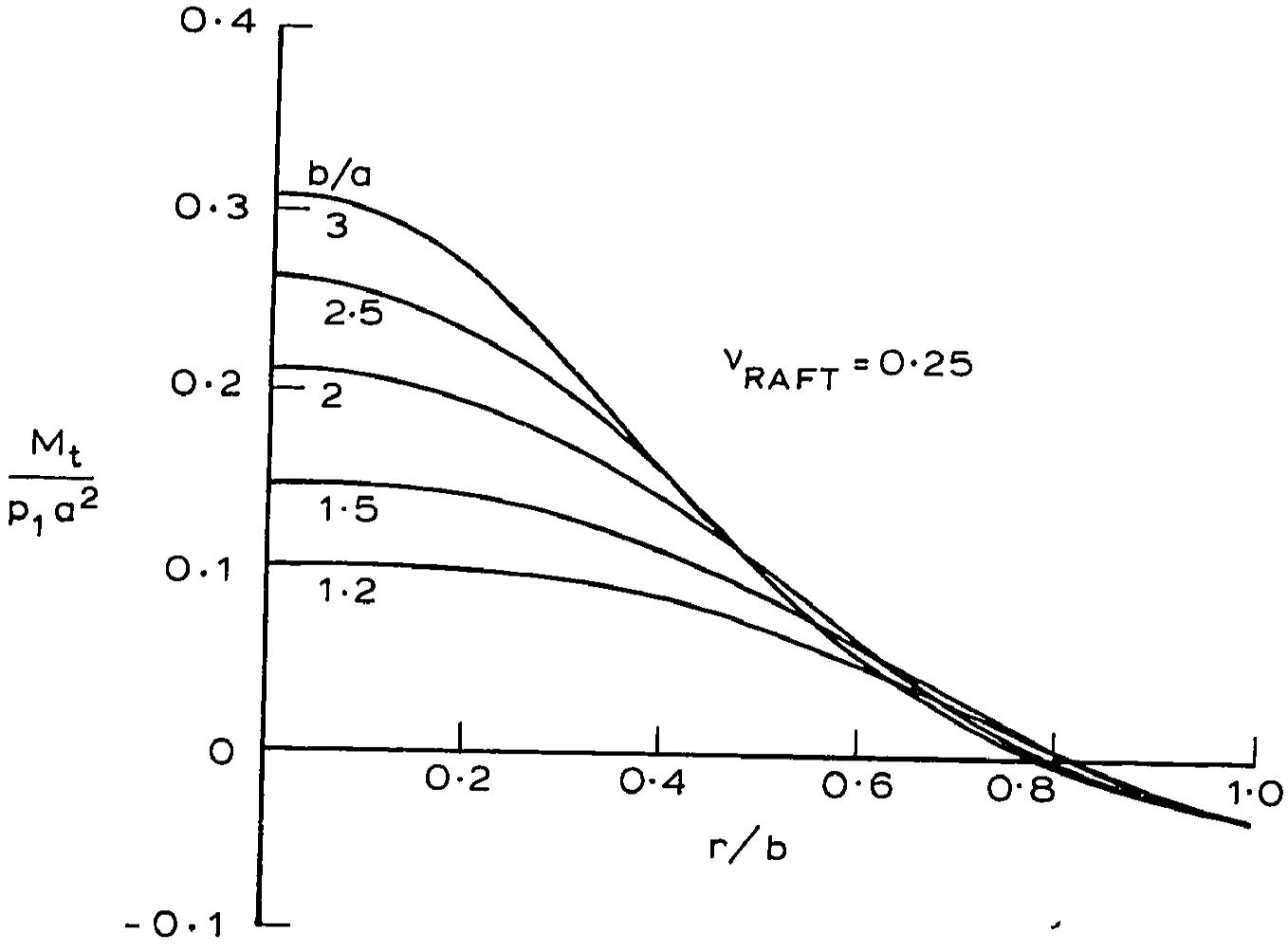

FIG. 7·19 TANGENTIAL BENDING MOMENT DIAGRAMS

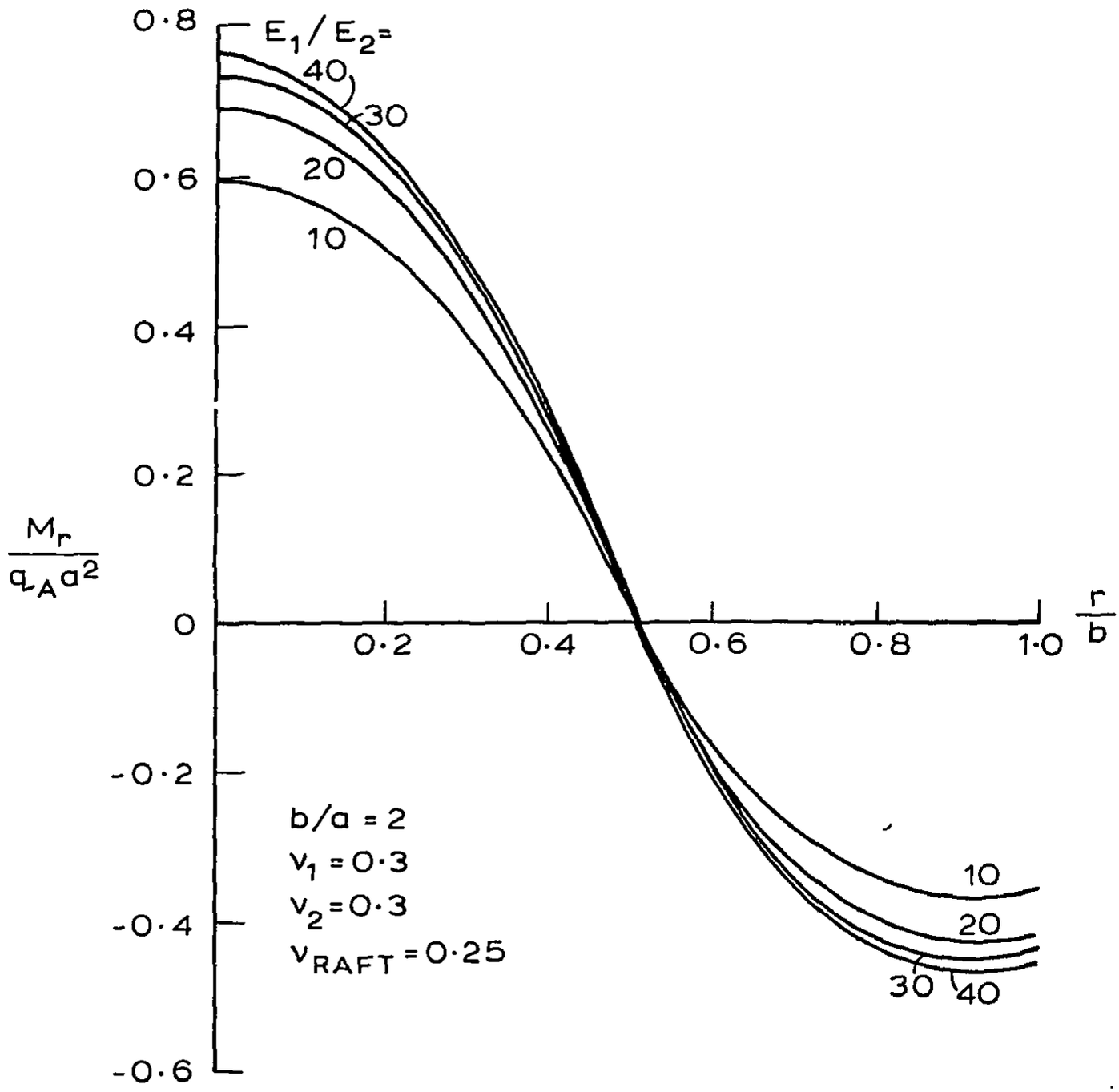

FIG. 7·20 EFFECT OF STIFFNESS RATIO E_1/E_2 ON RADIAL BENDING MOMENT

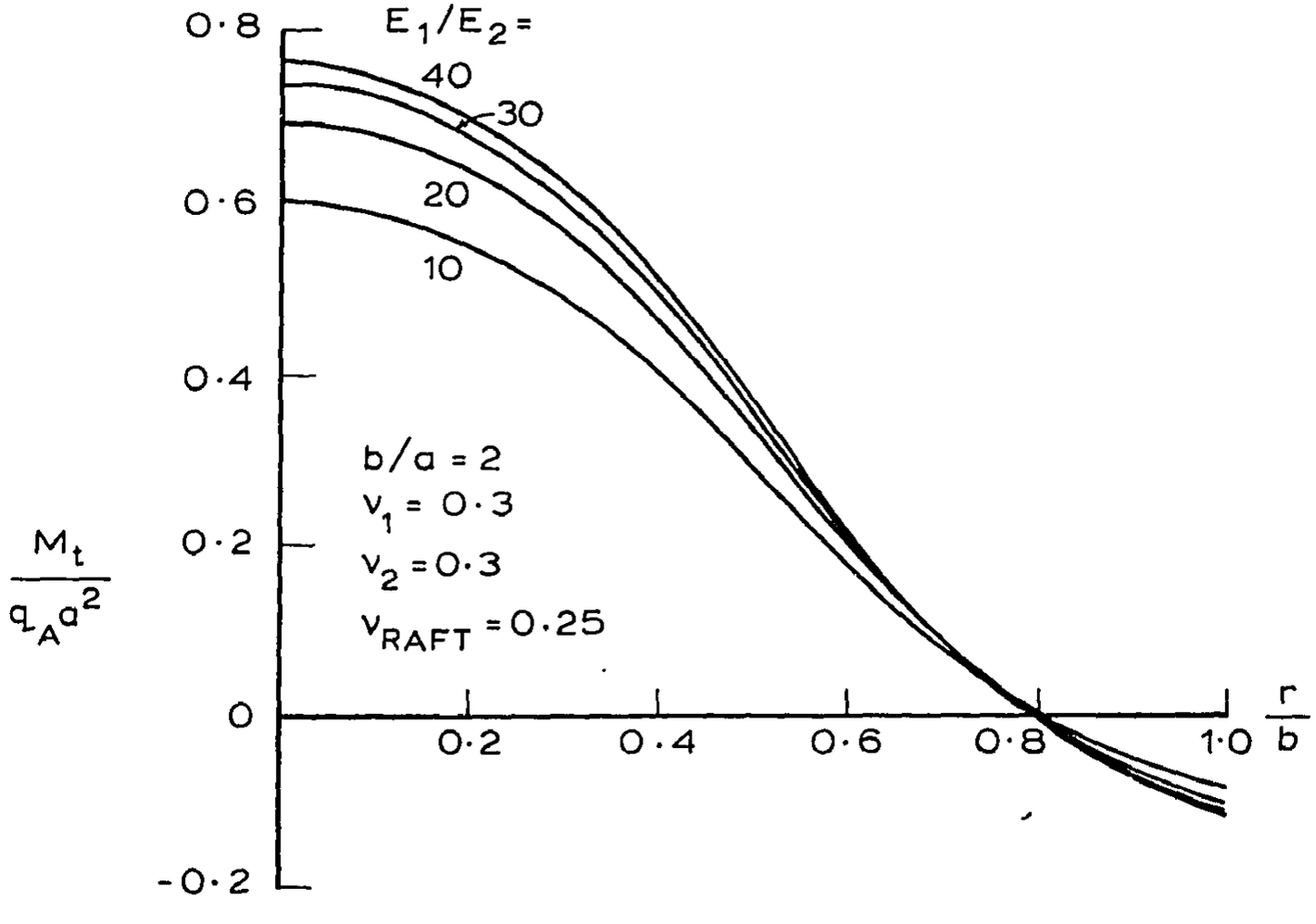

FIG. 7·21 EFFECT OF STIFFNESS RATIO E_1/E_2 ON TANGENTIAL BENDING MOMENT

The shear force diagrams for the triangular and square arrangements of the piles, corresponding to an equivalent circular domain of influence in which $d_e/d = 1.5$, are shown in Fig. 7.22. These diagrams are not coincident at the shear free edge because the requirement that the domains of influence have equal area results in the distance from the centre to an edge being dependent upon the shape of the domain. The shear force profile is less sensitive than the moment distributions to the arrangement of the piles. The discrepancy is not significant and thus the distribution of shear for the equivalent circular domain of influence can be used for both the triangular and square arrangement of piles.

The shear force diagrams for the circular domain of influence are shown in Fig. 7.23 for representative values of b/a. The maximum shear force occurs at the pile-soil interface with zero shear at the centre of the piles and the edge of the domain. The magnitude of this maximum shear force is determined by the diameter of the piles and the reaction pressure p_1 which increases with b/a. Thus, for a given diameter of piles, an increase in the spacing results in a larger maximum shear force. The shear force is also a function of the stiffness ratio E_1/E_2; the effect of the stiffness ratio on the shear force distributions is shown in Fig. 7.24 when $b/a = 2$ and $\nu_1 = \nu_2 = 0.3$. As would be expected, increasing the stiffness ratio results in larger shear forces.

7.4 ANALYSIS OF THE TIME-DEPENDENT BEHAVIOUR

In this section the different pile arrangements are analysed using an equivalent circular domain of influence, and the time-dependent

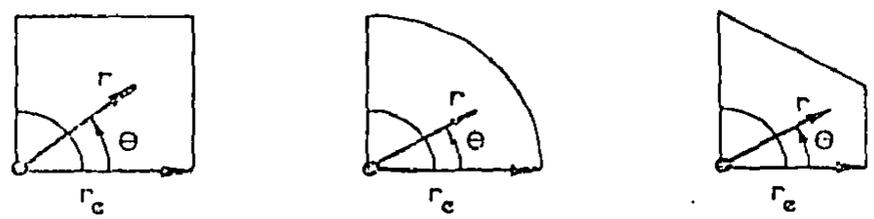

(a) Square (b) Circular (c) Hexagonal

Domains of Influence

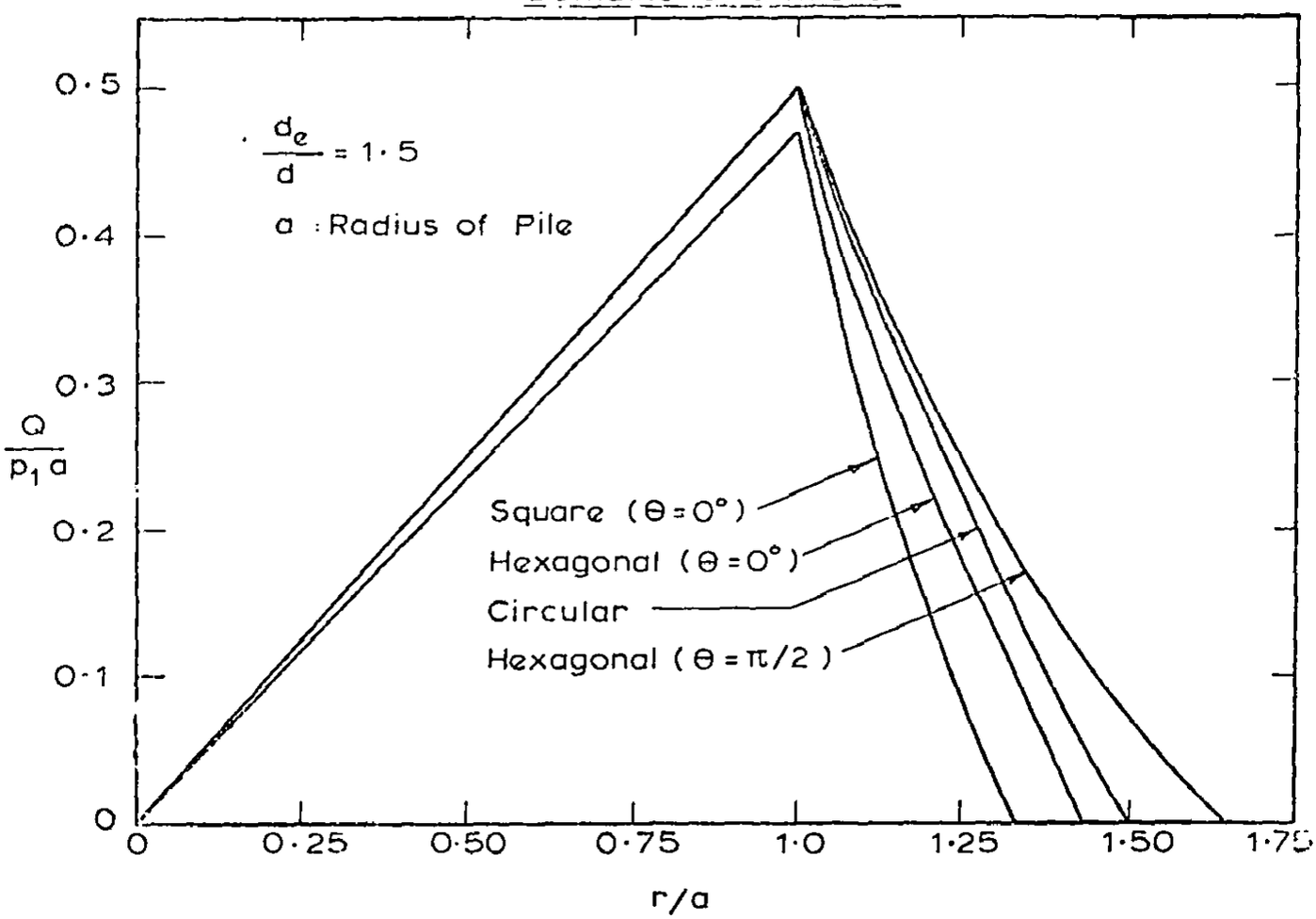

FIG.7·22 COMPARISON BETWEEN SHEAR FORCE DIAGRAMS FOR TRIANGULAR AND SQUARE ARRANGEMENTS OF PILES.

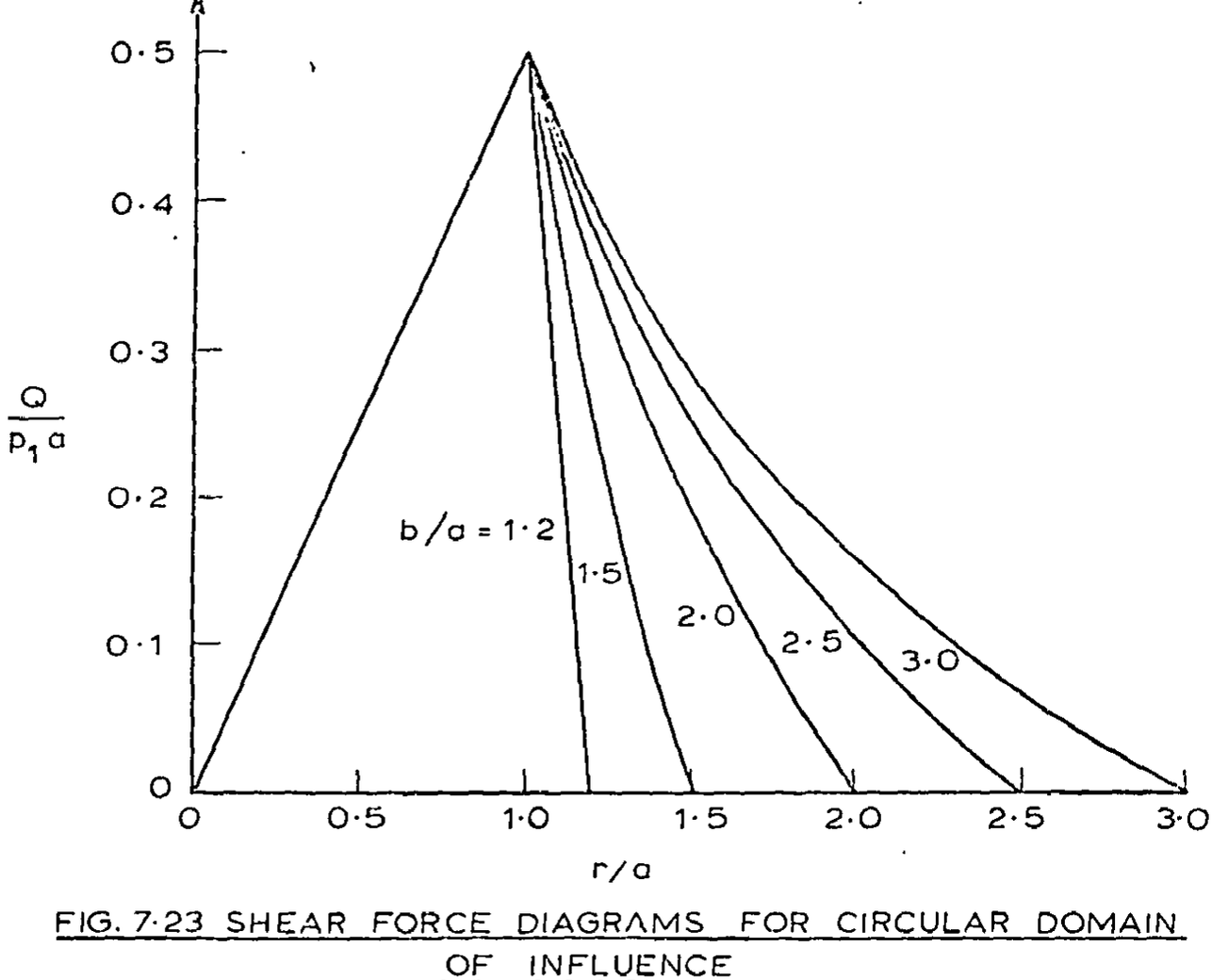

FIG. 7·23 SHEAR FORCE DIAGRAMS FOR CIRCULAR DOMAIN OF INFLUENCE

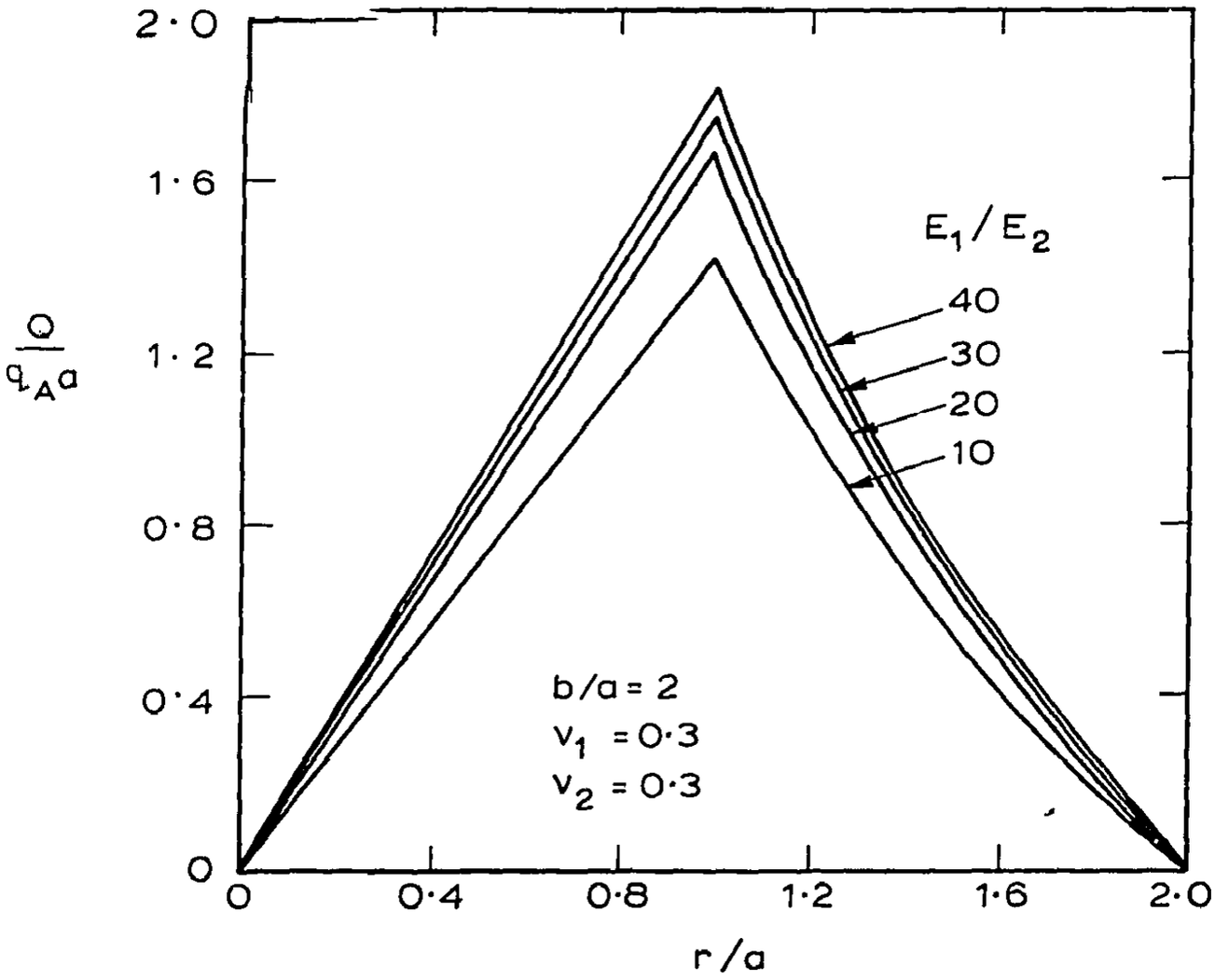

FIG. 7·24 EFFECT OF STIFFNESS RATIO E_1/E_2 ON THE SHEAR FORCE DISTRIBUTION

behaviour of the rigid raft is investigated using an axi-symmetric finite element solution to the equations of consolidation derived by Biot (1941). These equations combine the effects of diffusion and the elastic deformations resulting from the dissipation of the excess pore pressures. The numerical method used for solution of Biot's equations in this chapter is the same as used in Chapter 6, and is identical to that presented by Booker and Small (1975).

When the load is initially applied the soil behaves as an incompressible material but there is a small initial settlement of the raft due to the presence of the compressible stone columns. If the raft is impermeable and seated directly on the soil the excess pore pressures in the soil dissipate by radial flow to the columns. Barron (1948) has presented a solution for the excess pore pressure at any point within the soil mass subjected to equal vertical strain in which both a resistance to flow into the well (stone column) and smear around the well are taken into account. However, this solution assumes that the initial excess pore pressures in the soil are non-uniform whereas initially the bulk stress and therefore the excess pore pressures will be constant.

In Fig. 7.25 the boundary conditions are defined and the finite element mesh used for the analyses is shown. The rate of consolidation from analyses using this mesh (mesh No.1) and a finer mesh (Fig. 7.26) were initially compared and the discrepancy found to be insignificant. In addition, close agreement was obtained when the effective stresses at the completion of consolidation (mesh 1) were compared with those computed from Solution C. The results of these comparisons are shown in Figs. 7.27 and 7.28. Thus mesh 1 was employed for a parametric study of

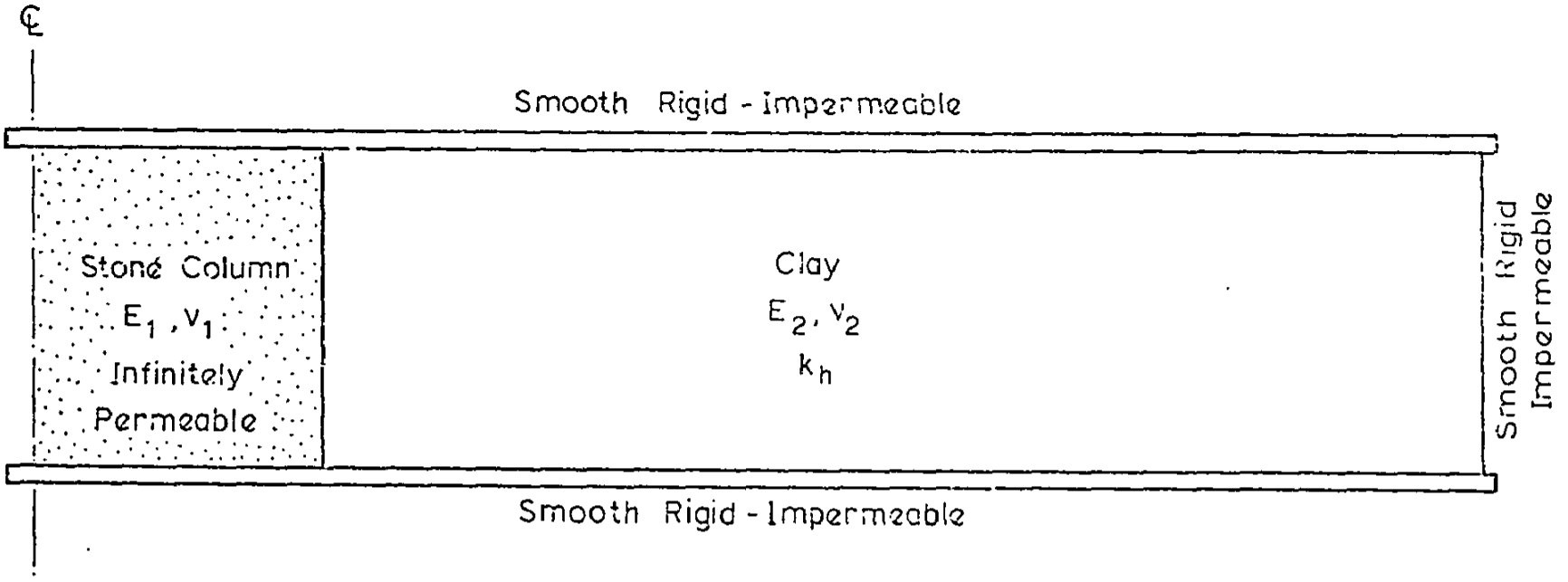

(a) Definition of Boundary Conditions

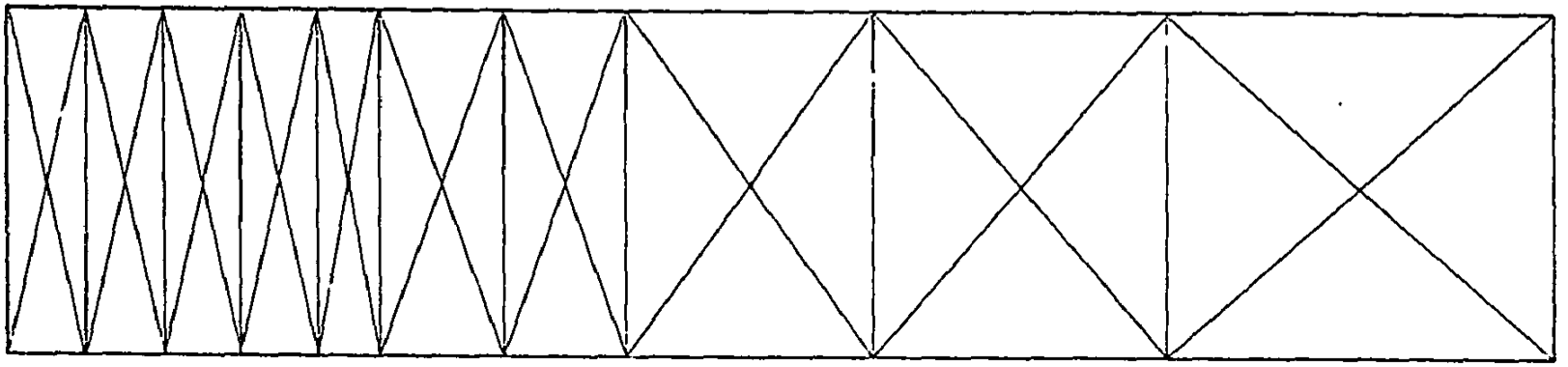

(b) Finite Element Mesh

FIG. 7-25 PROBLEM DEFINITION

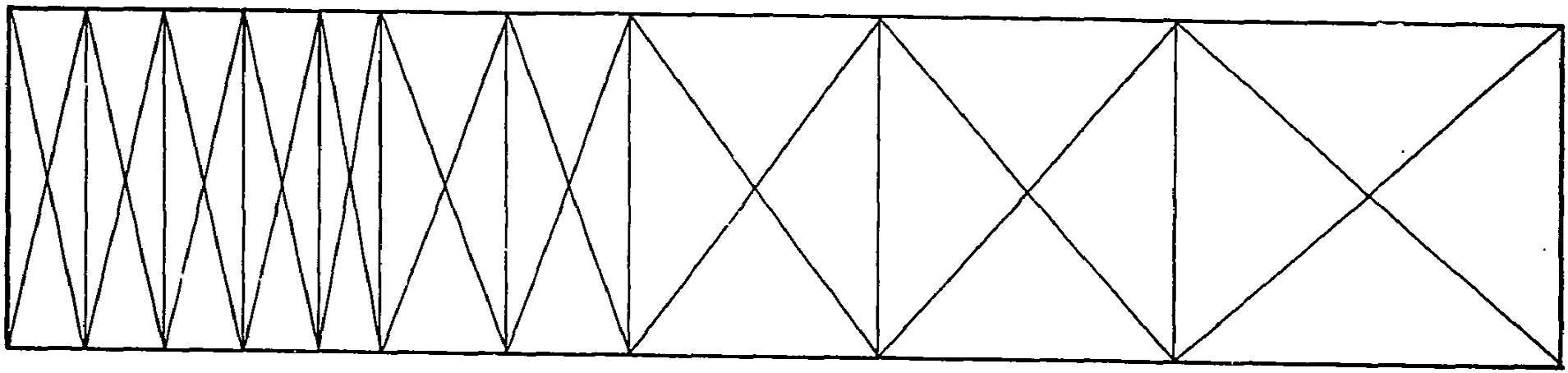

(a) Finite Element Mesh No 1

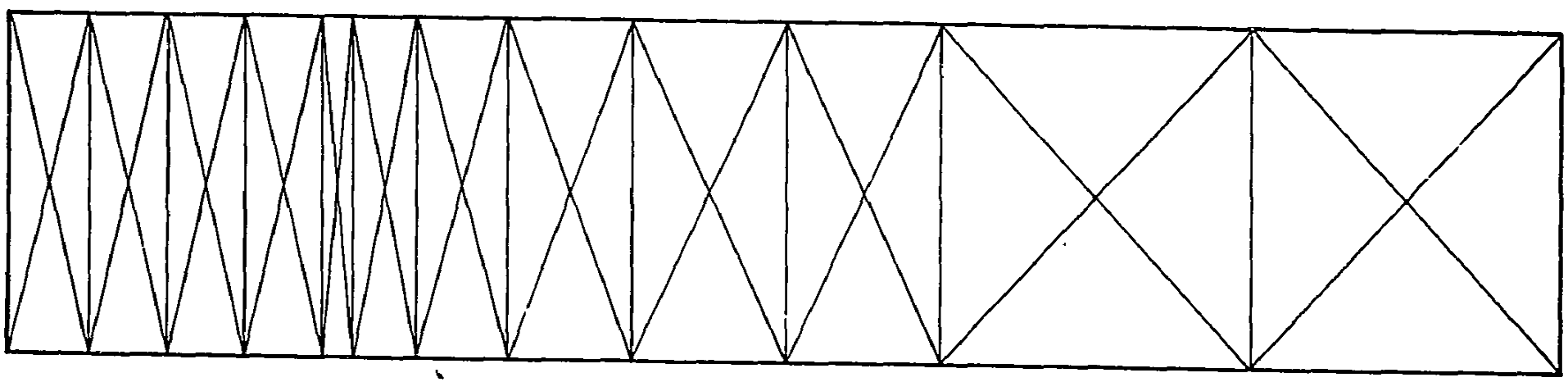

(b) Finite Element Mesh No 2

FIG.7·26 INVESTIGATION OF THE EFFECTS OF MESH ON CONSOLIDATION RATE

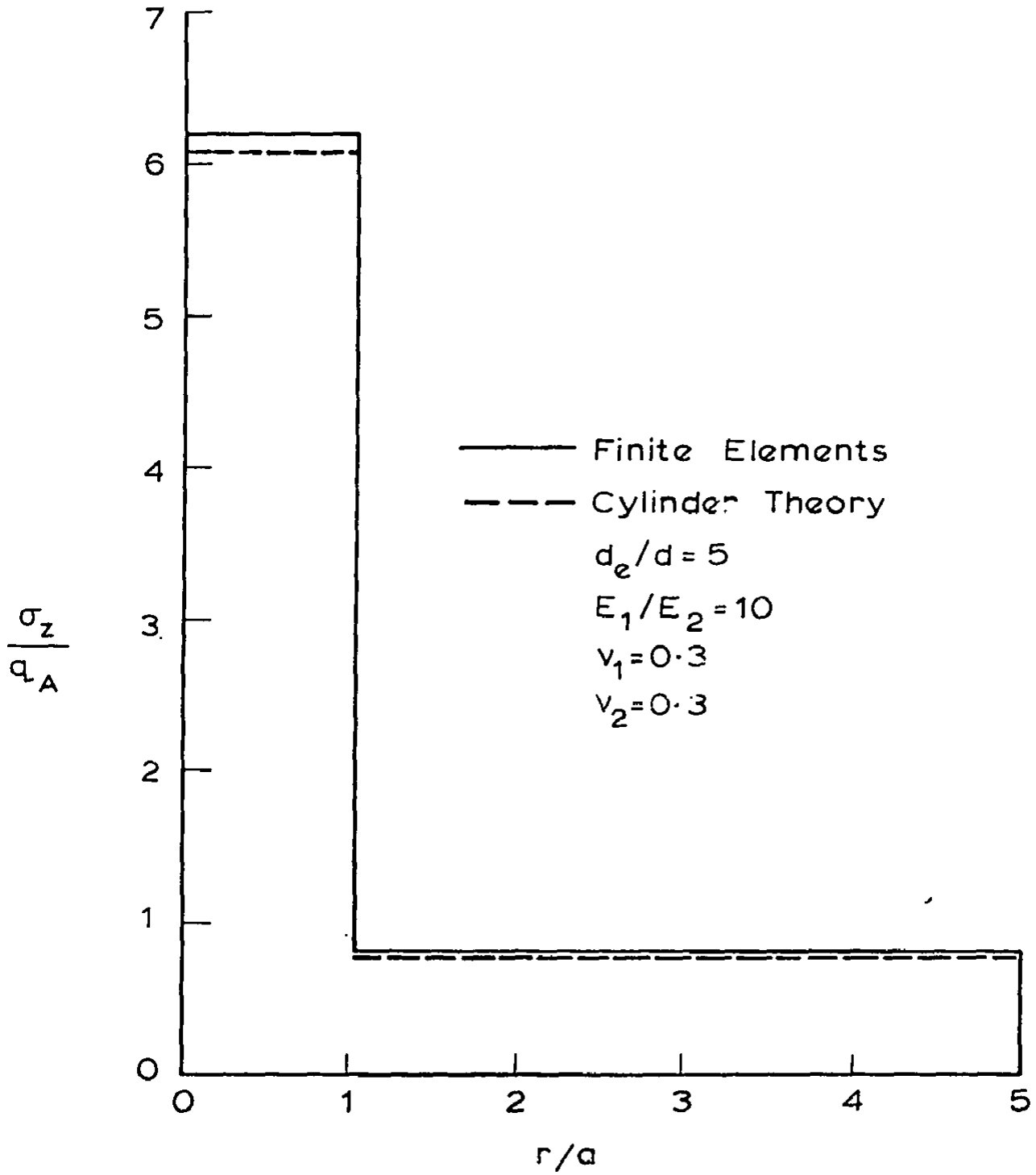

FIG. 7·27 FINAL VERTICAL STRESS FOR $d_e/d = 5$

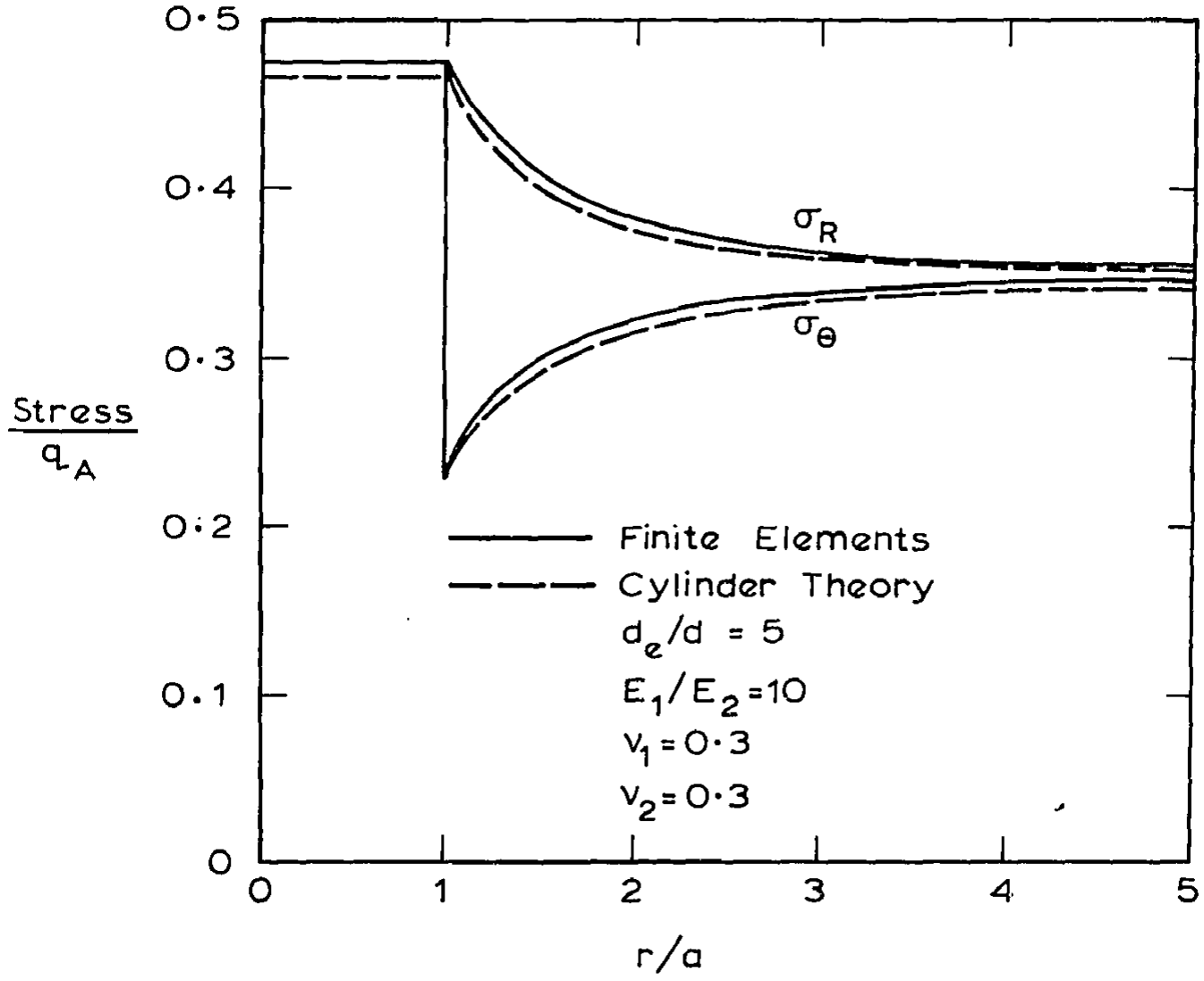

FIG. 7·28 FINAL σ_R & σ_θ STRESSES FOR $d_e/d=5$

the factors affecting the rate of settlement of the raft.

The rates of consolidation are shown in Figs. 7.29 to 7.33 for d_e/d = 1.5, 2, 2.5, 3.5 and stiffness ratios under drained conditions E_1/E_2 = 1, 10 and 40 when $\nu_1 = \nu_2 = 0.3$. The stone columns are assumed to be infinitely permeable whereas the soil is assigned a horizontal permeability k_h. A time factor T_h is defined in terms of the radial coefficient of consolidation c_{rl} where

$$c_{rl} = \frac{k_h E_2 (1-\nu_2)}{\gamma_w (1+\nu_2)(1-2\nu_2)} \qquad (7.15)$$

The degree of settlement U_s is defined as

$$U_s = \frac{S_t - S_i}{S_{TF} - S_i} \qquad (7.16)$$

where S_t = settlement of raft at time t

S_i = initial settlement of raft

S_{TF} = total final settlement of raft.

Also plotted with these results are the average degree of pore pressure dissipation U_p, obtained from Barron's solution. The finite element solutions are in reasonable agreement with the Barron solution when E_1/E_2 = 1 but for practical values of this ratio the Barron solution predicts a slower rate of consolidation. This discrepancy arises because the Barron solution takes no account of the relative stiffnesses of the column and clay materials whereas the results from the elastic Biot theory show that, for a given spacing of columns, as the stiffness ratio increases, the columns take a greater proportion of the applied load and the rate of consolidation increases. However, numerical studies show

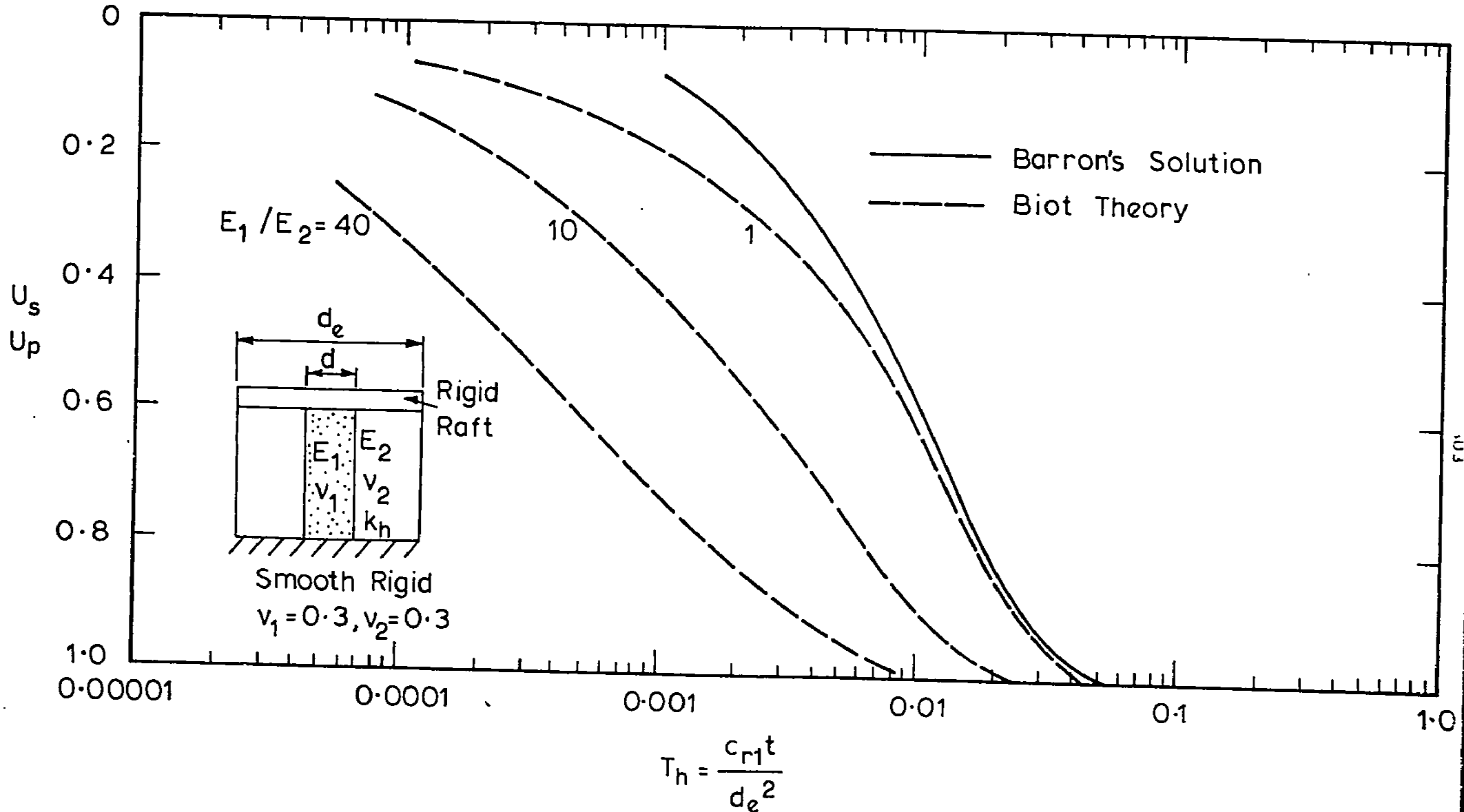

FIG. 7·29 RATE OF SETTLEMENT OF RIGID RAFT ; $d_e/d = 1·5$

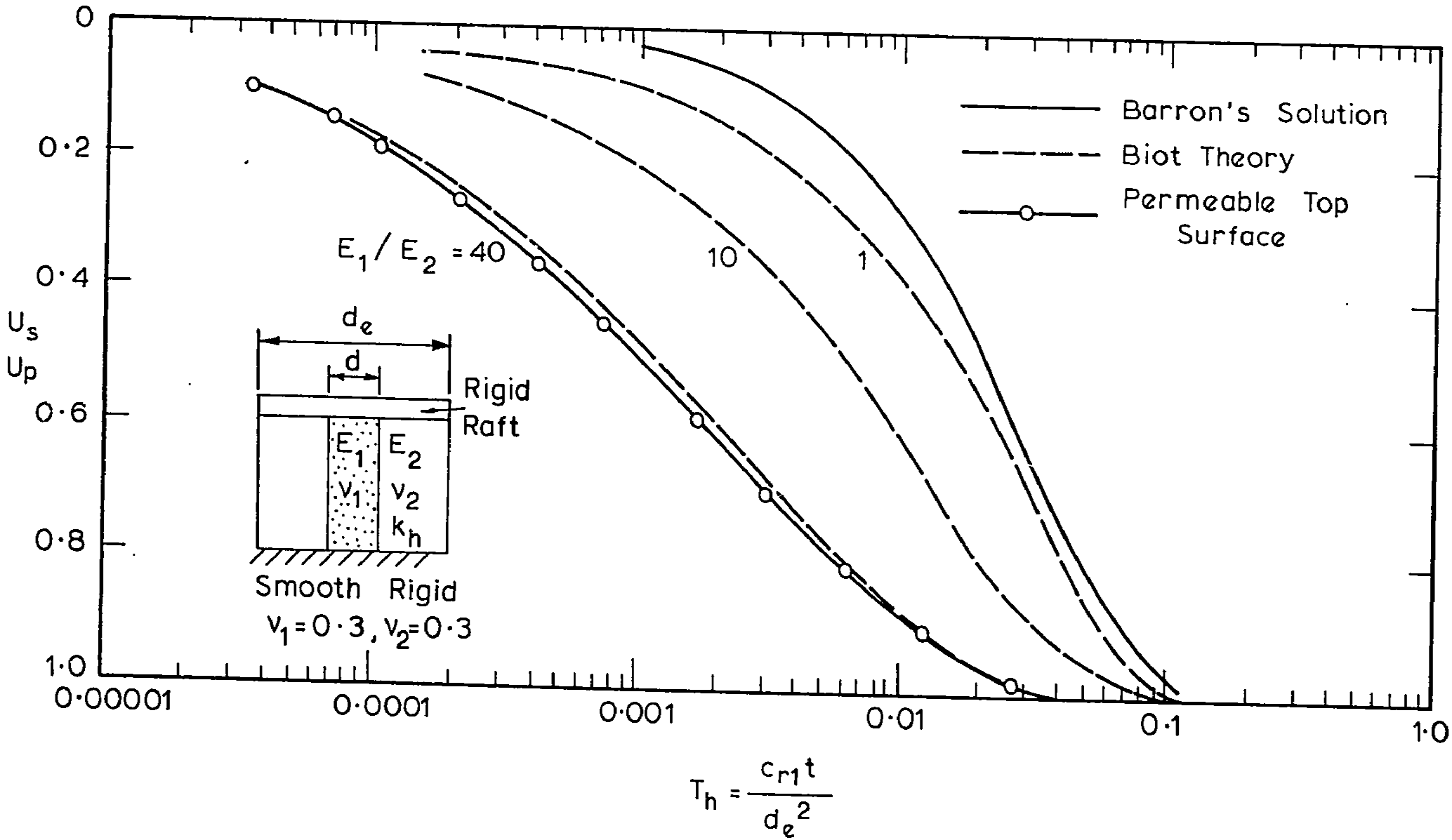

FIG. 7·30 RATE OF SETTLEMENT OF RIGID RAFT; $d_e/d = 2$

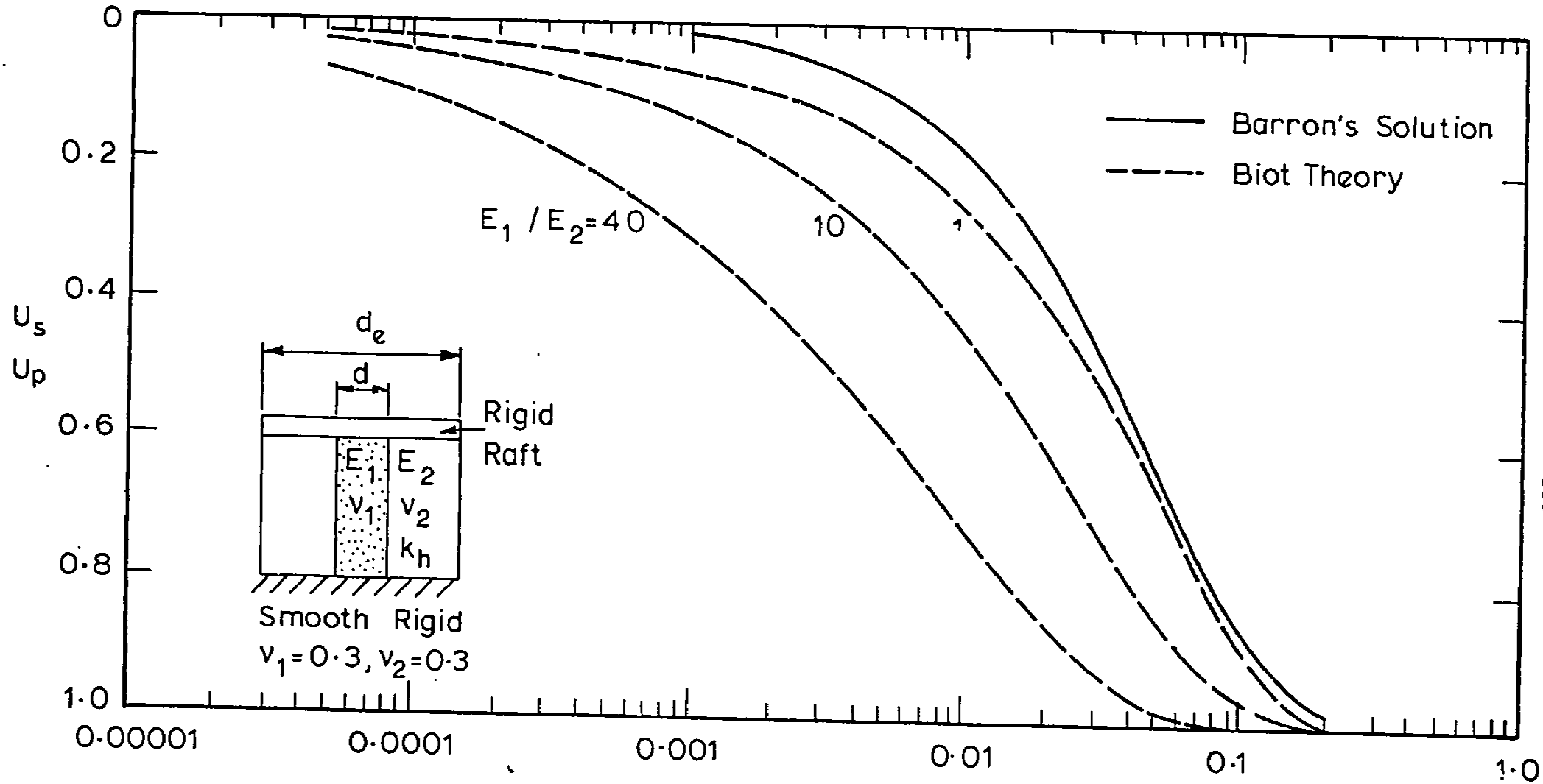

FIG. 7·31 RATE OF SETTLEMENT OF RIGID RAFT; $d_e/d = 2·5$

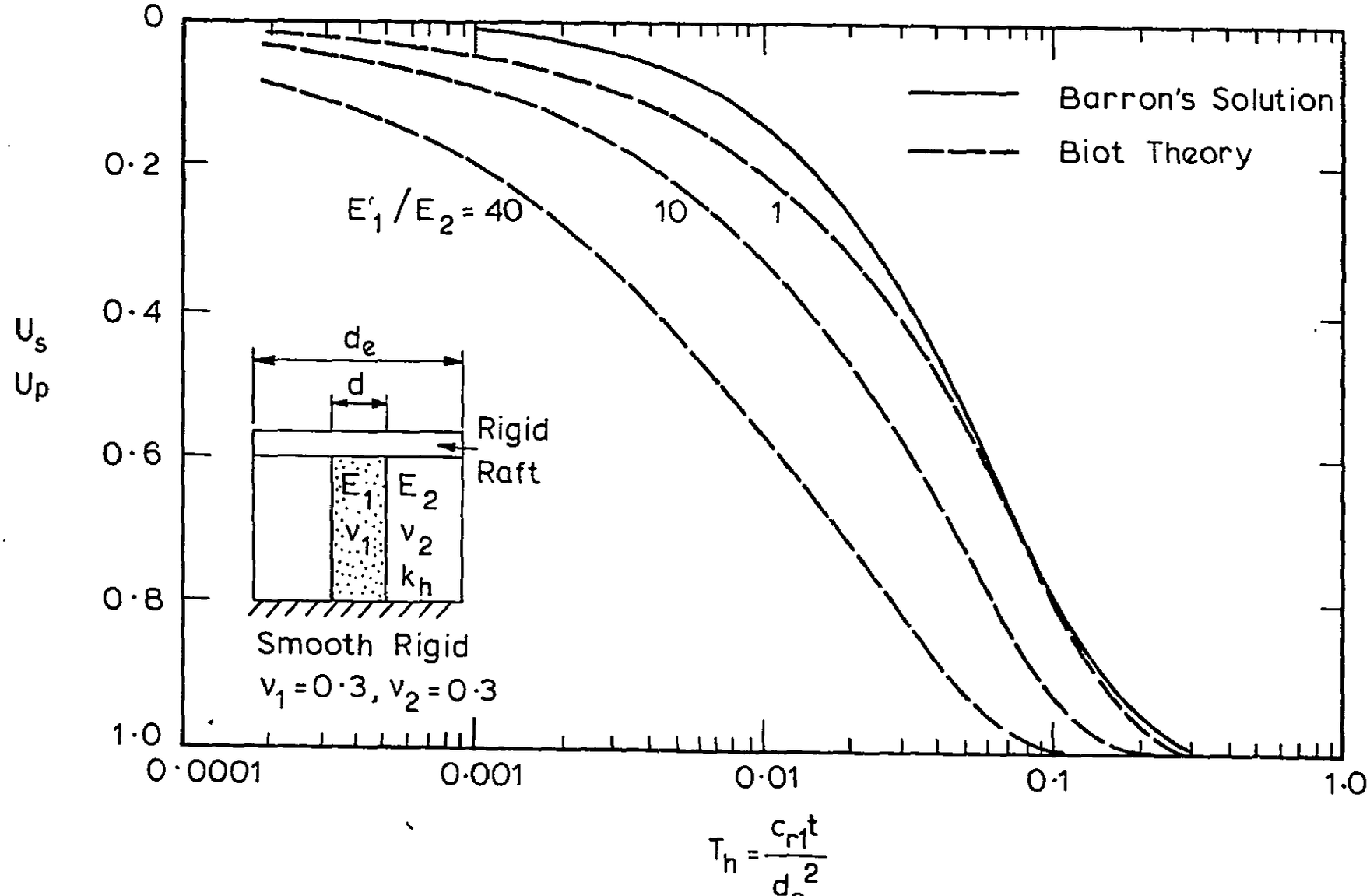

FIG. 7·32 RATE OF SETTLEMENT OF RIGID RAFT ; $d_e/d = 3$

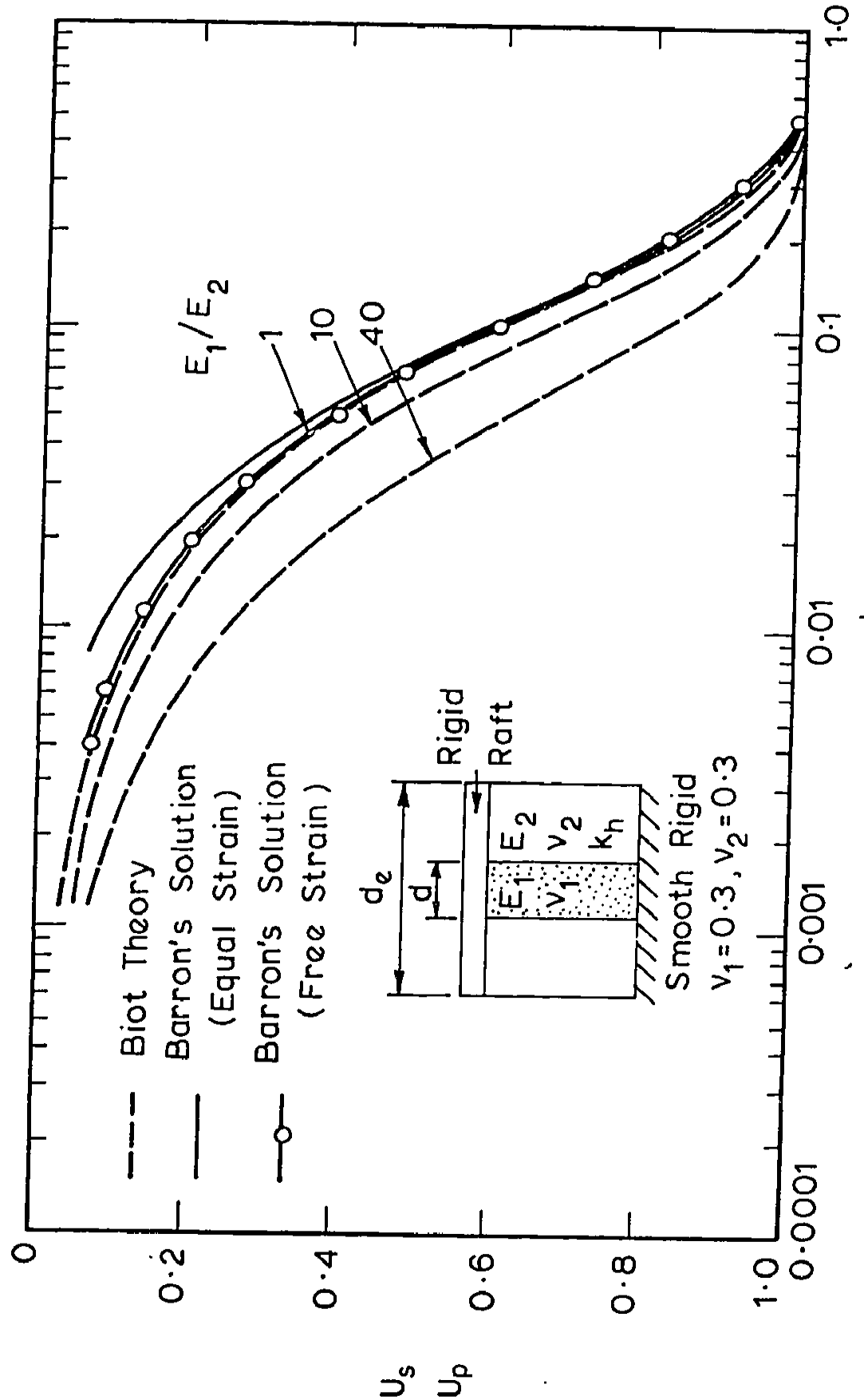

FIG. 7·33 RATE OF SETTLEMENT OF RIGID RAFT ; $d_e/d=5$

that the effect of the ratio E_1/E_2 on the rate of consolidation is not significant for the case of a uniform applied pressure (ie. free strain) which was considered in the previous chapter. This difference in behaviour between the equal and free strain cases may arise because for equal strain the load intensity on the clay is largely time-dependent. The load intensity on the clay is initially greater than that on the column but as consolidation proceeds this is reversed and at the completion of consolidation the intensity on the column is far greater than on the clay (for realistic values of E_1/E_2). Thus, the rate of change of the bulk stress with time $\frac{\partial\theta}{\partial t}$ (equation 6.1) in the clay is significant and dependent on E_1/E_2 (ie. it has an increasing effect as the ratio of E_1/E_2 increases). In contrast, for the free strain case the load intensity on the clay is insensitive to E_1/E_2 and nearly constant with time and this may therefore account for the rate of consolidation being nearly independent of E_1/E_2 and for the much closer agreement between the Biot and diffusion theory solutions for this case.

In Fig. 7.33 the results are shown of a comparison between the Biot theory solutions for the degree of settlement and the Barron solutions for average degree of pore pressure dissipation for both cases of free and equal vertical strain. It is evident that an anomaly exists; the Barron solution for the free strain case is in closer agreement with the Biot theory for a rigid raft ($E_1/E_2 = 1$) than the equal strain solution. This is largely due to Barron's solution for the equal strain case being derived from a physical argument regarding flow in which the initial excess pore pressure distribution is non-uniform whereas that obtained from the theory of elasticity is uniform. However, a uniform initial distribution is adopted for the Barron solution of the free strain case which results in the anomaly that this so-

lution gives closer agreement with the Biot theory solution than the equal strain solution.

In some practical situations the raft would be separated from the stabilised soil by a layer of permeable sand or gravel. In this situation dissipation of the excess pore pressures in the soil occurs by radial flow to the columns and vertical flow to the permeable top surface. For a typical case, ie. $h/d = 10$, $d_e/d = 2$, $E_1/E_2 = 40$ and $\nu_1 = \nu_2 = 0.3$, solutions were obtained for both cases of an impermeable and permeable top surface. The soil was taken to be isotropic. This comparison showed that the vertical component of flow did not cause a significant increase in the rate of consolidation (Fig. 7.30) and thus the solutions for radial flow only, can be used to predict the rate of settlement of a raft placed on a gravel mat overlying the stabilised soil.

As consolidation proceeds and settlement takes place, the strain of the stone columns increases causing an increase in the contact stress σ_z between the columns and raft and a decrease between the soil and raft from equilibrium. The contact stresses are shown in Fig. 7.34 for various times for the case where $d_e/d = 2$, $E_1/E_2 = 40$ and $\nu_1 = \nu_2 = 0.3$. As expected, due to the one-dimensional strain conditions, the rate of increase in the uniform stress on the stone columns is identical to the rate of settlement. Thus, if the non-uniform contact stress distribution on the soil is replaced by an equivalent uniform stress, the results presented in the previous section can be used to estimate the magnitude of the moments and shears at various times. The rate of increase of the moments and shears is then identical to the rate of settlement.

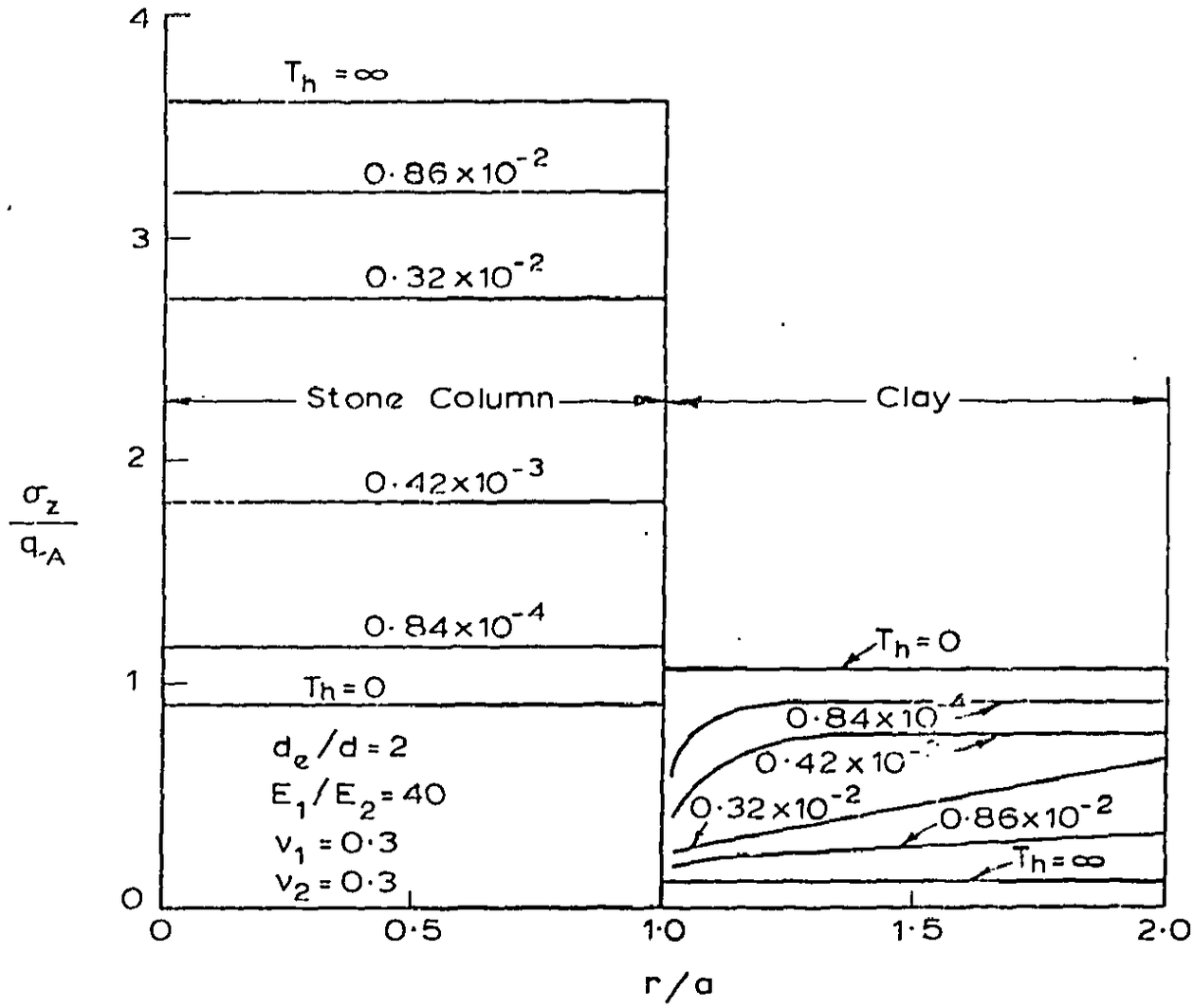

FIG. 7·34 CHANGE IN VERTICAL STRESS WITH TIME

7.5 SUMMARY AND CONCLUSIONS

In the last three chapters solutions for the magnitude and rate of settlement of foundations supported by soil reinforced with granular piles have been presented. In the present chapter consideration has been given to the situation in which the foundation is rigid and supported by a regular array of fully penetrating granular piles.

An analytic solution using elasticity has been developed for the settlement of the rigid foundation by considering a typical cylindrical pile-soil unit. Expressions for evaluating the moment and shear distributions across the foundation are given. The two regular arrangement of piles used in practice (square and triangular) have been considered in detail. For these arrangements each pile-soil unit has a square or hexagonal plan area respectively. The effect of treating this area as an equivalent circular area has been investigated by use of a finite element analysis (for settlement) and the development of expressions for the moments and shears in a square and hexagonal domain of influence. The results presented show that the errors in the stresses (and thus settlement) by assuming an equivalent circular area are negligible. However, although the shear force distribution is relatively insensitive, the moment distributions are largely dependent on the arrangement of piles. Thus, in a sophisticated analysis of the raft where the profiles of principal moments are to be employed, the expressions given in this chapter enable these profiles to be evaluated. If however, the design is to be based on the maximum and minimum values of the moments, then the solutions for the cylinder can be employed.

Numerical solutions to Biot's theory of consolidation have been

presented for the rate of settlement of the raft. These solutions quantify the increased rate of consolidation of the reinforced soil with increasing stiffness ratios of the piles and soil. Finally, it is of interest to note that the solutions show that by increasing the stiffness ratio of the piles and soil the settlements are reduced and the rate of settlement increased but to counteract these, the moments and shears are increased in the raft.

CHAPTER EIGHT

EXPERIMENTAL RESULTS

8.1 INTRODUCTION

In this chapter the results of two experimental programmes are presented. The first of these programmes was undertaken to provide more evidence as to the applicability of the finite element analysis presented in this thesis for the analysis of a single granular pile. Also, the analysis for the settlement of small groups of granular piles (Chapter 4) is used to predict the results of an experiment. The second programme was designed to verify the theoretical predictions using elastic theory (Chapter 7) for the magnitude and rate of settlement of a rigid raft seated on a clay reinforced by large numbers of granular piles.

The first experimental programme consisted of a set of four model footing tests which were performed in a closed pressure vessel in order that the clay (kaolin) was normally consolidated. The experimental results are compared with the theoretical predictions and the agreement is found to be good for the load-settlement response of a single granular pile. However, for a small group of granular piles, the analysis presented in Chapter 4 seriously underestimates the settlement of the model footing.

The primary aim of this experimental program was to investigate the reduction in settlement of a circular footing supported by conventional piles and stone columns.

lysis that the settlement can be predicted by considering one pile-soil unit was used in the design of the experimental set-up. A P.V.C. cylinder filled with kaolin was consolidated under one-dimensional conditions by a rigid raft and the settlement for a given stress range compared to

the settlement when the clay was reinforced by a granular pile. This enabled a settlement reduction for a given diameter of pile to be computed. The results of the experiments are shown to be in close agreement with the elastic theory.

8.2 PRESSURE VESSEL TESTS

Four pressure vessel tests were performed in which the load carrying capacity of model circular footings (10.16 cm diameter) placed on the surface of a normally consolidated bed of kaolin was determined. The following model footings were loaded to failure

1) a circular footing
2) a circular footing supported by an aluminium pile
3) a circular footing supported by a granular pile
4) a circular footing supported by a group of three granular piles.

8.2.1 Apparatus

The pressure vessel in which the clay was consolidated and the footings loaded to failure is shown diagrammatically in Fig. 8.1. The vessel has an inside diameter of 30.48 cm and a depth of 38.1 cm. The lid of the vessel N and the base L were secured to the body M by socket headed bolts. A groove was machined into the flanges at the top and base of the vessel so that a 33 cm diameter rubber O-ring could be fitted to give a water-tight seal. A central hole P in the base of the vessel allowed the pore water drainage system to be connected, a similar tapping Q was provided at the top of the vessel to allow two-way drainage. The lid of the vessel contained the pressurised water for consolidation.

A: Air Filter
B: Precision Pressure Regulator
C: Pressure Gauge
D: Air-Water Pressure Cylinder
E: Filter Paper-Gauge Drain
F: Model Pile
G: Clay
H: Loading Plunger
I: Displacement Transducer
J: Magnetic Clamp
K: Rubber Membrane
L: Pressure Vessel Base
M: Pressure Vessel Body
N: Pressure Vessel Lid
O: Rubber Membrane
P: Base Drainage Tapping
Q: Side Drainage Tapping
R: Filter Drainage Tapping
S: Sealing Cap
T: Automatic Recorder
U: Load Transducer

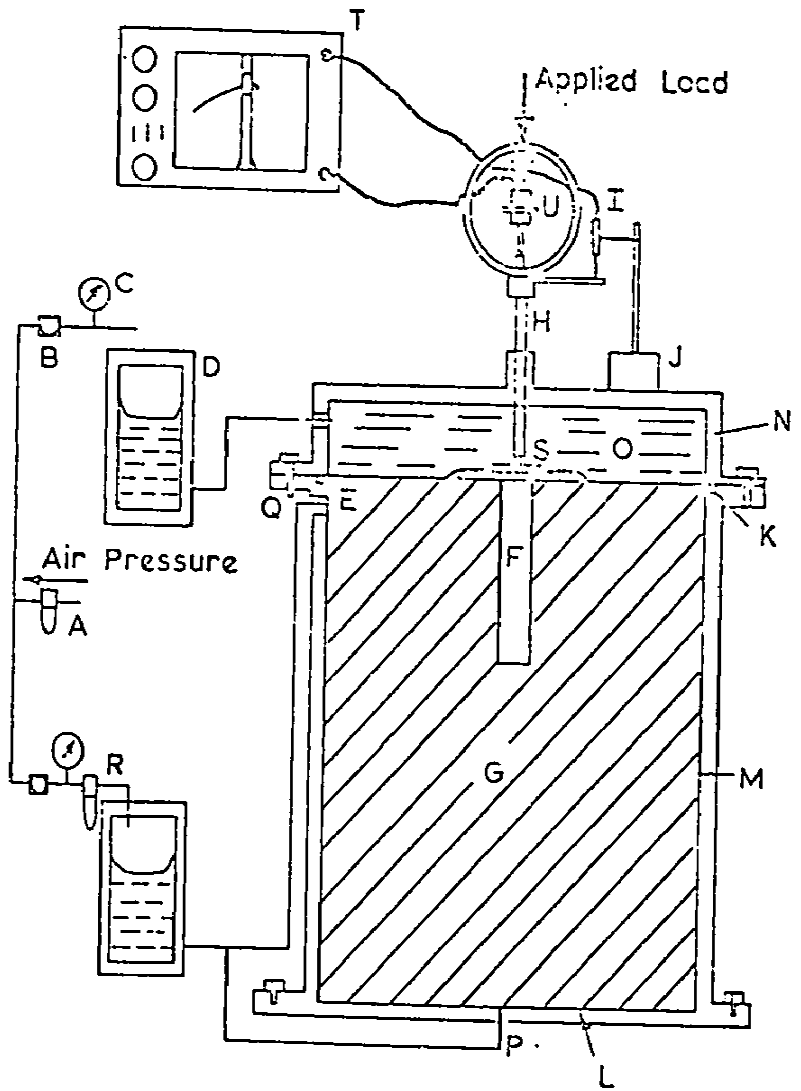

FIG. 8·1 APPARATUS SET-UP FOR PRESSURE VESSEL TESTS

A rubber membrane O, separated the water from the footing and clay beneath. A screw-in sealing cap S was provided on top of the footing to secure the rubber membrane to the footing. A hole in the lid enabled a loading plunger to be seated onto the footing.

The pressure was supplied via an air-water exchange bottle using a Norgren (0-413kPa) pressure regulator coupled with a Budenberg Standard Test Gauge.

8.2.2 Test Procedure

The kaolin had a liquid limit of 41% and a plastic limit of 32% and was mixed at 50% moisture content and placed into the vessel under vibration in an attempt to reduce the air content to a minimum. The clay was then consolidated under a pressure of 173kPa. A back pressure of 69kPa was used in order to dissolve any trapped air in the system. Thus at the completion of this consolidation the effective stress was 104kPa. After this initial consolidation the pressures were relieved and the lid removed. A 'dishing' effect of the top surface of the clay occurs because the centre settles considerably more than the sides.

The surface of the clay was then levelled and the footing (10.16 cm in diameter) placed on the surface although for the latter three tests the piles were installed at this stage and then the footing seated on the piles. For the installation of the aluminium pile a hole 2.54 cm in diameter and 12.7 cm in length was bored in the clay and the pile seated into the hole. The same procedure of forming the hole was

used for the 'gravel' piles, which were composed of Nepean River Sand and poured into the hole in three 'lifts'. After each lift the sand was firmly tamped with a brass rod. The footing was then placed concentrically onto the piles and the lid secured to the body of the vessel. The clay was then further consolidated under a pressure of 207kPa and a back pressure of 69kPa. When the consolidation was completed the drainage taps were closed and the loading plunger seated onto the footing.

The load was applied at a constant rate of penetration with the maximum load being applied within one minute so that conditions could reasonably be expected to be undrained. The load-deformation behaviour was recorded automatically using direct current load and displacement transducers which were connected to a Hewlett-Packard 7046A X-Y recorder.

8.2.3 Experimental Results and Theoretical Predictions

The tests were performed in order to verify the results of the finite element analysis presented in Chapter 4. In order to predict the load-deformation behaviour of the model footings using this analysis, the material properties of the clay and piles are required.

The results of four K_o' triaxial tests on the kaolin are shown in Table 8.1. The apparatus and test procedure used in these tests is identical to that outlined in detail by Davis and Poulos (1963) and thus no detailed description of either is given here.

TABLE 8.1

Test	Undrained Cohesion c_u kPa	Coefficient of lateral earth pressure K_o'
1	55	0.37
2	62	0.40
3	62	0.37
4	-	0.50

In these tests the final vertical effective stress was 138 kPa which corresponds to the effective stress in the pressure vessel prior to loading the footing. The Young's modulus obtained from these tests showed considerable scatter. The modulus used in the finite element analyses was therefore backfigured from the elastic portion of the load deflection curve obtained from the first model footing test.

Standard drained triaxial tests were performed on the sand to obtain the strength and deformation properties. A summary of the results from nine tests is shown in Table 8.2.

TABLE 8.2

Cell Pressure kPa	Young's Modulus (E_{50}) kN/m^2		Angle of Dilatancy	
	Average	Range	Average	Range
68.9	19300	15800-24800	10°	10°-11°
103.4	26200	16200-37200	5°	4°-7°
172.4	33100	28300-37200	4°	0°-6°

The drained cohesion c' was zero and the angle of internal friction ϕ was 40°. The Poisson's ratio ν_s' was found to be 0.37.

The circular footing test will be considered first. This test provided a means of backfiguring the Young's modulus of the kaolin and verifying the value of cohesion and K_o' measured from the K_o' triaxial testing. Young's modulus of the kaolin was backfigured using an elastic finite element analysis by adjusting the value until the theoretical and experimental responses were in agreement. A value of 15500 kN/m^2 was obtained and was used for the subsequent analyses.

The mechanism of failure of the rigid circular footing was by 'punching' into the kaolin. This is shown schematically in Fig. 8.2. This 'punching' or shearing of the kaolin at the edge of the footing can be taken into account in a finite element analysis by inserting dual nodes along the rupture plane and allowing slip to occur when the nodal forces in the direction of shear reach their limiting values. This procedure has been investigated and used successfully on a variety of problems by Rowe and Davis (1977) with particular emphasis on anchor plates. The finite element mesh used to analyse the circular plate is shown in Fig. 8.3. Dual nodes are inserted along the rupture plane.

From the results of the K_o' triaxial testing the coefficient of lateral earth pressure was taken as 0.40 and the undrained cohesion as 60 kPa. The friction angle ϕ_u was assumed to be zero. The kaolin was assigned the backfigured Young's modulus E_u of 15500 kN/m^2 and Poisson's ratio $\nu_u = 0.48$. The comparison between the measured load-settlement response and the results of the finite element analysis are shown in Fig. 8.4. The good overall agreement suggests that the

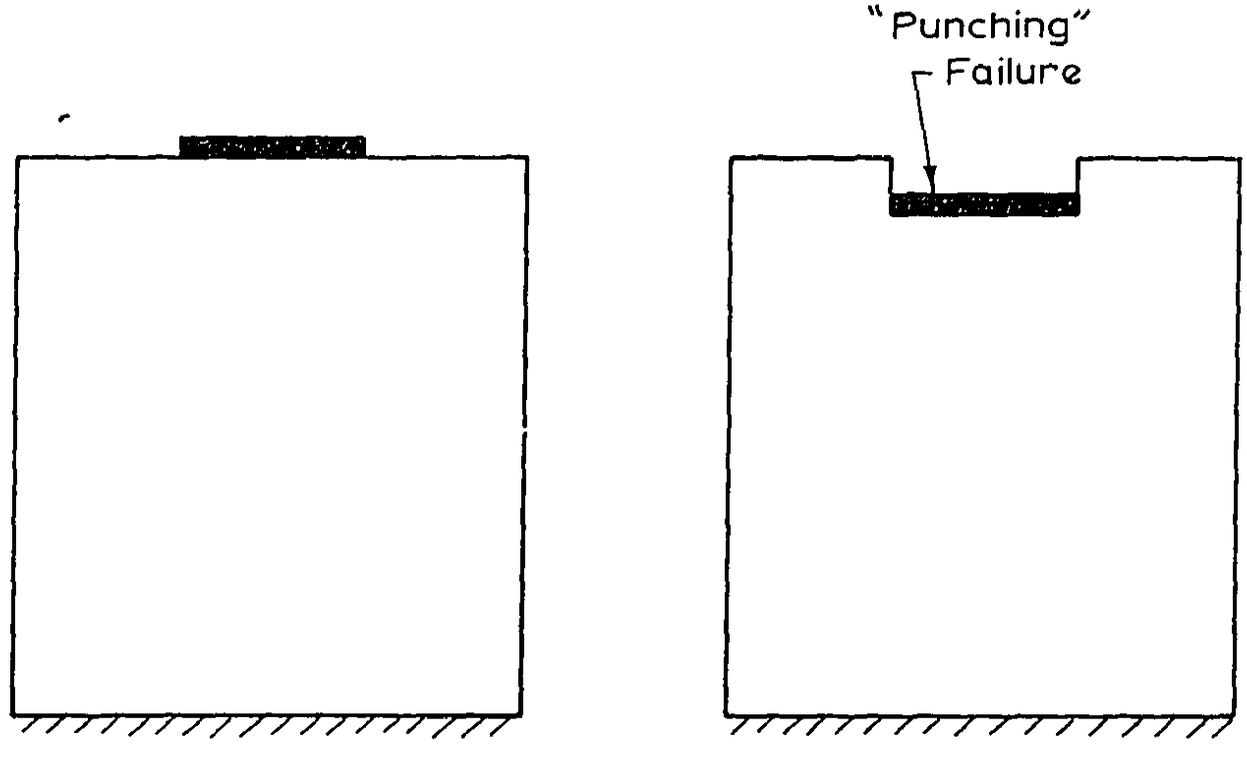

FIG. 8·2 SCHEMATIC DIAGRAM OF FAILURE MECHANISM

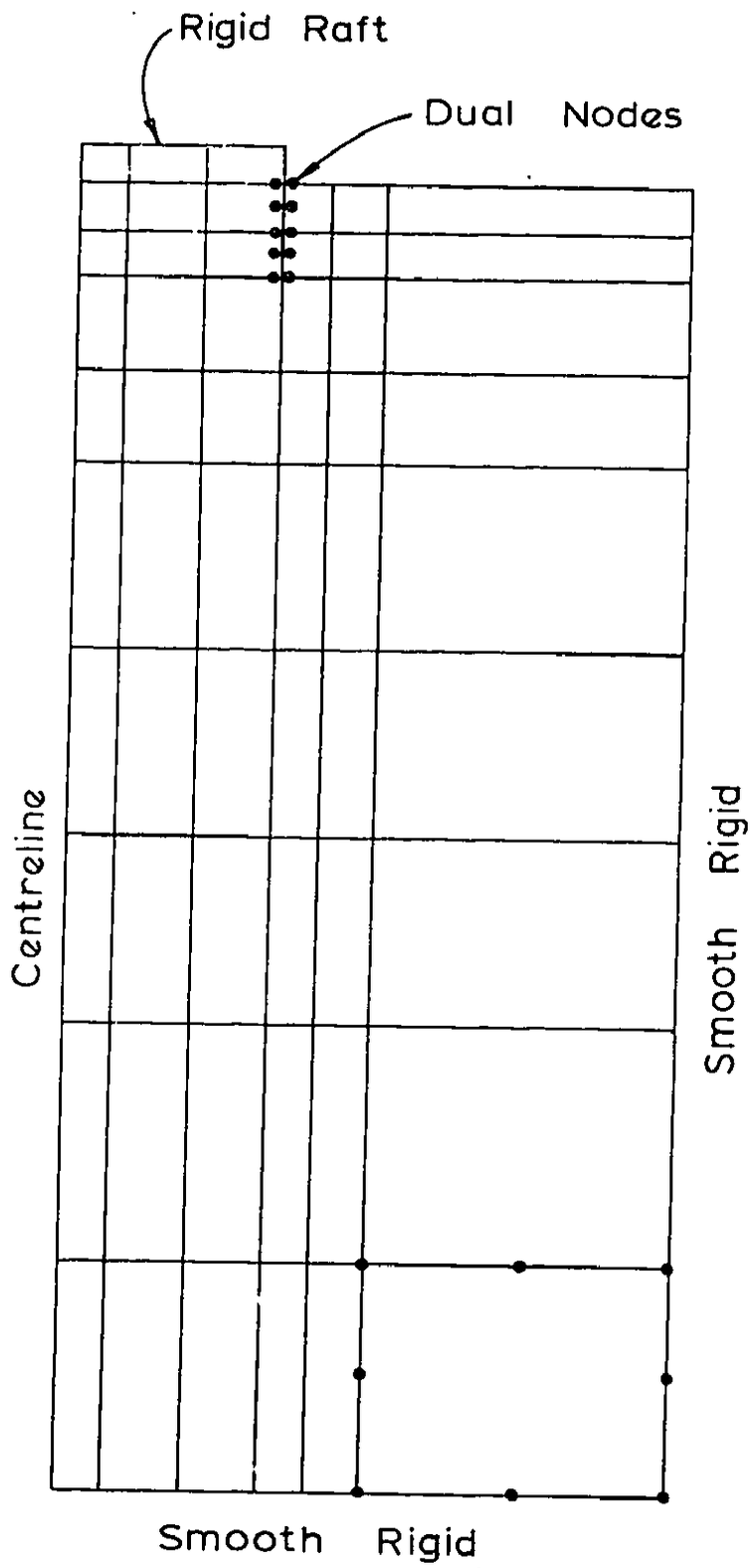

FIG. 8·3 ISOPARAMETRIC MESH USED FOR ANALYSIS OF RIGID RAFT

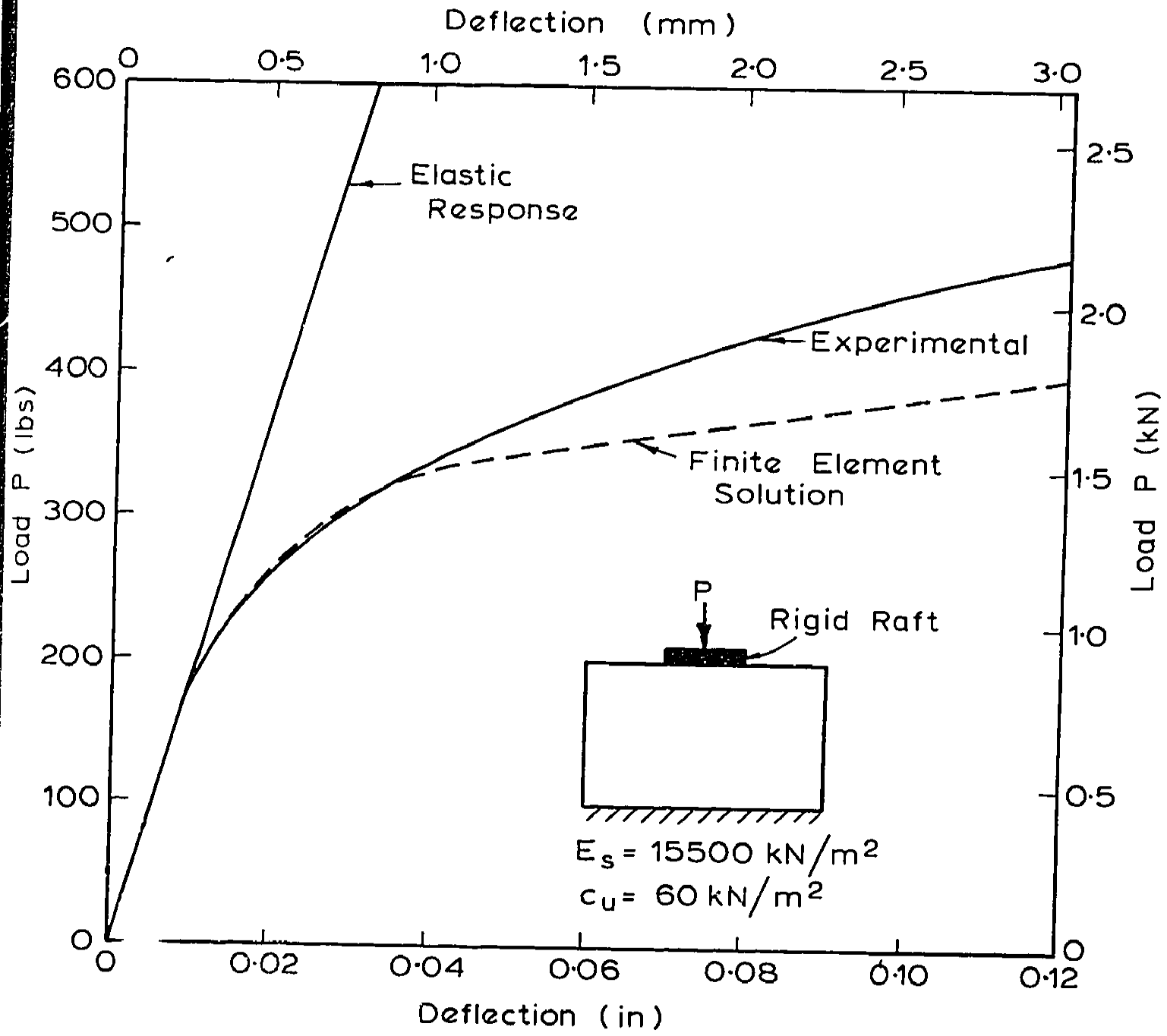

FIG 8·4 ANALYSIS OF RIGID RAFT

measured values of the material properties are in close agreement with the actual values and the failure mechanism has been modelled correctly. The growth of the plastic zone obtained from the finite element analysis is shown in Fig. 8.5.

The size of the sand pile (12.7 cm long, 2.54 cm diameter) used in the second test was not sufficient to cause a significant increase in the load carrying capacity of the circular footing. However, because the sand is stiffer than the clay, reduced settlements were measured. The finite element analysis used to reproduce the results of this test also allowed for a rupture plane at the edge of the footing in addition to slip at the granular pile-clay interface and yielding within the clay and sand. The finite element mesh used for this analysis and also the analysis of the aluminium pile is shown in Fig. 8.6.

From the results of the triaxial testing, the sand was assigned zero cohesion, a friction angle ϕ of 40° and an angle of dilatancy ψ = 7°. The Poisson's ratio ν_s' was taken to be 0.37 and a Young's modulus E_s' of 22000 kN/m^2 was considered appropriate. The coefficient of lateral earth pressure K_o' was assumed to be 0.4. The properties of the kaolin were taken to be the same as used in the previous analysis, ie. a cohesion of 60 kPa, ϕ_u = 0, E_u = 15,500 kN/m^2, K_o' = 0.4 and ν_u = 0.48. The results of the finite element analysis are shown in Fig. 8.7 along with the experimental results. While the agreement is fair, it could be improved if the cohesion of the clay were increased and the angle of friction of the and reduced. The elastic response obtained from this analysis is in close agreement with the measured response. The growth of the plastic zone is shown in Fig. 8.8.

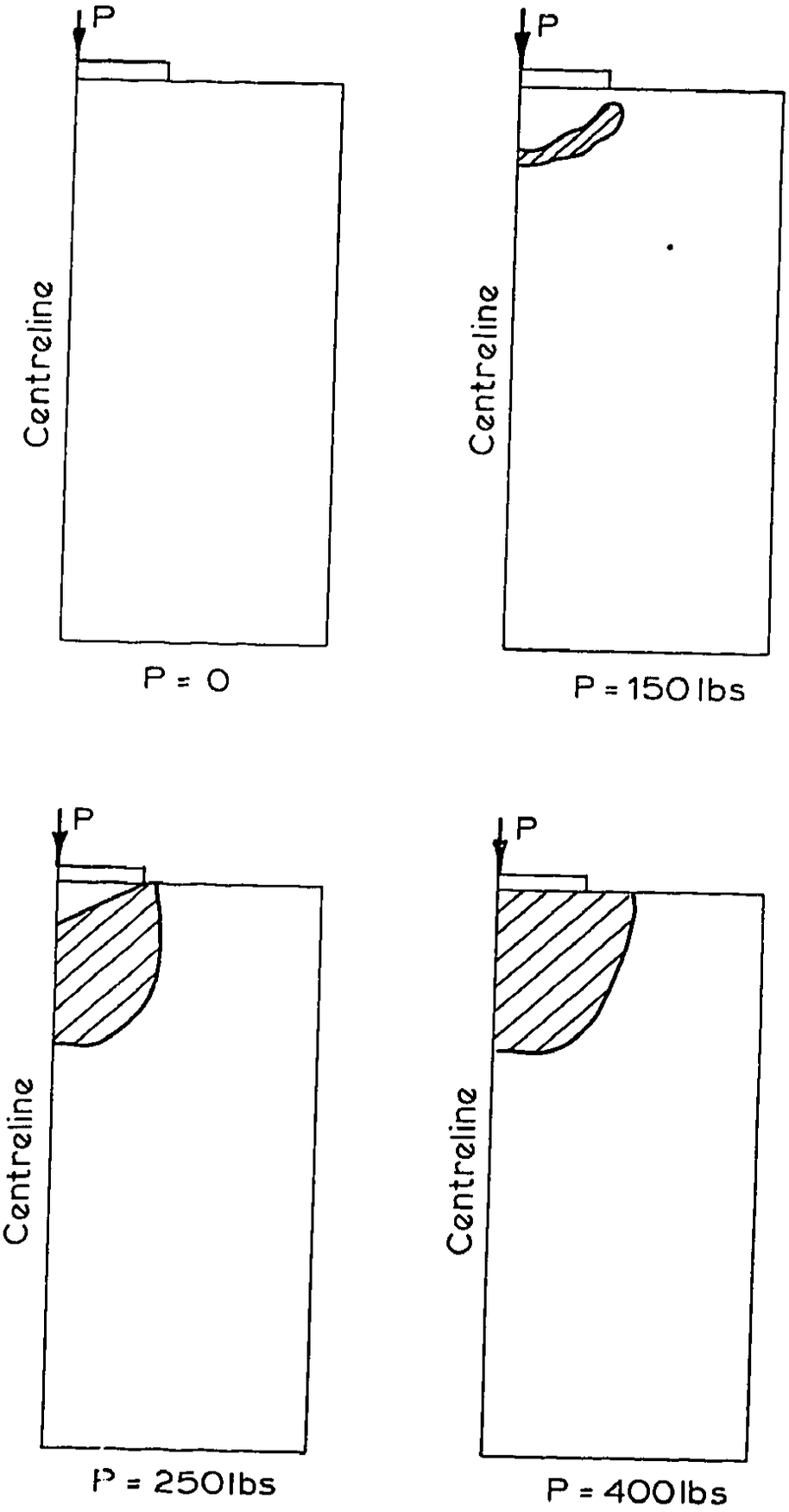

FIG. 8·5 GROWTH OF PLASTIC ZONES FOR CIRCULAR FOOTING TEST

The applicability of the solutions presented in the previous chapter for the magnitude and rate of settlement of a rigid raft was investigated in the second programme. The assumption used in the analysis that the settlement can be predicted by considering one pile-soil unit was used in the design of the experimental set-up. A P.V.C. cylinder filled with kaolin was consolidated under one-dimensional conditions by a rigid raft and the settlement for a given stress range compared to

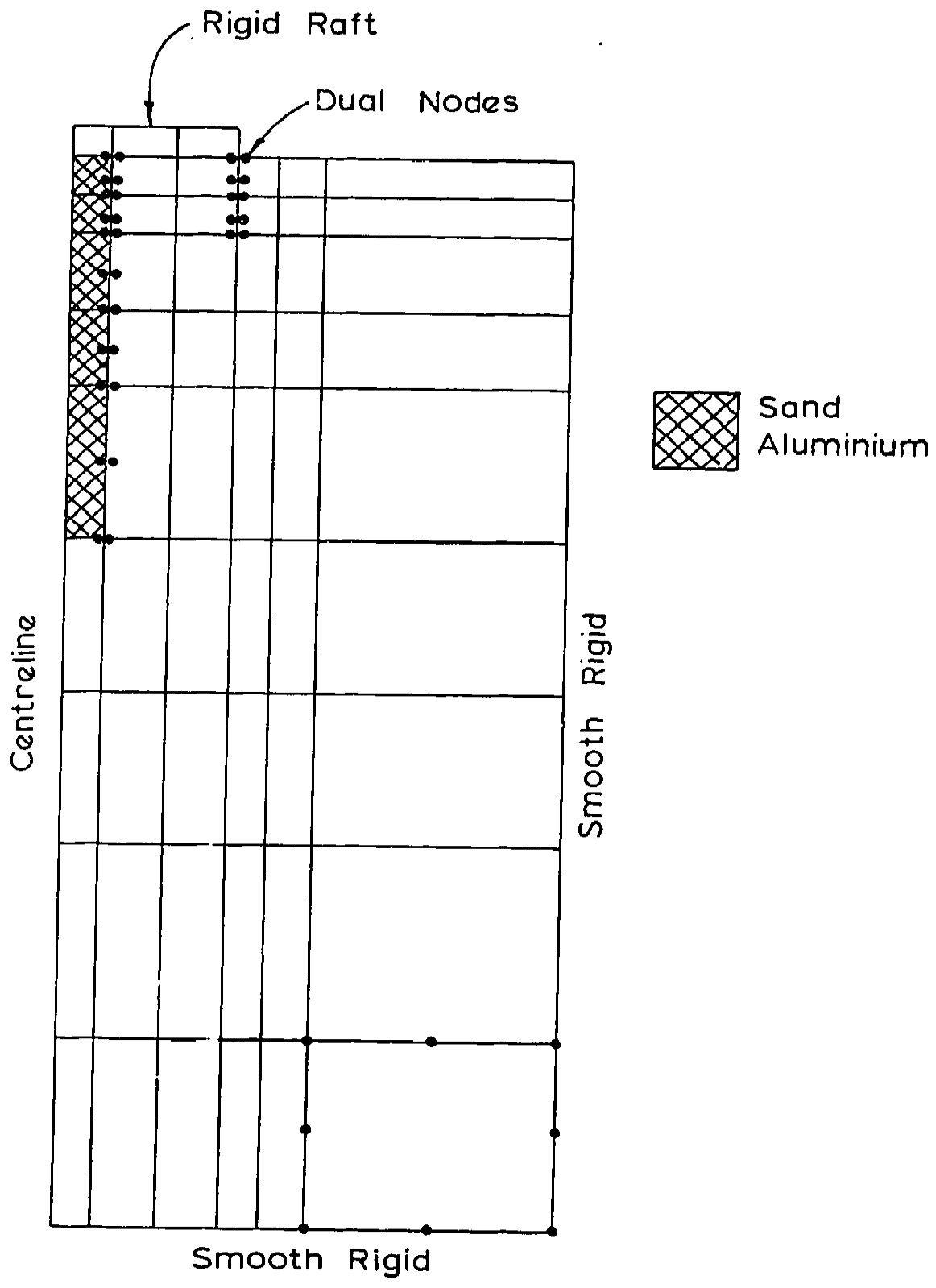

FIG. 8·6 ISOPARAMETRIC MESH USED FOR ANALYSIS OF GRANULAR AND ALUMINIUM PILES

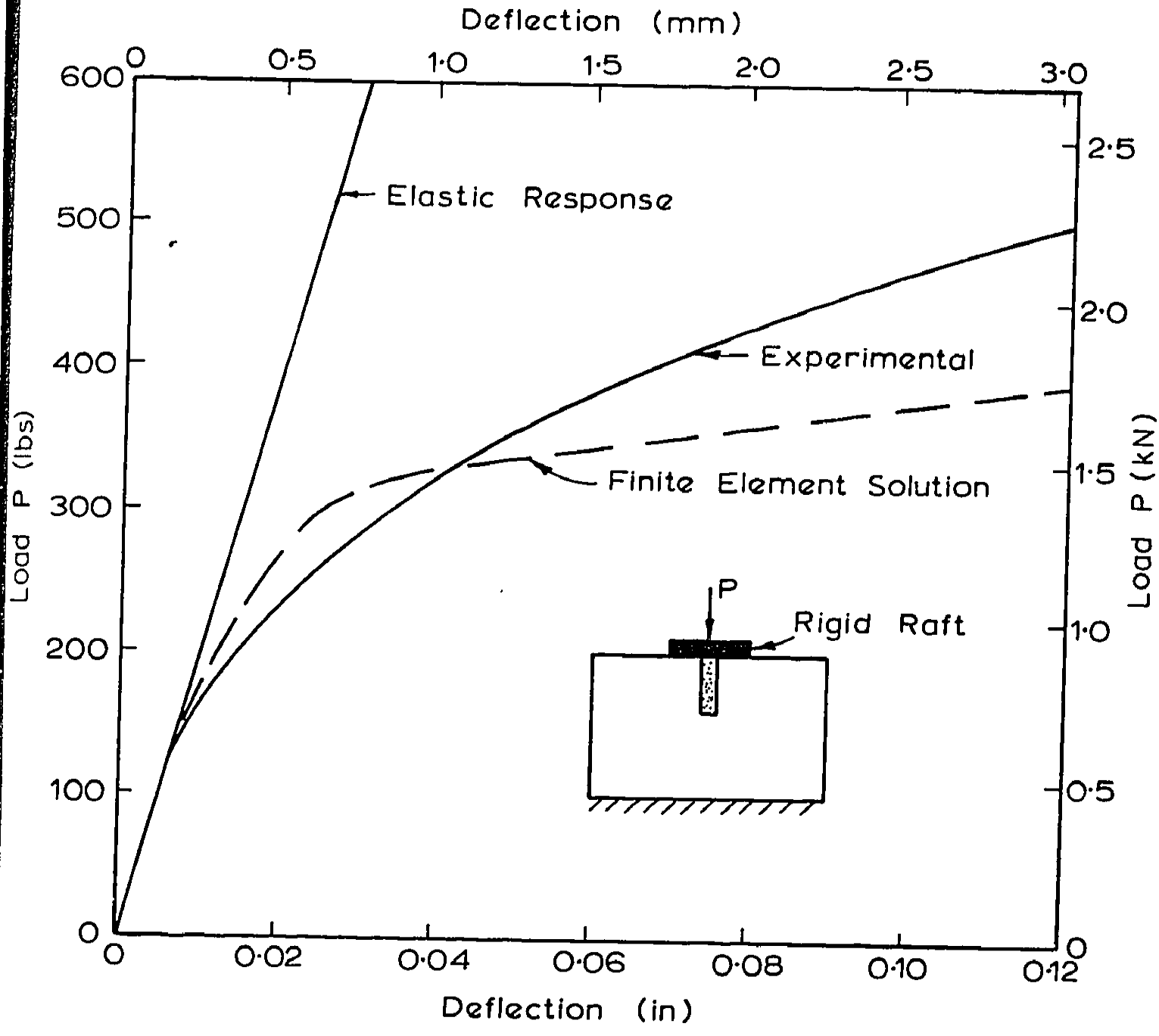

FIG. 8·7 ANALYSIS OF SINGLE GRANULAR PILE

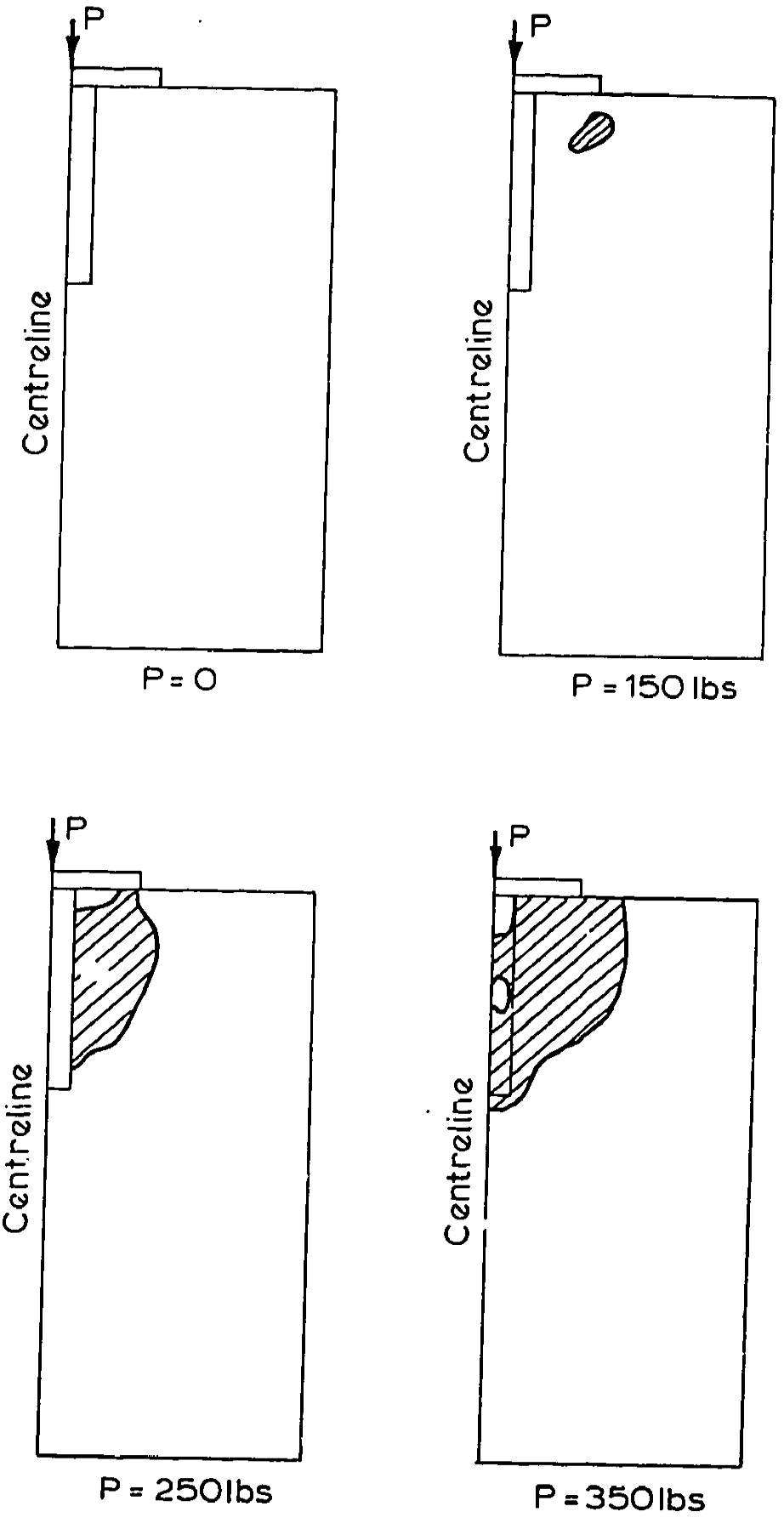

FIG. 8-8 GROWTH OF PLASTIC ZONES FOR GRANULAR PILE

The use of an aluminium pile to support the circular raft resulted in a significant increase in the load carrying capacity of the raft when compared to a sand pile with the same dimensions. The results of a finite element analysis are shown along with the experimental results in Fig. 8.9. The aluminium was assigned a Young's modulus $E_p = 68.95 \times 10^6$ kN/m^2 and a Poisson's ratio of 0.3. In this analysis failure of the pile material was not taken into account. The pile-clay adhesion c_a was taken to be equal to the cohesion c_u. The overall agreement between the predicted and measured results is reasonable.

Finally, the results from the finite element analysis of a single granular pile can be used in conjunction with the interaction factors presented in Chapter 4 to estimate the load-settlement response for the circular raft supported by three sand piles. The method of constructing the load-settlement curve is outlined in detail in section 4.3.1. The piles of diameter 2.54 cm were placed on the vertices of an equilateral triangle with sides 2.54 cm. From Fig. 4.15 the sum of the interaction factors for this arrangement of piles is approximately 1.6. In Fig. 8.10 the load-settlement curve for the rigid circular raft constructed from the results of the single granular pile analysis is compared with the experimental results. The theoretical and experimental results are in poor agreement. This discrepancy may be due to the use of elastic interaction factors for the construction of the entire load-deflection curve. However, more theoretical and experimental (field and laboratory) work is required before firm conclusions can be reached regarding the settlement of small groups of granular piles.

In Table 8.3 the results are shown of comparisons between the

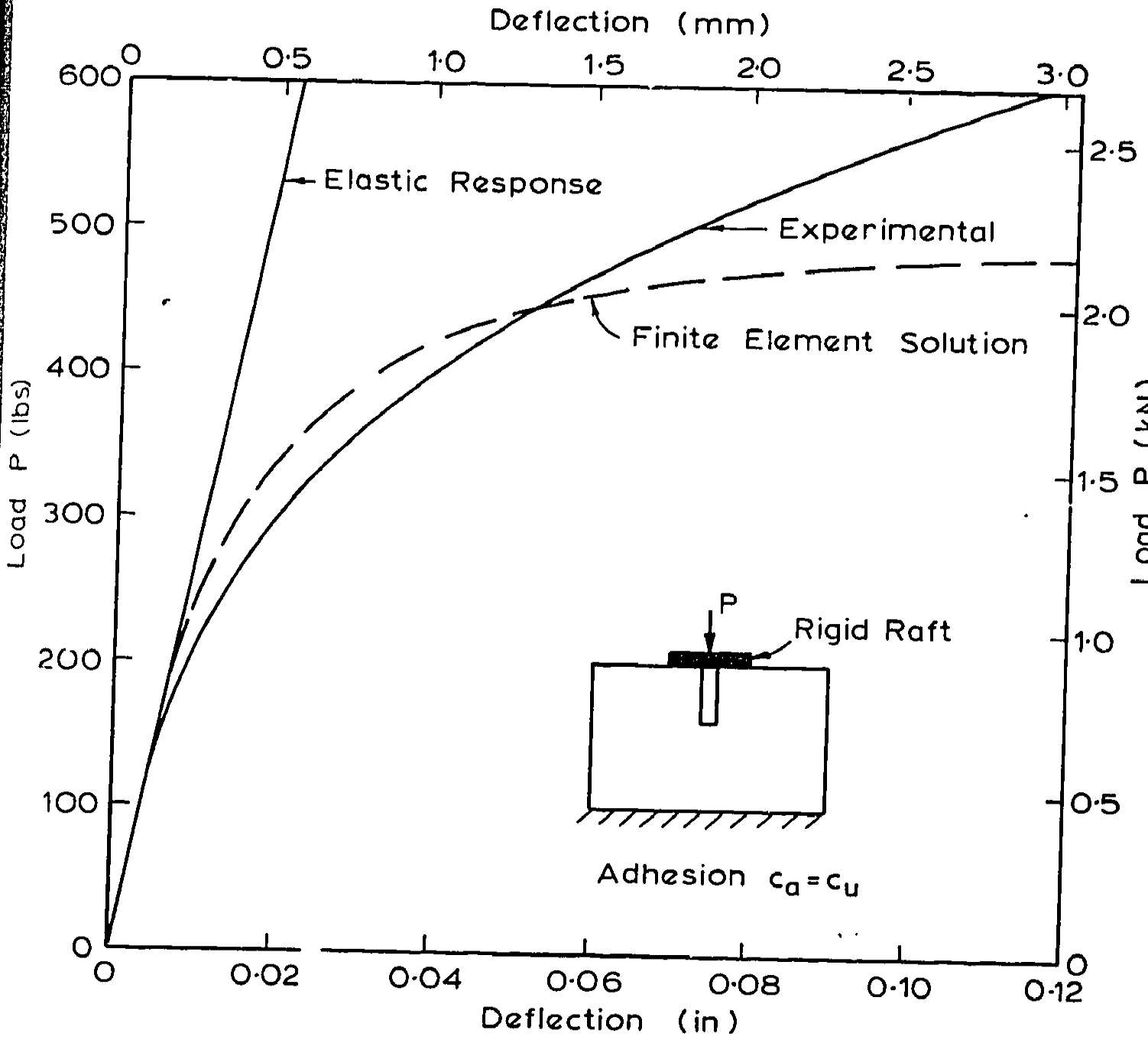

FIG. 8·9 ANALYSIS OF SINGLE ALUMINIUM PILE

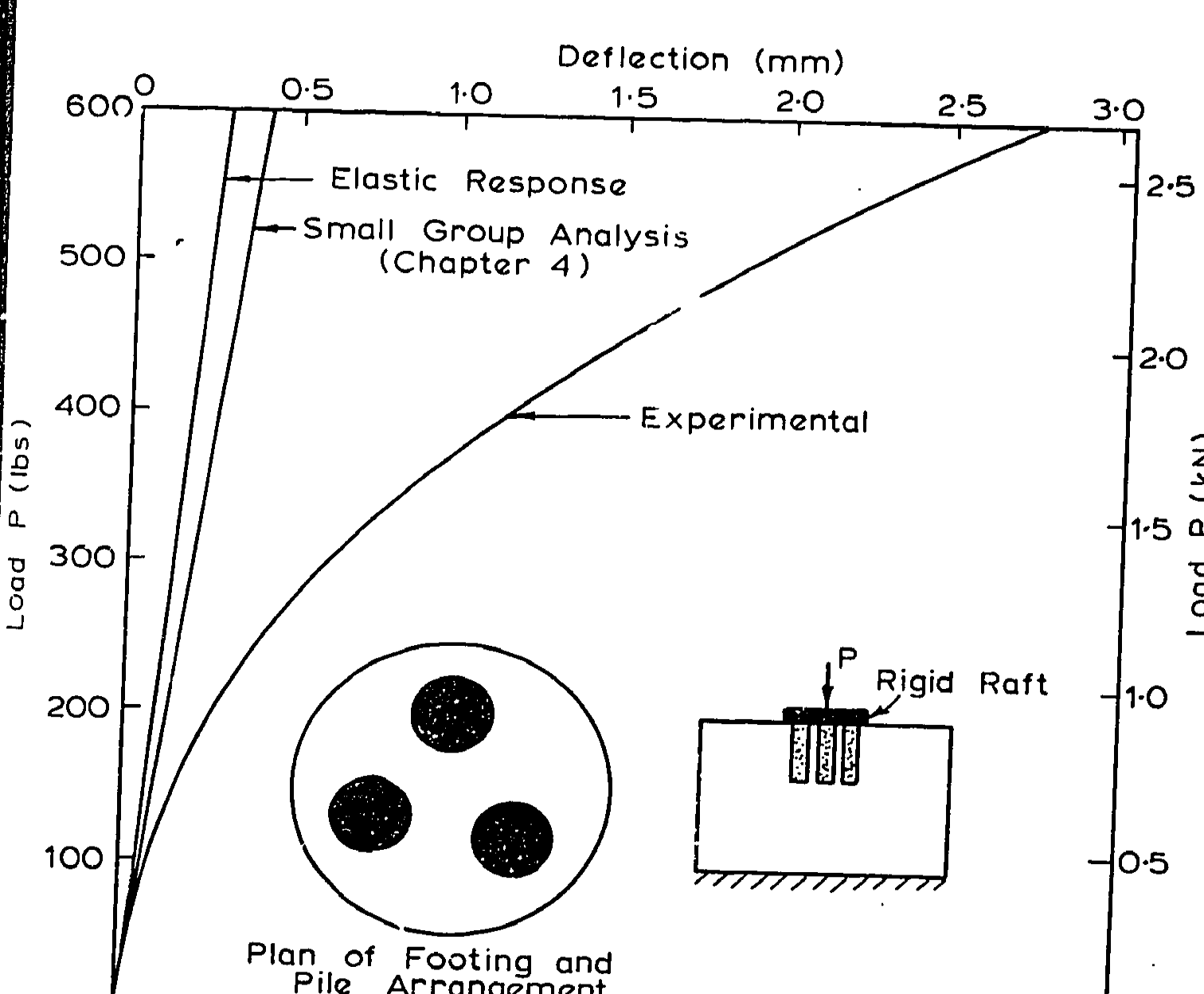

FIG. 8·10 ANALYSIS OF SMALL GROUP OF GRANULAR PILES

predicted and measured settlements for these four tests at load levels of 0.5 and 1 kN. Although the overall agreement between the predicted and measured load-deflection behaviour in these four model tests is only reasonable, good agreement is obtained, (except for the group of three piles) at load levels representative of the normal working load range.

TABLE 8.3

COMPARISON BETWEEN MEASURED AND PREDICTED DEFLECTIONS

	P = 0.5 kN		P = 1.0 kN	
	Experimental (mm)	Theoretical (mm)	Experimental (mm)	Theoretical (mm)
No Pile	.30	.30	.38	.38
Granular Pile	.31	.30	.48	.38
Aluminium Pile	.10	.10	.28	.23
3 Granular Piles	.10	.075	.33	.15

In conclusion, the results of these four model tests indicate that when the material properties and insitu stresses are known, the finite element analysis gives a reasonable prediction of the load-settlement response of a single granular pile. However, this analysis used in conjunction with elastic interaction factors for the analysis of small groups of granular piles may lead to a significant underestimate of settlement.

8.3 CYLINDER TESTS

The elastic theory presented in the previous chapter was used to predict the settlement of a rigid die seated on the surface of a cylinder of clay reinforced by a fully penetrating granular pile. The experimental procedure consisted of measuring the settlement of the rigid die for a given stress range and then comparing this to the settlement when the clay is reinforced by a granular pile. This enabled a settlement reduction for a given diameter of pile to be computed which was compared with the theoretical predictions.

8.3.1 Apparatus and Test Procedure

The cylinder was cut to a length of 30 cm from P.V.C. tubing which was 10.16 cm inside diameter and .5 cm thick. The tubing was cast into a concrete base for stability. A perspex disc in which a hole had been drilled was placed on the bottom of the cylinder and a Klinger cock screwed in to allow control over drainage. This apparatus is shown schematically in Fig. 8.11.

The diameter of 10.16 cm enabled investigations of practical values of $^{de}/_{d}$.

greased with petroleum jelly. A comparison between the coefficient of volume decrease (m_v) measured in the cylinders and small oedometer tests indicated that this was effective. Kaolin mixed at 60% moisture content was then poured into the cylinder and the clay consolidated to a vertical stress of 45 kPa.

At the completion of this initial consolidation the rigid die

The test procedure was as follows; firstly, in an attempt to ensure that the cylinder had smooth shear-free sides, the tubing was greased with petroleum jelly. A comparison between the coefficient of volume decrease (m_v) measured in the cylinders and small oedometer tests indicated that this was effective. Kaolin mixed at 60% moisture content was then poured into the cylinder and the clay consolidated to a vertical stress of 45 kPa.

At the completion of this initial consolidation the rigid die

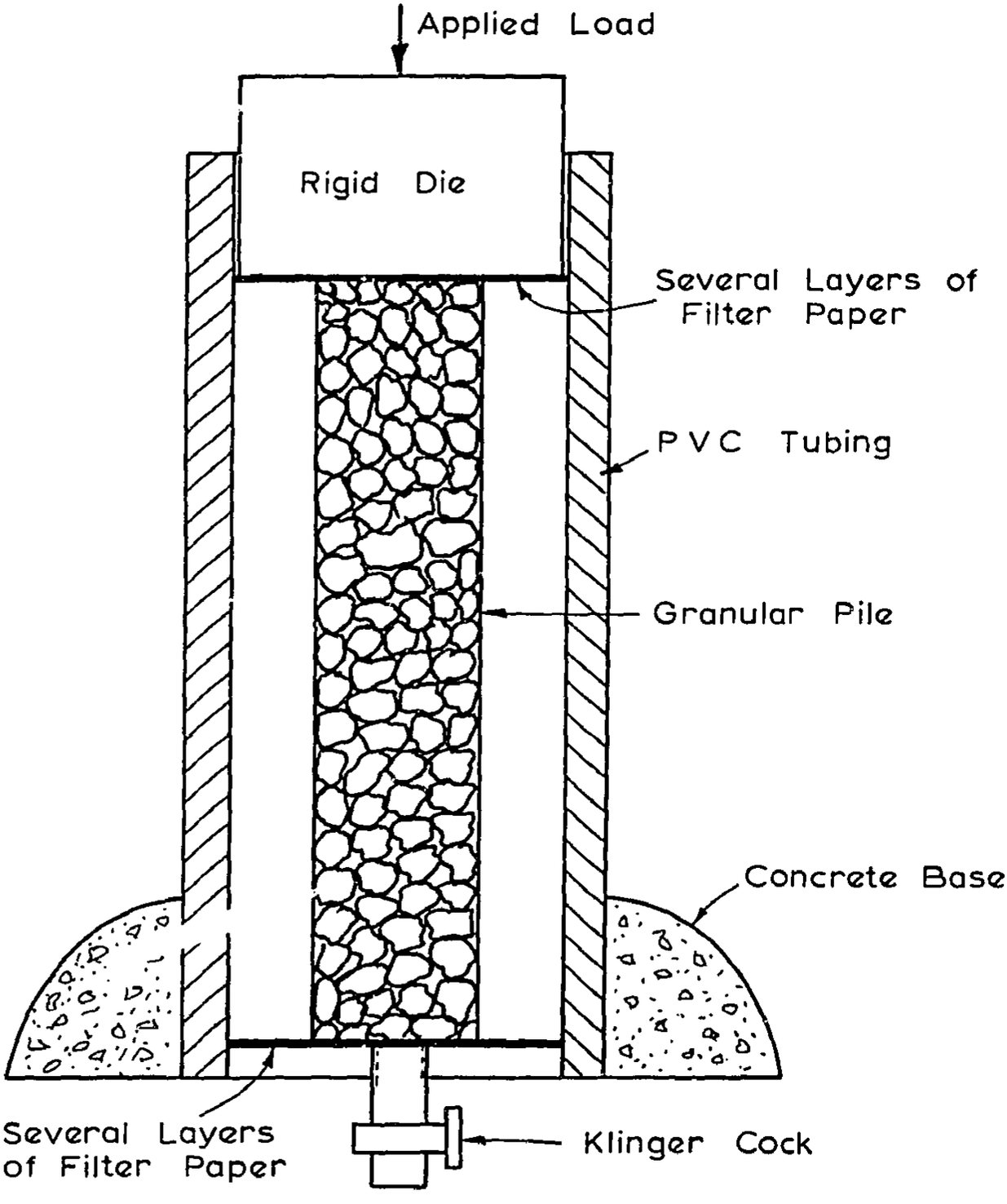

FIG.8·11 SCHEMATIC DIAGRAM OF CYLINDER TEST APPARATUS

and applied loads were removed and the height from the top of the cylinder to the surface of the clay recorded. Also, in this initial consolidation stage, any clay which may have squeezed between the rigid die and the cylinder was removed. The die was then seated on the clay and the clay reconsolidated to 45 kPa. At the completion of this reconsolidation, an increment of 27.4 kPa was then applied and the total final settlement of the die determined from the consolidation curve. A further 54.9 kPa were added and the corresponding settlement recorded. Thus, for the stress ranges of 45-72.4 kPa and 72.4-127.3 kPa, values of m_v for the clay were determined.

The only difference in the experimental procedure used for the granular piles was that before the reconsolidation to 45 kPa, a sampling tube of the required diameter was pushed into the clay to the base of the cylinder. The clay on the interior of the tube was then removed and the tube slowly withdrawn. The clay was sufficiently stiff for the hole to remain open. A coarse fraction from the Nepean River sand was then poured into the hole in several 'lifts'. Water was added after each 'lift' so that the sand was fully saturated. The sand was then tamped firmly with a brass rod to achieve maximum density. However, excavation of the piles at the completion of the tests showed that neither the applied loads or tamping caused significant migration of the sand into the clay and that the initial diameter of the sand pile had not increased. The amount of sand used for construction of the pile was recorded and used to calculate the unit weight of the piles. The average unit weight achieved was approximately 15.7 kN/m^3. The two increments in pressure (27.4 and 54.9 kN/m^2) were then applied and the time-settlement behaviour recorded. The reductions in settlement due to the presence of the granular pile were then computed.

8.3.2 Comparison Between Theoretical and Experimental Results

Four tests were conducted to determine the compressibility of the sand. In these tests the cylinder was filled with sand and a pressure of 45 kPa applied. The stress increments of 27.4 and 54.9 kN/m^2 were then applied and the total final settlements recorded. Consolidation was almost immediate. A Poisson's ratio of 0.3 was estimated for the coarse fraction of the Nepean River Sand and the clay (under drained conditions) and thus these tests enabled a ratio of the Young's modulus of the sand (E_1) and clay (E_2) to be determined. The ratio of E_1/E_2 varied between approximately ten and twenty.

The theoretical settlement reductions from the previous chapter are reproduced in Fig. 8.12 along with the experimental results for values of a/b (radius of granular pile to radius of cylinder) equal to 0.25, 0.5 and 1.0 (all sand). Thus, although the tests are simple the agreement is good and thus some experimental evidence has been obtained which indicates that the properties of the clay and gravel can be determined from oedometer tests of this size.

In Chapter 7 solutions for the rate of settlement of a rigid die supported by clay reinforced with gravel piles were presented. Assuming the modular ratio of the sand and clay E_1/E_2 is 10 and the Poisson's ratios ν_1 and ν_2 are both 0.3, interpolation of these results enable the ratio of times at 50% consolidation (t_{50}) to be computed for the two cases, ie. no pile (one-dimensional consolidation) and the fully penetrating pile (predominantly radial flow to the pile). These ratios have been evaluated for the two geometries considered, ie. a/b = .25 and .5, using the average t_{50} obtained from the no-pile tests. A comparison

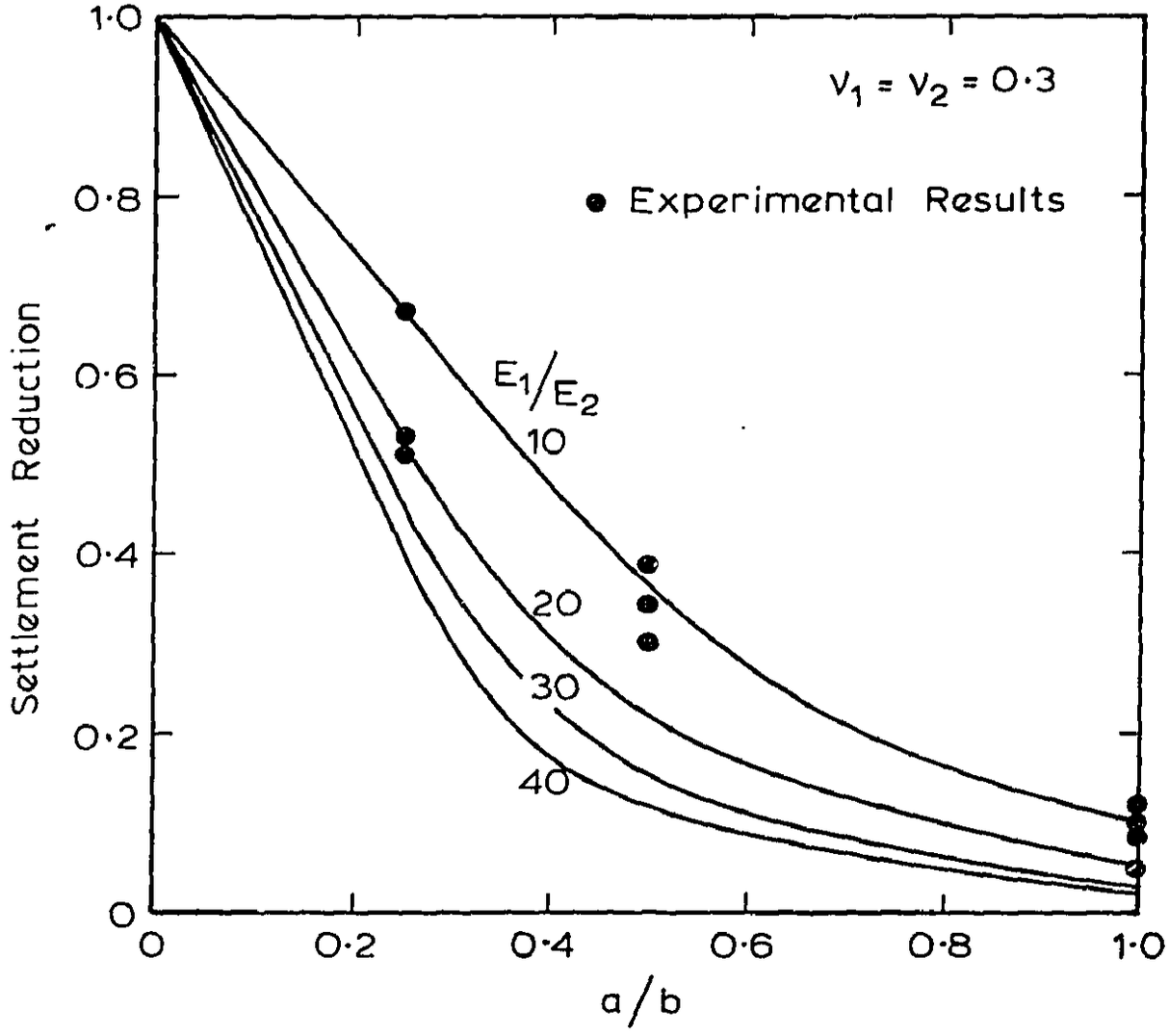

FIG. 8·12 COMPARISON BETWEEN THEORETICAL AND EXPERIMENTAL SETTLEMENT REDUCTIONS

between the measured ratios and the theoretical values are shown in Table 8.4. The agreement between the measured and theoretical values is good.

TABLE 8.4

a/b	Ratio of Times for 50% Consolidation	
	Theoretical	Experimental
.5	.024	.027 .023 .031
.25	.160	.147 .121 .182

8.4 CONCLUSIONS

In this chapter two experimental programmes have been described and the results presented. The experimental results for the load-settlement response of a single granular pile are in good agreement with the finite element analysis presented in this thesis for the analysis of single granular piles. In addition, the elastic settlement analysis and the finite element solutions for the rate of settlement of a rigid raft are in good agreement with the results obtained from a series of cylinder or oedometer tests.

However, the analysis of settlement for a small group of gra-

nular piles underestimates the settlements and more experimental (field and laboratory, evidence) is required before reliable conclusions regarding the reasons for this lack of agreement can be made.

CHAPTER NINE

CONCLUDING REMARKS

In this thesis methods of analysis have been developed which enable a rational assessment of the load-settlement response of foundations supported by single stone columns or small groups of stone columns, or by an extensive area stabilised by large numbers of stone columns.

The most fundamental problem to consider is the ultimate load carrying capacity of a single stone column (granular pile). The pile's load carrying capacity generally decreases as the rate of load application increases. When the load is applied rapidly enough the soil will behave as a purely cohesive incompressible material whereas the response of the pile material will be that of a purely frictional dilatant material. Thus, an analytic solution to this problem is only possible if radical simplifications are made. A finite element analysis has been presented in which the three modes of failure most likely to occur in the granular pile-soil system are taken into account. These are:

(a) interface slip between the granular pile and soil

(b) failure under undrained conditions within the soil mass

(c) failure under drained conditions within the granular pile.

The formulation for slip at the interface overcomes the need for a variable stiffness approach to be adopted as the nodal forces at the interface, and not the deflections, are treated as unknowns. The analysis allows for adhesive, adhesive-frictional, and dilatant interface behaviour.

This analysis has been used to identify the most important parameters affecting the ultimate load of a single column. These parameters are

(a) friction angle of pile material

(b) depth to which the pile is installed

(c) cohesion of the insitu soil.

The analysis has also been used to reproduce the results of a previously published full scale load test. The data presented has enabled an intuitive assessment of the required properties for the soil and pile materials. The results from this comparison have shown that, if the material properties are well defined, the analysis is capable of predicting the response of a single column accurately when the interface strength is specified as purely adhesive. However, the equation developed by Hughes and Withers (1974) for the ultimate load of a single stone column also closely predicts the measured ultimate load and thus presents itself as a convenient alternative to a time-consuming finite element analysis. If however, the site is non-uniform, the finite element analysis eliminates the element of subjectivity required in applying the Hughes and Withers equation.

A comparison has also been made between the results of this load test and the results from the analysis presented by Mattes and Poulos (1969) for determining the load-deflection behaviour of conventional piles. The overall agreement is poor although the initial elastic settlement is in good agreement with the measured values when appropriate moduli were specified. The settlements at small working loads are underestimated by the Mattes and Poulos analysis because of the extent of local yielding within the soil and pile materials. Therefore, caution should be exercised in using the results from conventional pile analyses as a preliminary design aid to predict the behaviour of stone columns.

A method has been described to predict the load-settlement behaviour of footings supported by small groups of granular piles. In this method, the results from a finite element analysis of a single pile are used in conjunction with settlement interaction factors obtained by an elastic analysis of two identical piles. Firstly, a load deflection curve for the single pile is determined taking into account the increased settlement due to the interaction between the piles. Then, for a given value of deflection, the corresponding load on the single pile is multiplied by the number of piles in the group to obtain the load the group can support. This is repeated for successive values of deflection until the entire load-deflection curve for the group has been constructed.

The elastic analysis was employed to backfigure the soil modulus from previously published full scale tests on single piles at a site in India. It was then used to predict the elastic settlement of a small group of seven columns installed at the same site. As only limited soil data was reported it was not possible to construct the theoretical load-settlement response for the group. The predicted settlements were too small, although the modulus backfigured from an analysis of one pile gave reasonable agreement with the measured settlement.

An entire load deflection curve using this method has been constructed for a group of three columns and compared with the results from [illegible] agreement as a [illegible] while-[illegible], it is the [illegible]'s [illegible] more comparisons of this type are required before [illegible] conclusions [illegible] this method.

If an extensive area is stabilised by large numbers of stone columns a mechanism for a bearing capacity type failure only exists at the edges of the loaded area. The likelihood of this type of failure can be assessed by conventional slip circle analyses in which the piles are treated as an equivalent 'trench' of purely frictional material situated in a purely cohesive environment. If an adequate factor of safety is calculated the design of the required layout and size of the piles is determined from the permissible settlements.

Elastic finite element solutions have been presented for the settlement of a flexible foundation supported by clay stabilised by the installation of large numbers of piles. As the loading pressure is increased contained plastic flow will develop within the pile and/or soil. However, it has been shown through an elasto-plastic finite element analysis that, because the discrepancy between the elastic and elasto-plastic settlements is not significant, the effects of various changes in a pile-soil unit can be determined to satisfactory accuracy by means of elastic analyses. It has been assumed that because the regular array of piles is extensive each pile-soil unit away from the edges of the loaded area will behave in precisely the same manner and therefore the settlement of the foundation can be determined from an analysis of an isolated pile-soil unit. In addition, for the two regular arrangements of piles used in practice (ie. triangular and square), the corresponding domains of influence (hexagonal and square) of each pile are replaced by an equivalent circle of equal area. The same assumptions have been used in the development of an analytic solution from elasticity theory for the settlement of a rigid foundation.

Solutions have been presented for the reduction in settlement

of a foundation due to the introduction of the stone columns which reinforce the insitu clay. These solutions show that the piles are more effective if the foundation is rigid because more load is carried by the stiffer piles as the rigidity of the foundation increases. To counteract this, the very high ratios of vertical to horizontal stress from an elastic analysis will cause contained yielding within the pile. For significant reductions in settlement the piles need to be closely spaced ($s/d \leq 5$) and penetrate through to at least half the depth of the clay layer. It is anticipated that these solutions will be used to optimise the size and spacing of the piles for a given required settlement reduction.

The available published field results for the reduction in settlement of flexible foundations have been compiled and compared with the finite element solutions and Greenwood's (1970) empirical curves. For small spacings of the piles the agreement between the measured, finite element and Greenwood values is good. For pile spacings in excess of 2.3m, field data is unavailable and it is for these spacings that the finite element solutions predict significantly larger reductions in settlement than those suggested by Greenwood.

The results computed from the analytic solution for the settlement of a rigid foundation have been compared with measured values obtained from a limited programme of laboratory tests. The agreement is good, and it is therefore inferred that when elastic moduli are assigned to the pile and soil materials for the appropriate stress range, the theoretical results presented can be used to predict the settlement of foundations supported by clay stabilised by the stone columns.

The improvement in the performance of the stabilised clay is not only due to the presence of the stiffer pile material which results in reduced settlements. The stone columns act as sand drains and therefore increase the rate of consolidation. Only short periods of preloading would be required for significant increases in strength and stiffness of the clay. Finite difference solutions to diffusion theory have been presented in the form of a parametric study for the rate of pore pressure dissipation. These solutions can be used to predict the rate of settlement of a flexible foundation or to estimate the strength and deformation properties of the clay after a period of preloading prior to subsequent loading. The rate of settlement of rigid foundations has been investigated by the use of finite element solutions to Biot's theory of consolidation. These rates of settlement are in good agreement with values measured in the laboratory tests. Thus, the solutions for the rate of settlement can be used in conjunction with those for the magnitude of settlement to construct the time-settlement behaviour of a rigid or flexible foundation supported by the stabilised clay.

In summary, an attempt has been made in this thesis to develop and verify methods of analysis for the load-settlement behaviour of foundations supported by either a single stone column, a small group or an extensive regular array of columns. In general, good agreement has been found between the observed and theoretical behaviour of single columns and large groups of stone columns. The finite element analysis has proved a useful tool for examining the mechanism of behaviour of a single column and has enabled the important parameters influencing this behaviour to be isolated. This analysis can be used as a design tool although its most valuable practical use may be in confirming the accu-

racy of existing design approaches such as that proposed by Hughes and Withers. The theory for large groups of stone columns also appears to be in good agreement with field and laboratory data and it is believed that the solutions presented herein provide a reasonable basis for design. The least satisfactory aspect of the investigation has been the analysis of small groups of stone columns supporting isolated foundations. The available published data is scant but that which is available does not appear to be in good agreement with the proposed theory. Future research into the behaviour of stone columns could profitably be directed towards the analysis of small groups.

REFERENCES

ABDELHAMID, M.S. and KRIZEK, R.J. (1976), "At Rest Lateral Earth Pressure of a Consolidating Clay", JGED, ASCE, Vol. 102, No. GT.7, pp. 721-738.

BALAAM, N.P., POULOS, H.G. and BOOKER, J.R. (1975),"Finite Element Analysis of the Effects of Installation on Pile Load-Settlement Behaviour," Geotechnical Engineering, Vol. VI, No. 1, pp. 33-48.

BARRON, R.A. (1948), "Consolidation of Fine-Grained Soils by Drain Wells", Trans, ASCE, Vol. 113, pp. 718-754.

BAUMANN, V. and BAUER, G.E.A. (1974), "The Performance of Foundations on Various Soils Stabilized by the Vibro-Compaction Method", Canadian Geotechnical Jnl., Vol. 2, pp. 509-530.

BIOT, M.A. (1941), "General Theory of Three-Dimensional Consolidation", J. App. Physics, Vol. 12, No. 2, pp. 155-164.

BISHOP, A.W. (1958), "Test Requirements for Measuring the Coefficient of Earth Pressure at Rest", Proc. Brussels Conf. on Earth Pressure Problems, Vol. I, pp. 2-14.

BOOKER, J.R. (1973), "A Numerical Method for the Solution of Biot's Consolidation Theory", Quart. J. Mech. App. Math., Vol. 26, Part 4, pp. 457-470.

BOOKER, J.R. and SMALL, J.C. (1975), "An Investigation of the Stability of Numerical Solutions of Biot's Equations of Consolidation", Int. J. Solids Structures, Vol. 11, pp. 907-917.

BOUSSINESQ, J.V. (1885), "Applications des potentials à l'etude de l'équilibre et du mouvement des solides élastiques", Gautier-Villars, Paris.

BROWN, P.T. (1969), "Numerical Analyses of Uniformly Loaded Circular Rafts on Elastic Layers of Finite Depth", Geotechnique, Vol. XIX, No. 2, pp. 301-306.

BROOKER, E.W. and IRELAND, H.O. (1965), "Earth Pressures at Rest Related to Stress History", Canadian Geotechnical Journal, Vol. 2, No. 1, pp. 1-15.

CAMPANELLA, R.G. and VAID, Y.P. (1972), "A Simple K_o-Triaxial Cell", Canadian Geotechnical Journal, Vol. 9, No. 3, pp. 249-260.

CARRIER, W.D. and CHRISTIAN, J.T. (1973), "Rigid Circular Plate Resting on a Non-Homogeneous Elastic Half Space", Geotechnique, Vol. XXIII, No. 1, pp. 67-84.

CHRISTIAN, J.T. (1971), "Finite Element Deformation Analysis" M.I.T. Special Summer Program 1.34S Soft Ground Construc[illegible] 971.

CHRISTIAN, J.T. and BOEHMER, J.W. (1970), "Plane Strain Co[illegible]ition by Finite Elements", Journal of the Soil Mechanics and Foundations Division, ASCE, Vol. 96, No. SM4, pp. 1435-1457.

CLOUGH, R.W. (1969), "Comparison of Three-Dimensional Finite Elements", Proc. of Symposium on Application of Finite Element Methods in Civil Engineering, Vanderbilt University, Tennessee, pp. 1-26.

COOK, R.D. (1974), "Concepts and Applications of Finite Element Analysis", John Wiley and Sons Inc., N.Y.

D'APPOLONIA, D.J. and LAMBE, T.W. (1970), "Method For Predicting Initial Settlement", J. Soil Mech. Found. Div., ASCE, Vol. 96, SM2, pp. 523-545.

DAVIS, E.H. (1968), "Theories of Plasticity and the Failure of Soil Masses", Ch. 6, of Soil Mechanics, Selected Topics, ed. I.K. Lee, Butterworth.

DAVIS, E.H. and POULOS, H.G. (1963), "Triaxial Testing and Three-Dimensional Settlement Analysis", Proc. 4th Aust. - N.Z. Conf. S.M. & F.E., Adelaide, pp. 223-243.

DAVIS, E.H. and POULOS, H.G. (1972), "Rate of Settlement under Two- and Three-dimensional Conditions", Geotechnique, Vol. XXII, No. 1, pp. 95-114.

DATYE, K.R. and NAGARAJU, S.S. (1975), "Installation and Testing of Rammed Stone Columns", Proc. IGS Speciality Session, Fifth Asian Regional Conf., Bangalore, pp. 101-104.

DATYE, K.R. and NAGARAJU, S.S. (1976), "A New Technique for Ground Improvement", International Conference on New Horizons in Construction Materials, Lehigh University, Vol. I, pp. 187-198.

DATYE, K.R. and NAGARAJU, S.S. (1977a), "Reinforced Granular Columns - A New Design Concept", IX International Conference on S.M. and Foundation Eng. Speciality Session No. 10. Tokyo.

DATYE, K.R. and NAGARAJU, S.S. (1977b), "Behaviour of Foundations on Ground Improved with Stone Columns", IX International Conf. on S.M. and Foundation Eng., Vol. 1, pp. 467-470.

ELLISON, R.D., D'APPOLONIA, E. and THIERS, G.R. (1971), "Load-Deformation Mechanisms for Bored Piles", J. Soil Mech. Found. Div., ASCE, Vol. 97, pp. 661-678.

ENGELHARDT, K. and GOLDING, H.C. (1975), "Field Testing to Evaluate Stone Column Performance in a Seismic Area", Geotechnique, Vol. XXV, No. 1, pp. 61-70.

ENGELHARDT, K. and KIRSCH, K. (1977), "Soil Improvement by Deep Vibratory Techniques", 5th S.E.A. Conf. on Soil Engineering. Bangkok.

FUDO (1971), "Design Manual For Co... ...System", compiled by Research Laboratory, Fudo Constructi... ...mpany, Japan.

GEOTECHNICAL ENGINEERS, Inc. (1976), "Laboratory Testing Program for Bluff Stability Study, Pump Storage Project, Boyd County, Nebraska",

Report Subm. to Chas T. Main Inc., Nov. 1976.

GIBSON, R.E. and ANDERSON, W.F. (1961), "In Situ Measurements of Soil Properties with the Pressuremeter", Civil Engineering and Public Works Review, Vol. 56, No. 658.

GIROUD, J.P. (1972), "Tables Pour Le Calcul des Fondations", Dunod, Paris.

GOODMAN, R.E., TAYLOR, R.L. and BREKKE, T.L. (1968), "A Model for the Mechanics of Jointed Rock", J. Soil Mech. Found. Div., ASCE, Vol. 94, pp. 637-659.

GREENWOOD, D.A. (1965), "Strengthening Sand", The Consulting Engineer, October 1965, pp. 39-42.

GREENWOOD, D.A. (1970), "Mechanical improvement of soils below ground surface", Proc. Ground Engineering Conference, June, Paper 2, pp. 9-20.

GREENWOOD, D.A. (1975), "Vibroflotation: Rationale for Design and Practice", Ch. 11 of Methods of Treatment of Unstable Ground. Ed. F.G. Bell, Newnes - Butterworths.

GREENWOOD, D.A. (1976), "Ground Treatment by Deep Compaction", Discussion, Institution of Civil Engineers, pp. 123-125.

HART, E.G., KONDNER, R.L., BOYER, W.C. (1958), "Analysis for Partially Penetrating Sand Drains", Journal of the Soil Mechanics and Foundations Division, ASCE, Vol. 84, No. SM4, paper 1812.

HUGHES, J.M.O. and WITHERS, N.J. (1974), "Reinforcing of Soft Cohesive Soils with Stone Columns", Ground Engineering, May, pp. 42-49.

HUGHES, J.M.O., WITHERS, N.J., GREENWOOD, D.A. (1975), "A Field Trial of the Reinforcing Effect of a Stone Column in Soil", Geotechnique, Vol. XXV, No. 1, pp. 31-44.

HWANG, C.T., MORGENSTERN, N.R., MURRAY, D.W. (1971), "On Solutions of Plane Strain Consolidation Problems by Finite Element Methods", Canadian Geotechnical Jnl., Vol. 8, pp. 109-118.

KIRKPATRICK, W.M. (1957), "The Condition of Failure for Sands", Proc. 4th Int. Conf. Soil Mechanics and Fndn. Eng., Vol. 1, pp. 172-178.

LADD, C.C. and FOOTT, R. (1974), "New Design Procedure for Stability of Soft Clays", Jnl. Geot. Divn., ASCE, Vol. 100, No. GT7, pp. 763-786.

LADD, C.C., FOOTT, R., ISHIHARA, K., SCHLOSSER, F., POULOS, H.G. (1977), "Stress-Deformation and Strength Characteristics", State-of-the Art Report. IX ICSMFE, Tokyo.

LADD, R.S. (1965), "Use of Electrical Pressure Transducers to Measure Soil Pressure", Res. Report R65-48, No. 180, Dept. of Civil Eng., Mass. Inst. of Technology, Cambridge, 79p.

LAMBE, T.W. (1964), "Methods of Estimating Settlement", J.S.M.F.D., ASCE., Vol. 90, No. SM5, p. 43.

McKENNA, J.M., EYRE, W.A., WOLSTENHOLME, D.R., (1975), "Performance of an Embankment Supported by Stone Columns in Soft Ground", Geotechnique, Vol. XXV, No. 1, pp. 51-60.

MATTES, N.S. and POULOS, H.G. (1969), "Settlement of Single Compressible Pile", J. Soil Mech. Found. Div., ASCE, Vol. 95, SM1, pp. 189-207.

MILOVIC, D.M. (1970), "Contraintes et déplacements dans une couche élastique d'èpaisseur limitée produits par une fondation circulaire", Le Génie Civil, 147, 5(Mai 1970), pp. 281-285.

MOORE, W.W. (1944), "Pacific Coast Quay Founded on Deep Clay", Civil Engineering, Vol. 14, No. 12, pp. 515-517.

MOREAU, NEIL and MARY (1835), "Foundations-Emploi du Sable", Annales des Ponts et Chaussees. Memoires, No. 224, pp. 171-214.

NEWMARK, N.M. (1942), "Influence Charts for Computation of Stresses in Elastic Soils", Univ. of Ill., Eng. Expt. Stn., Bull. No. 338.

PELLS, P.J.N. and POULOS, H.G. (1976), "Computer Programs for Geotechnical Engineering. Users Manual-Prime 300", School of Civil Engineering, University of Sydney.

POULOS, H.G. (1968a), "Analysis of the Settlement of Pile Groups", Geotechnique, Vol. 18, pp. 449-471.

POULOS, H.G. (1968b), "The Behaviour of a Rigid Circular Plate Resting on a Finite Elastic Layer", Civil Engineering Transactions, Australia.

POULOS, H.G. (1975), "Settlement of Isolated Foundations", from 'Soil Mechanics Recent Developments' Symp. Proc. Univ. New South Wales, Aust., pp. 181-212.

POULOS, H.G. and AHLSTON, A.T. (1974), "A Study of the Deformation Parameters of Kaolin", 1st Aust. Conf. on Eng. Materials, Univ. N.S.W., pp. 371-384.

POULOS, H.G. and DAVIS, E.H. (1974), "Elastic Solutions for Soil and Rock Mechanics", John Wiley and Sons, New York, 411p.

RAFFLE, J.F. and GREENWOOD, D.A. (1961), "The Relation Between the Rheological Characteristics of Grouts and their Capacity to Permeate Soil". Proc. 5th Int. Conf. Soil Mech. Fdn. Engng., Paris 2, 789.

RATHGEB, E. and KUTZNER, C. (1975), "Some Applications of the Vibro-Replacement Process", Geotechnique, Vol. XXV, No. 1, pp. 45-50.

RICHART, F.E. (1959), "Review of the Theories for Sand Drains", Trans.

ASCE, No. 124, pp. 709-738.

RING, G.J. (1975), "Elasto-Plastic Analysis of Stability Problems", Ph.D. Thesis, University of Sydney, Australia.

ROWE, R.K., BOOKER, J.R. and BALAAM, N.P. (1976), "Application of the Initial Stress Method to Soil Structure Interaction", Accepted for publication Int. J. Num. Meth. in Engng., see also Res. Report No. 294, School of Civil Engineering, University of Sydney.

ROWE, R.K. and DAVIS, E.H. (1977), "Application of the Finite Element Method to the Prediction of Collapse Loads", Res. Report No. 310, School of Civil Engineering, University of Sydney.

SANDHU, R.S. and WILSON, E.L. (1969), "Finite Element Analysis of Seepage in Elastic Media", Journal of the Engineering Mechanics Division, ASCE, Vol. 95, No. EM3, pp. 641-652.

SEED, H.B., MARTIN, P.P. and LYSMER, J. (1975), "The Generation and Dissipation of Pore Water Pressures During Soil Liquefaction", Earthquake Engineering Research Center, Report No. EERC 75-26, August 1975.

SEED, H.B. and BOOKER, J.R. (1976), "Stabilization of Potentially Liquefiable Sand Deposits using Gravel Drain Systems", Earthquake Engineering Research Center, Report No. EERC 76-10, April 1976.

SIMONS, N. (1958), Discussion of "Test Requirements for Measuring the Coefficient of Earth Pressure at Rest", Proc. Brussels Conf. on Earth Pressure Problems, Vol. III, pp. 50-53.

TANIMOTO, K. (1973), "Introduction to the Sand Compaction Pile Method as Applied to Stabilization of Soft Foundation Grounds", Division of Applied Geomechanics. Technical Report No. 16 CSIRO, Australia.

TERZAGHI, K. (1925), "Erdbaumechanik auf bodenphysikalischer Grundlage" F. D euticke, Vienna.

THORBURN, S. (1975), "Building Structures Supported by Stabilized Ground", Geotechnique, Vol. XXV, No. 1, pp. 83-94.

THORBURN, S. and MacVICAR, R.S.L. (1968), "Soil Stabilization Employing Surface and Depth Vibrators", The Structural Engineer, 46, No. 10, pp. 309-316.

TIMOSHENKO, S.P. and WOINOWSKY-KRIEGER, S. (1959), "Theory of Plates and Shells", McGraw-Hill Kogakusha, Ltd., Tokyo, Japan.

WATSON, G.H. and THORBURN, S. (1966), "Building Construction on Soft Alluvium", Civil E..gineering and Public Works Review, March, pp. 295-298.

WATT, A.J., de BOER, B.B., GREENWOOD, D.A. (1967), "Loading Tests on Structures Founded on Soft Cohesive Soils Strengthened by Compacted Granular Columns", Proc. 3rd Asian Regional Conf. on S.M. and Foundation Eng. Haifa pp. 248-251.

WOOD, R.H. (1968), "The Reinforcement of Slabs in Accordance with a Pre-Determined Field of Moments", Concrete, Vol. 2(2), February 1968, pp. 69-76.

WROTH, C.P. (1972), "General Theories of Earth Pressures and Deformations", General Report, Session 1, Proc. 5th European Conf. on Soil Mechanics and Foundation Eng. Madrid, Vol. II, pp. 33-52.

WROTH, C.P. and HUGHES, J.M.O. (1973), "An instrument for in situ testing of soft soils", Proc. 8th Int. Conf. Soil Mech. Fdn. Engng. Moscow 1, pp. 487-494.

ZIENKIEWICZ, O.C. (1971), "The Finite Element Method in Engineering Science", McGraw Hill, London.

ZIENKIEWICZ, O.C., VALLIAPPAN, S., KING, I.P. (1969), "Elasto-Plastic Solutions of Engineering Problems - Initial Stress Finite Element Approach", Int. Journ. Num. Methods in Eng. 1, pp. 75-100.